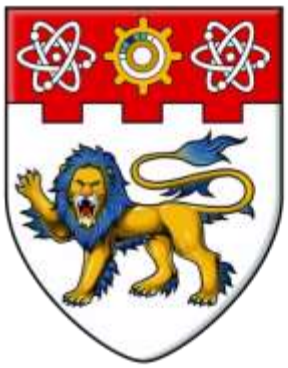

NANYANG TECHNOLOGICAL UNIVERSITY

DEVELOPMENT OF POLYMERIC MICROELECTRONICS PACKAGING ENCAPSULATION FOR HARSH ENVIRONMENT APPLICATIONS

ERIC PHUA JIAN RONG

SCHOOL OF MATERIALS SCIENCE AND ENGINEERING

2017

DEVELOPMENT OF POLYMERIC MICROELECTRONICS PACKAGING ENCAPSULATION FOR HARSH ENVIRONMENT APPLICATIONS

ERIC PHUA JIAN RONG

SCHOOL OF MATERIALS SCIENCE AND ENGINEERING

A thesis submitted to the Nanyang Technological University
in partial fulfilment of the requirement for the degree of
Doctor of Philosophy

2017

Statement of Originality

I hereby certify that the work embodied in this thesis is the result of original research and has not been submitted for a higher degree to any other University or Institution.

26-Aug-2017

. . . . . .

Date

. . . . . .

Eric Phua Jian Rong

Abstract

Epoxy has been the choice of mainstream polymer encapsulation in electronics packaging since the 1960s. Many present electronic applications require polymer materials which are stronger mechanically and functions at higher temperature due to increasing operation demands. Research was previously conducted on a polymer alternative known as phthalonitrile (PN) in the form of structural material but little work has been carried out in the use of phthalonitrile as an electronic packaging material.

Inspired by the extensive usage of epoxies, we propose that the low melting temperature resorcinol based phthalonitriles (PN) can be cured to form new high temperature composites reinforced by silica and alumina fillers that may be used and acceptable in the microelectronics packaging facilities.

In this thesis, the strategy is to evaluate and propose utilization of the new composite which comprises of strong covalent bonds between the matrix and its proposed fillers proven by both Fourier transform infrared spectroscopy (FTIR) and Density Functional Theory (DFT) analysis. PN can be cured to temperatures higher than 300°C and is a crucial binder in the proposed encapsulant and die attach material for furtherinvestigation.

This is the first treatise which extensively evaluates PN as an electronic material suitable for both bonding and as an encapsulant substitute for epoxy. Thermal degradation studies revealed that PN or its filled composites can sustain to temperatures 400°C and beyond. Mechanical characterizations reveal that PN and its filled composites do not encounter sudden failures when temperature is being elevated to 300°C. Other properties such as Coefficient of Thermal Expansion (CTE) can be tuned with fillers such as silica and alumina to match underlying substrates. Dielectric constants show that with 50 weight percent silica, it is possible to obtain dielectric constants of 3.99 which makes a filled version of PN highly comparable to existing epoxy molding compounds (EMC) that are filled with higher loadings of silica of up to 90 weight percent.

Systematic studies have also been implemented to study PN integrated with 24-pin standard alumina Dual in-line Package (DIP). Further High Pressure High Temperature (HPHT) integrated testing reveals that 50 weight percent silica filled PN can survive up to a maximum pressure and temperature of 190 MPa and 310°C respectively, because of the unique thermomechanical strength imparted from its molecular structure. Lastly, dome shaped polymer encapsulation designs are studied and enhanced using Workbench or SolidWorks™. These designs are then imported into ANSYS™ mechanical solvers for structural and thermal evaluation using coupled multi-physics studies. In conclusion, the integration of PN into electronic packages for harsh environment applications has been demonstrated through simulations and prototype testing.

Acknowledgements

First and foremost, I would like to express my utmost gratitude to Prof Gan Chee Lip for his supervision, valuable advices and guidance throughout the course of my candidature. As a mentor, Prof Gan did more than imparting research knowledge. He has demonstrated utmost dedication and principles in all projects accomplished. It is truly an honor to be under his tutelage.

I would also like to thank Prof Chen Zhong, Prof Hu Xiao, A/P Wong Chee Cheong and Dr Liu Ming who are critical in the project development and for their valuable advice which ultimately shape my thesis.

Also would like to extend my sincere gratitude to Dr. Riko I Made. He is both a mentor and a great collaborator.

Lastly, I would like to thank my parents and parent-in-laws for going to great extents taking care of my children as I juggle my part-time PhD studies, with the duties of my day job and roles in different organizations. And to my wife, Siew Chin and sons, Kayden and Jayven, you have been my pillars of joy, hope and support. I am indebted to all of you.

Table of Contents

Table Captions

Figure Captions

Abbreviations

BSE	Backscattered Electron
CTE	Coefficient of thermal expansion
DA	Die attached
DIP	Dual in Line package
EDS	Energy Dispersive X-ray Spectroscopy
EMCs	Epoxy mold compounds (typically industrial compounds)
FTIR	Fourier Transform Infrared Spectroscopy
LWD	Logging while drilling
LTCC	Low temperature co-fired ceramic
MWD	Measurement while drilling
SEM	Scanning Electron Microscopy
SEI	Secondary Electron Images
XRD	X-ray Diffraction
HP	High Pressure
HMC	Hybrid microcircuits
HTCC	High temperature Co-fired ceramics
HTHE	High temperature harsh environment
HTHP	High temperature high pressure
HTS	High temperature storage
PN	Phthalonitrile
RPh	Resorcinol based phthalonitrile
RTM	Rapid transfer molding
PMC	Polymer matrix composite
PCB	Printed circuit board
TM	Transfer molding
Wt%	Weight percent
10 A	10% alumina
10 S	10% silica
30 S	30% silica
30 A	30% alumina
50 S	50% silica

50 A	50% alumina

Chapter 1

Introduction

This chapter provides an overview of the properties required of polymers utilized in harsh environment applications. The motivation of this work is to investigate and propose the role of phthalonitrile (PN) and its behaviour in high pressure high temperature (HPHT) environment. Thermomechanical strength is a major concern in these materials and is discussed in details. Phthalonitrile has the potential to complement existing epoxy encapsulation technologies and be adopted for temperatures above 300°C. This is the temperature regime where scientific investigations to identify suitable polymer candidates are still ongoing. Suitable candidates have to possess similar properties as epoxies and yet maintain its structural integrity at even higher temperatures. Researches which has been performed previously on high temperature thermosets leading to PN as a structural material is explained. Detailed research hypotheses are formed and through a thorough investigation, the research aims to elucidate the effects of temperature, mechanical and environmental factors on new PN polymer composites suitable for electronics packaging. The effect of filler additions is also explained with new properties being analysed through various literatures. To add on, polymer formation mechanisms will also be discussed. The last section of this chapter presents an overview of the thesis organization along with a short introduction to each chapter that follows alongside the research areas which would reveal the practicality of PN as an electronic encapsulation.

Chapter 1.1: Overview of electronic materials for HTHE environments?

The evolution of the electronics industry in the last few decades has created materials which have helped to drive ruggedized electronics applications previously deemed impracticable. Harsh environment applications, also known as High Temperature Harsh Environment (HTHE) operations [1-5], have propelled the engineering frontier for such ruggedized electronics packages. Modern day HTHE operations typically exceed 150°C and are driven by application requirements from automobiles [6-8], aerospace industries [9-11] and oil drilling operations [12-16]. Besides temperature, other factors like high pressure also exist in some harsh environment such as oil drilling operations where pressure can concurrently exceed 69 MPa. The International Associate of Drilling Contractors (IADC) defined this operation requirement as HPHT (High Pressure and High Temperature) [17].

Increasing challenges both in temperature and pressure requirements for deep subsea oil drilling have set forth a need for electronics capable of surviving extremely harsh temperatures (>300°C) and high pressure 207 MPa (30,000 psi) when exposed. It is especially important for modern electronics to be able to operate at such high specifications as any unwanted stoppages or repair work in oil drilling operations typically cost upwards of a million US dollars a day [14]. Because of the operational extremities and high test standards, oil drilling and aerospace standards of electronics improvement could well serve as the benchmark for many other fields.

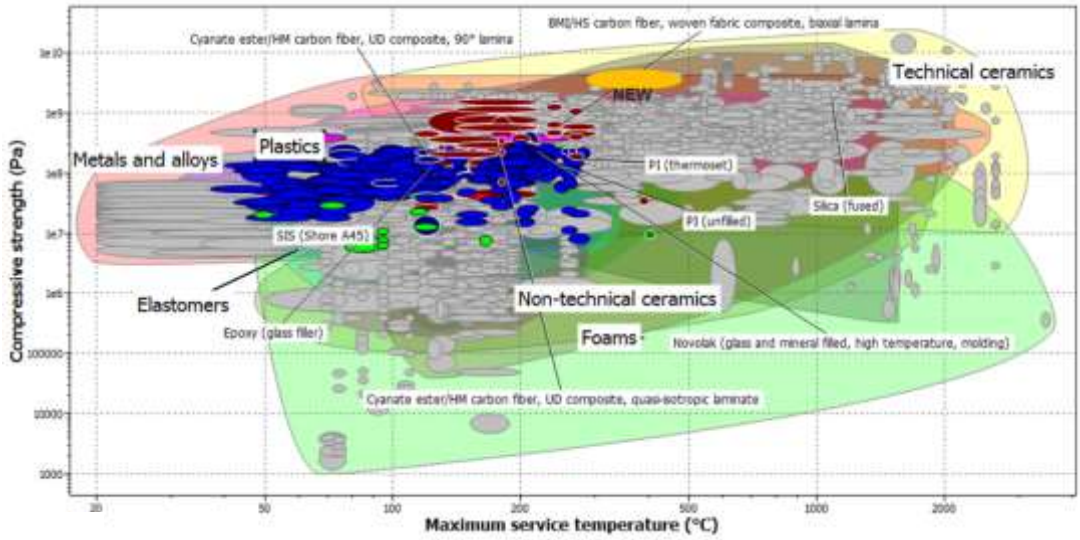

Figure 1- 1 Strength comparison between ceramics and polymers

Today, the requirements for high temperature operations have made it almost impossible for most commercial polymeric molding compound to survive harsh conditions such as that during oil drilling where temperatures can exceed 300°C in extremely deep wells. A huge demand for polymers exists (as shown in Figure 1-1) in the "new" region for high temperature materials where today's state-of-the-art epoxy cannot fulfill. Nevertheless, more than 99% of microelectronics devices are encapsulated in polymers [18] as they can easily be dispensed using the transfer molding or compression molding process. Other encapsulation methods involve using metal or ceramic lids to cover the chip on the substrate. However, more heat treatments are needed in these healing steps such as laser heating in metal welding [19-20] or high temperature bonding [21] in ceramic lid bonding.

Multichip modules (MCM) and hybrid microcircuits (HMC) manufacturing companies want inexpensive and solutions that can easily be integrated for suitable protection of their packages, especially when most of these packages are larger than standard ICs and thus harder to package [22]. Stringent requirements also exist for potting purposes on board level where components such as resistors and electrolytic capacitors also require good polymeric encapsulant as these components cannot survive hot sealing methods.

PN is a good heterocyclic polymer which has not been studied as an electronic encapsulant up to now. This material has high mechanical strength and possesses fire retarding properties. Hence, the glass fibre composite variant of the polymer has been approved for use in US submarines under stringent fire toxicity specifications of STD-MIL-2031. Figure 1-2 shows the various demands on a new packaging polymer material which has to be carefully considered for numerous industrial purposes.

1.2 Objectives and Scope of this research

The overall objective of this thesis is to explore the potential applications of PN encapsulation due to its exceptional thermomechanical properties, rendering it highly suitable for the niche High Temperature Harsh Environment (HTHE) market today. The three specific objectives are listed and further elaborated as below.

Figure 1- 2 Desired features of encapsulation material designed for HTHE operations

1. To develop an understanding of PN-based composites for high temperature electronics encapsulation through curing kinetics and bond relationship studies

The thermal stability is first explored in terms of post curing conditions and varied filler contents. Two main types of widely used fillers, namely alumina and silica, are evaluated in this study. Curing kinetics through the use of Kissinger's equations and degradation studies are implemented systematically to support the hypothesis made on the thermal characteristics which might in turn affect composite material performances under HTHE. Fourier Transform Infrared spectroscopy is used to identify potential new bonds formed between PN polymer components upon high temperature curing while Density Functional Theory (DFT) simulation techniques are used to verify the possibilities of such bond formation based on the theory of thermodynamic stability. This directly correlates to the crosslinking of polymer which influences the glass transition temperature.

2. To develop an understanding of the mechanical and electrical behaviors, and

moisture effect of polymer-filler composite through various characterization techniques. The encapsulation process parameters are optimized to suit standard commercial ceramic dual in line package (DIP). The encapsulation material is characterized by Field Emission Scanning Electron Microscopy (FESEM), Thermogravimetric Analyser (TGA), Thermo-mechanical Analyser (TMA), Dynamic Mechanical Analyser (DMA), nanoindentation and universal mechanical tester. Properties such as Coefficient of Thermal Expansion (CTE), tensile, compressive and flexural modulus and strength, and dielectric modulus are studied and compared with standard epoxy molding compounds. Moisture induced changes in mechanical performances will also be studied to understand the application of PN as an encapsulant.

3. To integrate PN as a die attach or encapsulant material and study the effects of fillers, bond stack and thermal ageing on its properties and test its performance in HPHT environment

The shear strength of three different bond stacks (alumina/alumina, alumina/silicon, silicon/silicon) are evaluated. Encapsulation morphologies are observed through optical or SEM imaging and discussed with respect to bond shear strength. It is essential to study the effects of fillers used in encapsulation materials as the encapsulant is placed in direct contact with the chip. An investigation into the material performance under HPHT environment is carried out and a redesign of the material in the form of glob top (dome encapsulant) is proposed with modelling performed in ANSYS^{TM} simulation. Lastly, the hermeticity of PN is also evaluated.

1.3 Dissertation Overview

This thesis is organized into 5 main chapters.
Chapter 1 introduces the HTHE market and the areas of focus for ruggedized applications. It also reveals the market demands which shape the development of this research on existing ruggedized electronics.

Chapter 2 reviews past literatures of interest pertaining to the work including high temperature resistant polymer encapsulation, preparation and properties, fundamentals of the packaging process in high temperature packages and acts as an introduction to filler

effects in composite encapsulation development. Detailed discussions on the development of HT encapsulation and its integration with existing systems of microelectronics packaging are provided.

Chapter 3 reports the synthesis methodologies adopted and the fabrication of filled PN composites. Detailed test methods are provided for each type of testing adopted. The test aims to characterize and evaluate the use of PN as both neat and filled materials such that these properties can be further correlated to their mechanical properties and behavior in later chapters.

Chapter 4 identifies PN to be a suitable candidate for high temperature encapsulation material. This chapter studies the thermomechanical behavior of PN both as a neat material and when fillers such as silica and alumina are added. Hypothesis on the factors related to the superior thermal properties are proposed and supported by systematic thermal investigations. Alongside are measurements which are conducted using FTIR to identify the possible bond formations. These are then verified using Gaussian09 DFT calculations.

Chapter 5 discusses the change in mechanical properties as PN goes from neat to samples filled with 50 weight percent of alumina or 50 weight percent of silica. Properties such as moisture adsorption which are of importance to mechanical changes of PN as encapsulation and packaging material are discussed. The moisture absorption behavior of PN in terms of diffusion behavior is discussed in detail.

Chapter 6 provides an overview to the integration of PN as a bonding material and subsequently as an encapsulant material. This chapter first discusses the adaptation of Resorcinol based phthalonitrile (RPh) as a bonding material with respective to the effects of fillers, bond stacks and thermal ageing. Experiments which feature the use of such encapsulated packages are evaluated both in High Pressure (HP) and High Pressure High Temperature (HPHT) environment applications while integrated onto existing commercial DIP packages.

Chapter 7 concludes the findings and addresses the extent to which the hypothesis is proven and the possible future works related to PN as the matrix material.

1.4 Findings and Outcomes/Originality

This thesis provides a first study and demonstration on the usage of resorcinol based PN (PN) as the matrix for electronics package encapsulation, and potentially as a die attach material (DA). Thermal studies established that stage curing not only helps to cross link existing molecules but also helps to form covalent bonds between silica and alumina to the existing polymer molecules resulting in a high strength molecular network. The compressive strength of neat PN is shown to be much higher than neat epoxy, and retain its mechanical properties in temperature regimes of 250°C and beyond. Hence, it is a suitable polymer matrix candidate for many varied forms of encapsulant, potting compound or as a die attach material.

Encapsulants using alumina or silica filler additions with the neat PN matrix to enhance strength and to negate thermal mismatches is made possible through melting and a flow process to integrate PN with the micron size fillers. The research also shows that PN's thermomechanical and electrical properties can be varied to suit different functions and optimize the properties according to its functions. Accelerated experiments such as 85%RH/85°C (JEDEC MSL 1 conditions) are conducted to demonstrate possible long term effects on PN. The last section of the thesis demonstrates the evaluation of PN as a die attach material and encapsulant which can be incorporated with various substrates to form a more robust package.

References

[1] M. R. Werner and W. R. Fahrner, "Review on materials, microsensors, systems and devices for high-temperature and harsh-environment applications," *IEEE Trans. Ind. Electron.*, vol. 48, no. 2, pp. 249–257, Apr. 2001.

[2] E. H. Amalu, N. N. Ekere, and R. S. Bhatti, "High temperature electronics: R & D challenges and trends in materials, packaging and interconnection technology," in *2nd International Conference on Adaptive Science Technology, 2009. ICAST 2009*, 2009, pp. 146–153.

[3] H. H. Yuan *et al.*, "Extreme high pressure and high temperature package development," in *Electronics Packaging Technology Conference (EPTC 2013), 2013 IEEE 15th*, 2013, pp. 379–383.

[4] M. Ohadi and J. Qi, “Thermal management of harsh-environment electronics,” in *Twentieth Annual IEEE Semiconductor Thermal Measurement and Management Symposium, 2004*, 2004, pp. 231–240.

[5] H. H. Yuan *et al.*, “Extreme high pressure and high temperature package development,” in *Electronics Packaging Technology Conference (EPTC 2013), 2013 IEEE 15th*, 2013, pp. 379–383.

[6] U. Scheuermann, “Reliability challenges of automotive power electronics,” *Microelectron. Reliab.*, vol. 49, no. 9–11, pp. 1319–1325, Sep. 2009.

[7] P. Lall, M. N. Islam, J. Evans, J. C. Suhling, and T. Shete, “Damage mechanics of electronics on metal-backed substrates in harsh environments,” *IEEE Trans. Compon. Packag. Technol.*, vol. 29, no. 1, pp. 204–212, Mar. 2006.

[8] B. M. Auguste, L. Pascal, G. Annabelle, and F. Helene, “Influence of Technological Parameters on the Behavior during Aging at High Temperature of Various Packages, in the Automotive Environment,” in *Physical and Failure Analysis of Integrated Circuits, 2007. IPFA 2007. 14th International Symposium on the*, 2007, p. .

[9] A. A. Shapiro, J. K. Bonner, O. A. Ogunseitan, J.-D. M. Saphores, and J. M. Schoenung, “Implications of Pb-free microelectronics assembly in aerospace applications,” *IEEE Trans. Compon. Packag. Technol.*, vol. 29, no. 1, pp. 60–70, Mar. 2006.

[10] J. Guofeng Bai, J. Yin, Z. Zhang, G.-Q. Lu, and J. D. van Wyk, “High-Temperature Operation of SiC Power Devices by Low-Temperature Sintered Silver Die-Attachment,” *IEEE Trans. Adv. Packag.*, vol. 30, no. 3, pp. 506–510, Aug. 2007.

[11] R. Pommer, “Challenges in aerospace packaging,” in *2013 IEEE Avionics, Fiber-Optics and Photonics Conference (AVFOP)*, 2013, pp. 77–78.

[12] “High-Pressure, High-Temperature Well Logging, Perforating and Testing (Oilfield Review), Schlumberger.” [Online]. Available: http://www.slb.com/resources/publications/industry_articles/oilfield_review/1998/or1998sum04_hpht_welllogging.aspx. [Accessed: 09-Sep-2011].

[13] P. Hagler, P. Henson, and R. W. Johnson, “Packaging Technology for Electronic Applications in Harsh High-Temperature Environments,” *IEEE Trans. Ind. Electron.*, vol. 58, no. 7, pp. 2673–2682, Jul. 2011.

[14] “Hot, Harsh, and Hostile | ECN: Electronic Component News.” [Online]. Available: http://www.ecnmag.com/Articles/2011/01/App-Solutions/Hot-Harsh-and-Hostile/. [Accessed: 09-Sep-2011].

[15] H. H. Yuan, H. Kuruveettil, E. W. L. Ching, E. P. J. Rong, G. C. Lip, and D. R. M. Woo, "Development of ruggedized timer and temperature sensor packaging for 300 °C 30kpsi downhole environment," in *Electronics Packaging Technology Conference (EPTC), 2014 IEEE 16th*, 2014, pp. 606–610.

[16] E. P. J. Rong *et al.*, "Electronic packages for high pressure applications: A dome-shaped cavity design," in *Electronic Components and Technology Conference (ECTC), 2013 IEEE 63rd*, 2013, pp. 2342–2348.

[17] "Definition of High Pressure and High Temperature Wells (HPHT Wells)," *IADC Lexicon*.

[18] H. Ardebili and M. Pecht, *Encapsulation Technologies for Electronic Applications*. William Andrew, 2009.

[19] T. A. Mai and A. C. Spowage, "Characterisation of dissimilar joints in laser welding of steel–kovar, copper–steel and copper–aluminium," *Mater. Sci. Eng. A*, vol. 374, no. 1–2, pp. 224–233, Jun. 2004.

[20] B. S. Yilbas, A. F. M. Arif, and B. J. Abdul Aleem, "Laser welding of low carbon steel and thermal stress analysis," *Opt. Laser Technol.*, vol. 42, no. 5, pp. 760–768, Jul. 2010.

[21] R. Gordon and J. G. Ciallella, "Ceramic lid assembly for hermetic sealing of a semiconductor chip," US4291815 A, 29-Sep-1981.

[22] P.K. Khanna, S.K. Bhatnagar, and W. Gust, "Analysis of packaging and sealing techniques for microelectronic modules and recent advancesnull," *Microelectron. Int.*, vol. 16, no. 2, pp. 8–12, Aug. 1999.

Chapter 2

Literature review

In this chapter, a review of current high temperature electronics market demands is provided in the perspective of high temperature harsh environment (HTHE). Electronics which are made to survive in such environment are generically branded as ruggedized electronics. A myriad of materials has existed to cater for such high temperature applications but most of them come at a high cost or involve highly sophisticated processes that demand greatly on resources, money and time. This study aims to introduce a new type of polymer which could gain popularity in the coming years with increasing demand in high temperature electronics. Traditional high temperature polymers unable to survive more than 250°C but have since changed with new findings in polymer science. Various high temperature thermosets will be introduced and a new variant, phthalonitrile will be discussed in detail. Its potential applications in HTHE electronics with filler modified characteristics are further touched upon in this chapter.

2.1 Overview of microelectronics packaging for high temperature harsh environment (HTHE) applications

Microelectronics packaging typically refers to protective enclosures which are made to shield sensitive parts such as integrated circuit chips. Such protection is necessary against external agents which might cause mechanical damage or degradation brought forth from environmental exposure such as moisture.

Figure 2-1 shows a cross sectional schematic of a leaded test package. For environmental demanding applications, features such as wire bonds, leads, solders, die attach (DA) materials and encapsulation could all be enhanced with better materials to suit their functions such as those in HTHE microelectronic packages. Cressler *et al.* have recently published a review on materials for extreme high temperature packages [1] and the reliability of such materials.

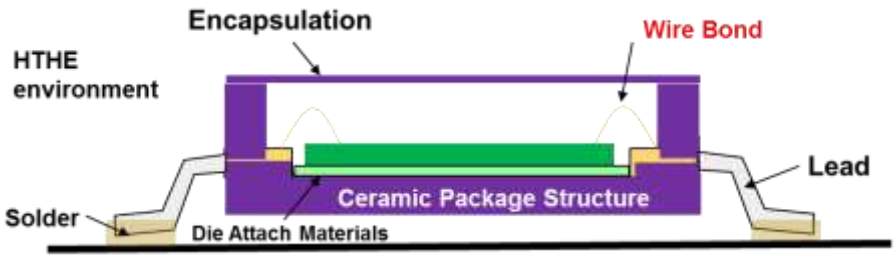

Figure 2- 1 Ruggedized package for HPHT

Traditional methods of packaging for high temperature electronics use ceramic packages made from aluminium oxide (Al_2O_3) or aluminium nitride (AlN), and fabricated with metallization using Low Temperature Co-fired Ceramic (LTCC) [2-5] or High Temperature Co-fired Ceramic (HTCC) [6] processes. The LTCC/HTCC packaging processes involve many hours of sintering at high temperatures. Even for LTCC processes, temperature of 800°C is commonly used. For HTCC, temperatures exceeding 1000°C is required. Sealing of ceramic packages also requires use of metallic bonding or glass frit sealing techniques. This increases the time required for high temperature encapsulation although such sealing techniques produce packages which are hermetic and is sometimes necessary for Microelectromechanical (MEM) devices. This encapsulation process is critical as it may lead to points of weakness [7] if not optimized properly and the package would fail readily when placed under high environmental stress. High

temperature glass frit sealing requires melting temperature above 400°C [7, 8] and may not be suitable for all devices.

Greater economies of scale can be achieved through the use of polymer packaging which has been widely adopted since the 1970s [9] to protect integrated circuits against environmental induced deterioration, such as those arising from contact with air and moisture [32]. The challenge however is that even when high temperature polymers are used. They rarely last beyond 300°C which is currently a common operation temperature in adverse environmental applications such as deep subsea drilling and for packaging high power devices [11].

Historically, silicone was the first adopted mold material which has been widely used for encapsulation. Epoxy was subsequently produced in Europe and USA in the early 1930s and is largely a cheap thermoset that became popular in the 1970s. Epoxy has a myriad of advantages such as excellent properties of mechanical strength , adhesion and reliability [9] and a host of dispensing methodologies has been developed such as mold transfer, resin transfer moulding (RTM) with a choice of vacuum assist, and also fast curing recipes. The earlier epoxies contain hydrolyzable chloride [9] in 1000 ppm levels which is undesirable as aluminium, the earlier commonly adopted wirebond metal is easily corroded by halogens. With epoxy, it is also possible to achieve volume resistivity of more than 10^{12} Ω-cm to prevent possible parasitic effects between package leads [9].

Since its inception, a huge understanding has been collected on epoxy molding compounds (EMC) in the aspects of compatible release agents and suitable accelerators to obtain better gelation times were developed. Despite much research and modifications to the matrix over the years, it has not been completely successful to make epoxy capable of high temperature performance above 250°C while having compatible properties to underlying ceramic materials and silicon. Thermal mismatch between the encapsulation and the substrate/die is usually a concern during integration. High temperature resistance requires the use of materials such as Bromine (Br) and Antimony oxide ($Sb_2O_{3)}$ containing fire retardants which act to inhibit the flame propagation through the formation of antimony halides [12]. Pigments are often used to provide opacity. For molding processes, the epoxy used typically comes in pellet preforms ready to be heated and pressed into its final form. This is a complex mixture of accelerators, retardants,

release, fillers and main matrix materials. Conventional epoxy has a T_g just over 100°C and heavy modifications are needed to ensure that the matrix survives to temperatures beyond 200°C. Most filled epoxy molding compounds have a CTE ranging between 40-60 ppm/°C and a viscosity less than 5 Pa.s. However, thermal mismatch with a variation of substrates is a perpetual challenge. A large mismatch generates high mechanical stress during thermal transitions and makes such materials unfit for harsh environment operations [13, 14]. Table 2-1 shows a generic list of material CTEs for common packaging materials.

Table 2- 1 Coefficient of thermal expansion of typical packaging materials

Material	CTE (ppm/°C)
Aluminum Nitride	4.6
Alumina	6-7
Silicon	2.6
Epoxy	40-60
General polymers	50-200

PN is a heterocyclic thermoset material which is able to withstand temperatures of up to 600°C if adequately cross-linked at higher temperatures in an inert environment. Once cured, the material is able to resist high temperature and high mechanical pressures of up to 207 MPa, analogous to the high mechanical pressure which is experienced by drill tools during deep sub-sea oil drilling. Although the packages are typically protected within a Dewar flask, partial or full exposure is required for the package to assist in detection and to feedback real time parameters such as environmental pressure.. A tough encapsulation is thus necessary to protect the semiconductor chips encased within the package. The use of PN helps to fulfill the high structural strength requirements of such packages for HPHT applications utilizing simple curing profiles which cures the polymer providing coverage to package cavity and the chips. The temperature required in such curing is still lower compared to most glass frit curing processes. To obtain a high temperature resistance of 300°C, glass frit has to be treated to 430°C [15] whereas PN only needs to be cured to 360°C to achieve the high mechanical performance at a much lower cost if hermeticity is not a concern.

In the field of logging while drilling, working temperatures has seen an increase to 175°C

[16]. With reference to Figure 2-2, Schlumberger highlighted that plastic encapsulated electronics have evolved to ceramic type gradually as the operational temperatures climb to 175°C and above. Ever more stringent conditions are seen in locations such as Mexico, Australia, Malaysia and Indonesia, where bottom hole pressures have increased to above 207 MPa and temperatures rising above 300°C.

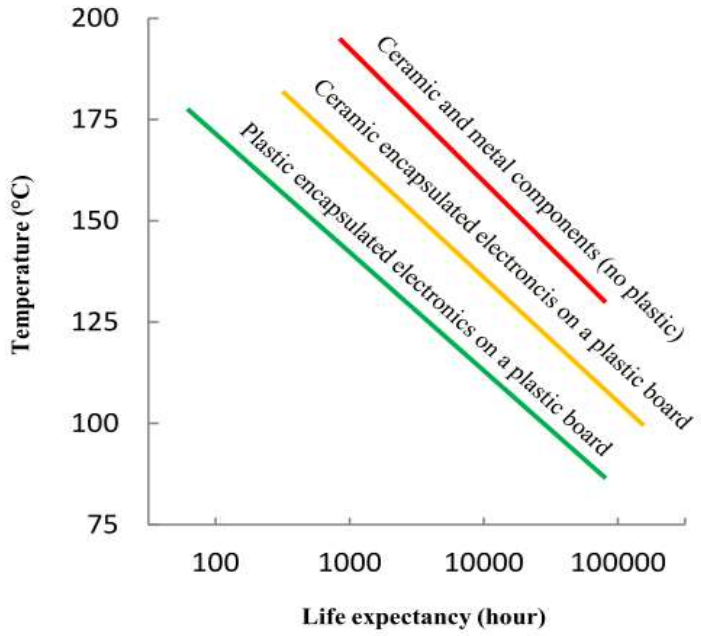

Figure 2- 2 Life expectancy of devices [16]

The average life expectancy of a device drops by about 10 times from 1000 hr to 100 hr when the working temperature increases from 150°C to 175°C [17]. Besides the widely used epoxy polymeric encapsulation, the option for hermeticity is also widely considered, especially when there is a requirement for placement of sensors within the package.

For HPHT applications, the most commonly used materials for electronic packaging are ceramic alumina and aluminum nitride. Because alumina nitride has a high thermal conductivity, its use in a high temperature environment as packaging material are restrained to prevent heat flow from the external environment into the chips or sensors. Hence alumina (96%) is more frequently used in the form of substrates and packaging.

2.2 Types of encapsulation materials

Electronic package encapsulants are materials that protect microelectronic devices (such

as chips) and interconnections (such as wire bonds and solder bumps) from environmental exposure which may lead to the package or device degradation. These factors include moisture, corrosion-inducing contaminants, and ultraviolet radiation. Adequate structural robustness is also required for packages to be exposed to structurally demanding applications.

In general, existing encapsulations can be divided into: hermetic and non-hermetic types. Traditionally, epoxy molding compound (EMC) contains a high amount of fillers (55%-70%)[18] and dominates about 97% of the global chip packaging market. To enhance the properties of EMC, additives such as flame retardants [19], plasticizers, catalysts and mold releases are added. Antimony oxide flame retardants [18] has been phased out due to environmental concerns. Appropriate fillers help to improve the thermal resistance and moisture resistance. It also changes the mechanical properties such as CTE.

Various other alternatives to EMCs for high temperature applications are investigated and some have already been put into industrial applications, such as BMI and cyanate esters [20]. With PN however, additives such as fire retardants are no longer required. PN by itself possess flame retarding properties, thus rendering it the only material approved for use as bulk composite in the US navy that meets MIL-STD-2031[21] specifications for fire toxicity. Most polymer systems with the exception of hybrid polymer systems, do not operate at temperatures over 300°C for extended durations as they gradually lose their mechanical strength. New hybrid polymer systems despite having high curing temperatures of 300°C or 500°C [22-24] and being able to operate to high temperatures have fairly complex processing. A further treatise is provided to show the high suitability of PN in the context of high temperature (HT) microelectronics packaging with special operations under extremely high mechanical stress.

2.3 High temperature thermosets for microelectronics packaging

Table 2-2 shows the comparison of high temperature polymer systems with epoxy that are currently available on the market. Most of these polymers are usually modified with fillers added to the matrix at high percentage loadings. The advantages and disadvantages of each system would be explained in the following sections.

Table 2- 2 Properties of various polymeric encapsulations [25]

Property	Epoxy	Phenolic	Toughened BMI	Cyanate ester
Density (g/cm$^{3)}$	1.2-2.5	1.24-1.32	1.2-1.3	1.1-1.35
Use temperature (°C)	RT-180	200-250	~200	~200
Tensile modulus (MPa)	3.1 - 3.8	3.1 - 5	3.4 - 4.1	3.1 - 3.4
Dielectric constant (1 MHz)	3.8 - 4.5	4.3 - 5.4	3.4 - 3.7	2.7 - 3.2
Cure temperature (°C)	RT-180	150 - 190	220 - 300	180 - 250
Mold shrinkage (mm/mm)	0.0006	0.002	0.007	0.004
TGA onset (°C)	260-340	300-360	360-400	400-420

2.3.1 Epoxy Molding Compounds (EMCs)

Epoxy resins are polyether resins containing more than one epoxy group. The epoxy group, otherwise known as oxirane, is bounded by separate bonds as shown in Figure 2-3 where the triangular functional group is fringed by four R groups that may vary greatly.

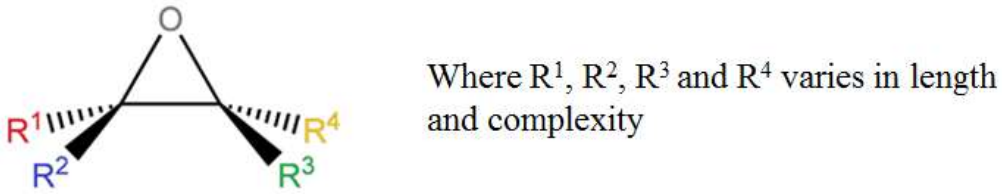

Figure 2- 3 Epoxy functional group with different R groups attached as side groups

Most encapsulants are based on epoxy with cresol novolac or phenol novalac [25,26], where cresol novalac is known to have better processability under melting compared to phenolic due to the presence of methyl groups which reduce the rate of reaction between epoxy and phenol [49].

Pre-cured epoxy resins can exist in various forms, ranging from low viscosity liquids to pre-form solids. To keep the viscosity low, most novalac epoxies are kept to a degree of polymerization of 5 [27]. Many methods such as ultraviolet (UV) or heat cure can be

employed to cure epoxy which is another added desirability of using epoxy based products. Epoxy has excellent properties such as good adhesion to most surfaces, toughness, chemical resistance to many dilute solvents, and low shrinkage. Moreover, fillers can easily be added to epoxies to tune their properties [29-31]. Commercially, an economy of scale has already been established for epoxies which is unparalleled and its use has been pervasive, ranging from industrial coatings to industrial adhesives.

The use of epoxies however is highly dependent on high mixing ratios of fillers and additives to tweak its engineering properties. It is well known that neat epoxy encapsulant used in most packaging industries does not fulfil all requirements of electronic applications. Neat epoxies encounter low thermal conductivity, brittleness, high thermal coefficient expansion (CTE) which generates high amount of thermal stresses between thermal cycles [32,33]. Hence, epoxies have limited potential for future development due to its temperature usage limits. Table 2-3 shows the generic properties of a commercially available epoxy.

Table 2- 3 Properties of generic commercially available epoxy [35]

Properties	Values
Glass transition temperature (Tg)	120 - 130 °C
Tensile strength	85 MPa
Tensile Modulus	2470 MPa
Elongation at break	0.8%
Flexural strength	112 MPa
Flexural Modulus	2470 MPa
Compressive Strength	190 MPa
Compressive Modulus	2470 MPa
Thermal Decomposition	350° C

Therefore, in order to improve its properties, epoxy can be loaded with fillers such as silica or alumina to improve the thermal expansion and conductivity properties [34,35].

Hence, in this work, the evaluation of PN is also completed by taking into consideration the effects of fillers which are commonly used in other thermoset matrixes such as silica and alumina.

Fire retardancy [36] is generally imparted into epoxies with the addition of bromine (6-13%) but has in modern times been replaced with chemicals such as phosphorus (at 1.1%) based compounds instead [37] where long sides chains such as 9,10-dihydro-9-oxa-10-phosphaphenanathrene 10-oxide (DOPO)[38-43] and 10-chloro-9,10-dihydro-9-oxa-10-phosphaphenanthrene (DOP-Cl) [37] are also utilized to increase Tg of the epoxies. This helps the epoxies to pass the UL-94 requirement (USA Standards for Safety of Flammability of Plastic materials for Parts in Devices and Appliances testing). UV cured epoxy resins[14,44] are also developed to simplify curing processes.
Epoxies are heavily customized since its creation for microelectronics packaging to reduce moisture absorption. Moisture absorption can range from 0.5% to 3%[45] as reported. This is highly favorable to reduce popping effect of polymer matrix composites (PMCs) at high temperatures.

2.3.2 Bismaleimides (BMI)

Figure 2-4 shows a typical bismaleimide structural formula with a centre variable R group. Bismaleimide (BMI)[46,47] , a promising form of polyimides, is highly popular in microelectronics packaging. With a suitable amount of additives, thermal stability, low water absorption and retention of mechanical properties can be achieved even at elevated temperature. Unlike polyimides, the moisture absorption of BMI is reportedly lower and hence is a more suitable material for microelectronics packaging and is often mixed with epoxy for printed circuit board (PCB) fabrication. However, there are reports which claim an increase in moisture diffusion at an operational temperature of 70°C which raises concern for its use as a standalone material [48].

In addition, BMI has low curing temperature and does not produce by-products during curing. As compared to epoxy, the imide linking groups in BMI yield higher polymer backbone stiffness. Moreover, it has better thermal and hydrolytic resistance due to its greater crosslinking density [49]. Conversely, their brittleness and high dielectric constant

may limit their applications.

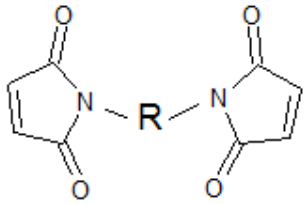

Figure 2- 4 Bismaleimide structural formula where R represents the benzene structure

Reports have also been made about the behavior of BMI moisture absorption which is closer to that of non-Fickian behavior [48]. This is important when the polymer is used in highly humid environmental conditions.

Polyimide thermosetting resins have been used in high temperature regimes exceeding 300°C, its usage is not wide as higher temperature tolerances couples with high mechanical strength are required for microelectronic packaging application particularly for oil drilling [50]. It is known that highly aromatic and heterocyclic rings polymer structures such as that in BMI can help to provide thermal stable structures. These cyclic rings limit the freedom of rotation in the polymer chains, thus resulting in better resistance to deformation, yielding higher glass transition temperatures (T_g) and melting points [51]. However, the presence of these aromatic rings tends to make the polymer to be brittle. Hence, flexible linkages are introduced into the polymeric backbone to provide flexible units while retaining the excellent thermal properties. Phthalonitrile resins behave similarly and has similar thermomechanical properties [50].

2.3.3 Cyanate Esters

Cyanate esters have been established as a substitute for both epoxies and bismaleimide products since the 1980s. The general formula of a cyanate ester is shown in Figure 2-5. It has glass transition temperatures between 190°C to 290°C with better toughness compared to both epoxies and bismaleimide. Cyanate esters are reported to possess excellent adhesion as a coating on metals at temperatures up to 250°C [52]. It is also comparable in terms of costs with bismaleimide although both materials are approximately twice the price of high temperature epoxies [52]. The Young modulus of cyanate ester is comparable to both epoxies and BMI. However, when cyanate esters are

blended with other monomers and prepolymers with more than 35% cyanate ester, it is prone to crystallization [52]. Cyanate ester mechanical properties may also be affected depending on the degree of trimerization. It has been shown that cyanate esters blended with alumina or quartz fillers could be a good encapsulation material as reported by Chidambaram *et al* [53].

Figure 2- 5 Structural formula of cyanate ester monomers

2.3.4 Novel polymers/blends/hybrids

Various mixtures of polymers have been combined to create intertwined materials with enhanced properties. A hybrid polymer can be a chemical combination of polymeric materials, a blend of polymers, or an interpenetrating network and these has been widely documented in the past. High performance combinations include BMI/cyanate containing hybrids [54,55], BMI/epoxy hybrids [56], epoxy containing hybrids [57][39]. BT is a class of polymers otherwise known as bismaleimide-triazine[58] resin, which is already available in the market as a PCB material. It can be mixed with polysiloxane [58] and post cured to high temperatures of 240°C and above. Heng Huo *et al.* [59] reported that a blended composition of glass composites, phthalonitrile and epoxy resin has higher glass transition temperature (T_g), and better thermal and oxidative stabilities. This is due to the increase in cross-linking. The research by Dominguez *et al* also showed similar results, whereby the degradation temperatures of phthalonitrile-epoxy polymer blends improved with or without curing additives [60].

A class of low viscosity silane-curing organic polymers which heat up to produce ceramics is gaining popularity where the first synthesis of such materials, such as polycarborane-siloxane-acetylene, dates back to twenty years ago [61]. Such materials are suitable for high temperature applications from 500°C to 1500°C and are reportedly easy to process [24][62] as most of them are either liquids at room temperature or low temperature melting solids. This new class of polymers largely comprises material from both the organic and inorganic groups. More complex hybrid polymers in recent times

also involve the use of polycarborane-siloxane-acetylene [79] and has been widely discussed by Keller *et al.* [61,63]. The cost of producing these hybrid materials however is still significantly higher than that of epoxy, bismaleimide or cyanate ester.

2.3.5 Novel Resorcinol Phthalonitrile (PN) based polymers

Phthalonitrile based polymers have not been characterized comprehensively as an microelectronics packaging material despite the postulation that it can be utilized by Keller *et al* [64]. The most commonly used encapsulation utilizes epoxy materials with a variation of curing agents, inert fillers, flame retardants, stress relief or coupling agents, mold release and colorants. However, PN and its variations do not require the use of flame retardants as the material is already a combustion inhibitor. Neither does it require the use of coloring agents as PN has a natural dark green coloration. Silicone mold release which is routinely used on epoxy does not work on PN. As such specialized molds and coatings are required when working with PN.

Modifiers and fillers can be added to PN to decrease the treatment temperature and to improve the CTE mismatch for it to be applied effectively in the field of microelectronic packaging, especially in applications involving high temperature coupled to high mechanical stresses.

The stringent and extreme operating environment has motivated the search of alternative or novel materials vital for electronic operations. Numerous electronic applications engage high temperature packaging to increase survivability under harsh conditions. In addition, endurance to high pressure is also essential in concurrently demanding operations such as subsea drilling, geothermal energy tapping and offshore marine studies. Such novel materials developed are typically also viable in high temperature environments such as that in aerospace and automotive applications.

The advancement in subsea drilling technology has pushed the exploration of electronic materials suitable to sensing and real time monitoring at operation temperatures exceeding 300°C and 207 MPa (30 kPsi). In tandem with the search for such advanced materials, other factors are also considered such as coefficient of thermal expansion (CTE) which should inherently matches with silicon and substrate materials such as

alumina that are commonly used in high temperature packaging. Inherently, material data such as compressive modulus provide important insights of the material's capability to survive in high pressure operations and thus have to be evaluated. PN has been evaluated in the literature research to be the best candidate for such adverse environment operations for electronics.

Phthalonitrile (PN), which is a high temperature thermoset adept of tolerating temperatures beyond 300°C, is the next generation of encapsulation materials both for niche packaging and for more industrial scale packaging.

Phthalonitrile (PN) based polymer can take on both forms of solid preforms or liquid resins depending on the processing variables such as the type of catalysts chosen and the solvents such as Tetrahydrofuran (THF) or Dimethyl sulfoxide (DMSO), which are used to prepare the monomer form of PN. The PN polymer has a high curing temperature and could produce, derivatives of:

1) Triazine: Produces greatly cross-linked ring structures and possibly bubble free formation [[65-67]. The cross-linking density increases with further post curing at high temperatures and for longer durations, resulting in increase in storage modulus [67].

2) Phthalocyanine: trimer based ABAB network of phthalocyanines resulting in prevalent cross linking branches. High temperature cyclotetramerization of phthalonitrile functional groups produce phthalocyanine structures with superior thermo-oxidative and mechanical properties.

3) Isoindolenine: The products which exist in minute quantities in PN

With increased crosslinking densities in polytriazine, polyphthalocyanine and polyisoindolenine, chain motions become more restricted, leading to much stronger and stiffer macromolecules [85].

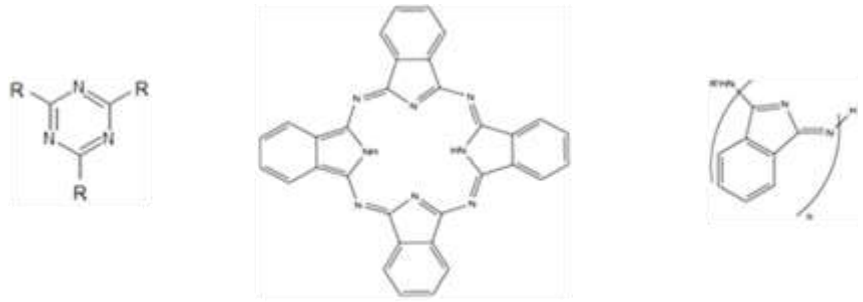

Triazine Phthalocyanine Isoindolenine

Figure 2- 6 Main structures of PN [69]

Initially, Keller and Griffith proposed activated copper as the catalyst of phthalocyanine formation from phthalonitrile resin, as described in Figure 2-5 [68]. On the other hand, Tomoda *et al.* suggested alkoxide to catalyze the formation of phthalocyanine, where the alkoxide anion could nucleophilic attack C≡N groups to form a 1-alkoxy-3-iminoisoindolenine intermediate.

This intermediate leads to the formation of phthalocyanine, as shown in Figure 2-7 [69].

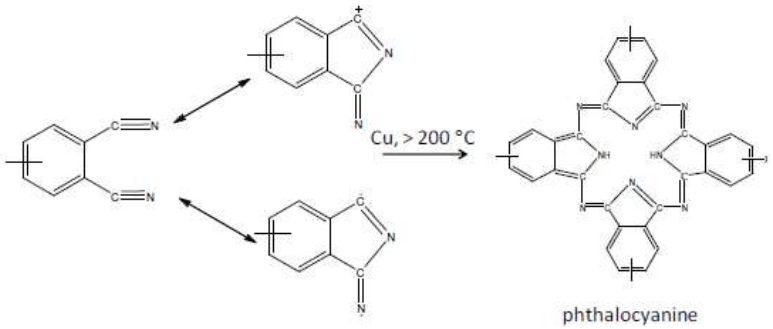

Figure 2- 7 Proposed reaction for the formation of phthalocyanine [70]

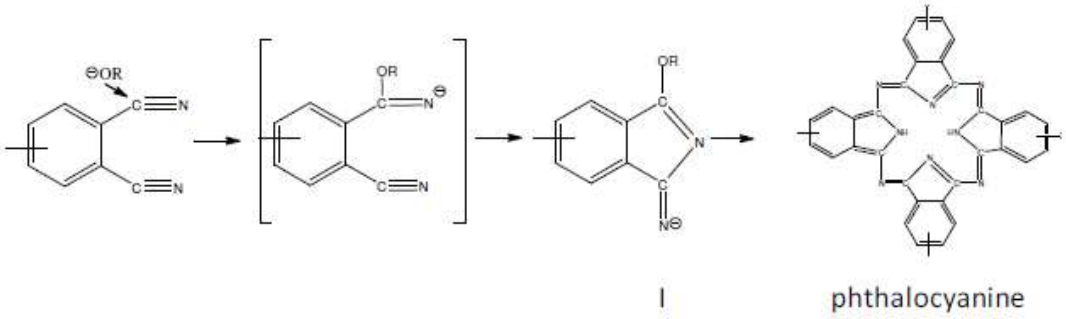

Figure 2- 8 Proposed reaction for the formation of phthalocyanine [71]

In addition to phthalocyanine, triazine is another major product from the polymerization process. Based on the proposed reaction by Burchill, the formation of the amidine groups occurs via initial protonation of the cyano group nitrogen, followed by nucleophilic attack by free base at the carbon [88]. Cyclization took place when three organic cyano compounds were transformed into amidine, ultimately produced a triazine which led to

the formation of polytriazine, as described in Figure 2-9.

Condensation of suitable tetranitrile with aromatic diamine under appropriate conditions produced thermally stable polymers consisting of macrocyclic units. At high temperature cyclotetramerization of phthalonitrile functional groups produced phthalocyanine macrocycle structures with superior mechanical and oxidative properties compared to other high temperature resistant polymers discussed.

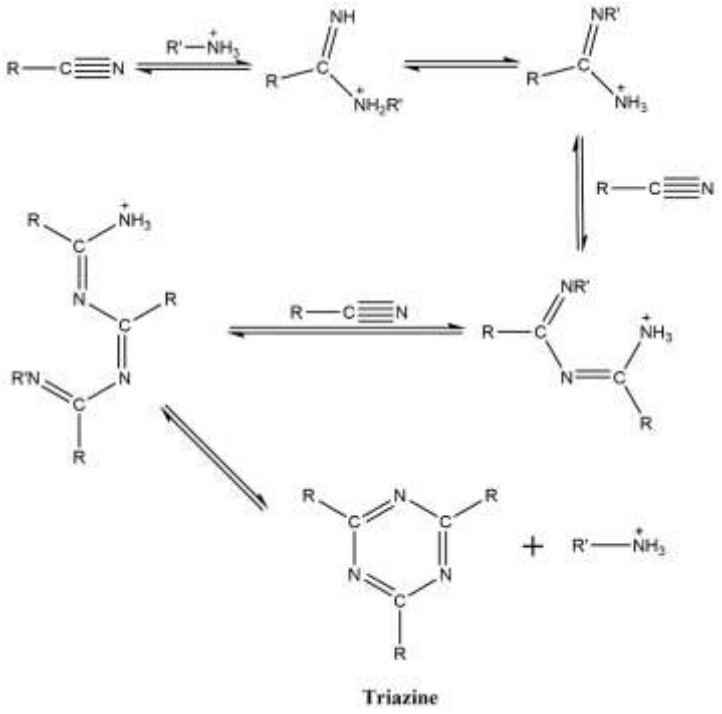

Figure 2- 9 Formation of triazine [68]

Different shaped components can be easily processed by heating the polymer to gelation, i.e. to heat to temperatures above its melting point and Tg [68]. Even when used without any additives or fillers, PN matrix shows good fire retardancy, and is superior to most thermoset-based composites. The cure mechanism of these systems leads to highly cross-linked and void-free network polymers, which could exhibit good mechanical properties, outstanding thermo-oxidative stabilities at elevated temperatures, superior fire resistance relative to other conventional polymers, and low water absorptivity [71].

By altering the terminal group of phthalonitrile, the compound may become more thermally stable due to its cross-linked structures [72], dissimilar to epoxy, which has a

linear architecture. Phthalonitrile has a dense network consisting of polymer units comprising of poly(triazine), poly(phthalocyanine) and poly(isoindolenine). This interpenetration network allows the polymer to be intra-bonded strongly, constituting to its advantageous high strength and thermal stability.

It is well known that high aromaticity in higher molecular weight polymers [73] provides the high resistance properties at temperatures of 300°C and above. In addition, flexible linkages are also required to complement high aromaticity to avoid the formation of brittle and intractable polymers. Most phthalonitriles predominantly exist in the high temperature melting zones, such as aromatic ether, imides, hexafluoropropylidene, sulfones, bisphenol A and aromatic ether phosphine oxide linkages incorporated amongst the terminal phthalonitrile units [22]. It is thus important to understand the influence of the fillers to matrix bonds and neat polymer matrix on the properties of packaging materials, especially in the aspects of high temperature microelectronics packaging. It is also imperative to determine if high temperature phthalonitrile would be adequate to withstand harsh environment conditions to complement or substitute epoxy systems for packaging applications.

Furthermore, it is crucial to note that the formation of polyimides through condensation polymerization would unfavorably produce water, which is highly undesirable because water aids corrosion of metal wires (such as Al, Ag, and Cu). Many PN systems are poor moisture absorbers and do not combust readily even under direct flames. A PEEK like liquid resin PN [75] has also recently been developed and can be melted at 70°C, but the processing temperature is much higher compared to the current PN but still a good alternative for molding and processing.

2.4 Fillers for microelectronics packaging

ASTM D-883 defines filler as inert materials included into plastics to modify its mechanical properties [27]. Mold compounds based on polymers have obvious constraints such as lower mechanical strength [94]. In order to improve the usage of epoxies and most other polymers, additions of particulate fillers of various nature help to produce better materials with more desirable properties. Physical modifications can be brought about through the use of plasticizers, fillers and lubricants whereas chemical

changes can be brought about through the use of heat stabilisers, antioxidants and fire retardants. The effects of fillers have been widely discussed and summarized in Table 2-4 from McGrath *et al* [77].

At micron size levels, most of the fillers help to provide mechanical strengthening through crack tip pinning, bowing, crack path deflection and crack bridging[78]. But this is not as valid once filler sizes go to nanometer scales[79].

In this thesis, fillers such as silica and alumina are selected and investigated in depth to be added to the PN matrix to improve its CTE and thermal properties. Moreover, in order to focus on the study of the influence of fillers on the matrix solely, no other surface treatments were provided to the fillers prior to mixing with the neat polymer.

Table 2- 4 Change in mechanical properties by fillers [97]

Change in filler property and/or test condition	Effect on modulus of elasticity	Effect on fracture toughness (K_{IC})	Effect on flexural strength
Increase in filler content	Increase	Increase	Limited to the matrix value
Increase in particle size	Constant	Slight decrease	Decrease
Increase in strength and modulus of filler	Increase	Increase	Increase
Improvement in adhesion	Constant	Increase	Decrease
Embedded in tougher matrix	Slight decrease	Increase	Decrease
Increase in rate of loading	Slight increase	Increase followed by plateau	Slight increase

2.4.1 Size and shape effect of fillers

Table 2-3 shows the filler properties where some of them are already widely used in microelectronics packaging, especially with epoxy as the matrix polymer [27]. This is done to both lower the cost and also to improve material properties.

Where fillers are added the Mooney equation is used to calculate the viscosity of the

system, whereby,

$$\ln \frac{\eta}{\eta 0} = \frac{K_e \Phi}{1 - \frac{\Phi}{\Phi_m}} \qquad \textbf{Equation 2-1}$$

Φ_m is the maximum packing fraction that can be achieved with ideal filler size distribution, K_e is the Einstein coefficient. Typically, it is possible to achieve only 60% of filler particles with a maximum loading of approximately 60vol % and 90vol% if a variation of filler sizes and shapes are utilized.

It has been proven scientifically that at micron size ranges, fillers do not have significant effects on polymers such as epoxies. As shown in Fu *et al*, [76] where silica particle additions have no effects on the Young's modulus to the epoxy matrix which it was added to. If the silica are angular shaped, the effect on modulus is marginal particularly between particle sizes of 2-47 µm.

In the context of alumina trihydrate additions [80], marginal changes to the tensile modulus is observed between 6.6 GPa to 7.4 GPa for particle sizes of 1-12 µm. And where the highest tensile modulus of 7.4 GPa is registered for particle sizes of 5 µm.

The impact on mechanical strength and rigidity however sets in when the size changes from micron to nanoscales. In the context of epoxy and spherical shaped silica, nano sized silica are reported to possess better mechanical characteristics [94]. For ranges between 20-80 nm, nano-silica is reported to have no size effect on fracture toughness or elastic modulus as reported by Liang *et al.* [81].

Dispersing such nano particles may become a challenge when the surface energies are high and the particles tend to stick together. Simpler methods which worked for micron size particles such as increasing mechanical shear forces through ultrasonic shaking and increased mechanical blending [82] might not work as well for such small particles. Such matters are raised more commonly amongst blending of carbon nanotubes with polymer to improve mechanical, electrical and thermal properties [82].

Table 2- 5 General filler properties [85, 86]

Filler Type	Epoxy	Boron Nitride	Silica	Alumina	Diamond
Density (g/cm^3)	1.19	2.25	2.2	3.98	3.5
Thermal Conductivity (W/m-K)	0.23	300	1.5	36	2000
CTE (µm/m °C)	75.18	< 0.5	0.5	6.6	0.8
Modulus (GPa)	2.3	43	74	385	1050
Poisson's Ratio	0.4	0.25	0.19	0.21	0.068
Filler Shape	-	Platelet	Spherical	Polygon	Polygon

Furthermore, improvements in the properties of polymer composites are not only determined by its concentration of fillers within the matrix but also governed by the filler particle size, shape and properties as well as the bonding strength with the polymer matrix [83]. Hence, non-spherical alumina, diamond and BN particles have better interactions among the filler particles than spherical filler particles since they have comparatively smaller contact areas between particles.

In this thesis, both alumina and silica fillers are investigated with focus on thermal conductivity, CTE and modulus, when they are loaded into resorcinol based phthalonitrile matrix. Addition of alumina and silica helps to strengthen the package mechanically yet does not drastically increase the rate of heat transfer as compared to AlN from external environments into the package. In addition, they are more cost-effective as compared to diamond. Boron nitride (BN) fillers were not selected due to its high viscous adhesive consistency. The maximum amount of BN which can be added to PN is found to be only 5 weight percent. Further addition leads to increase of air entraps in the samples, yielding thick and voided bond layers, which might affect test accuracy[84].

Table 2-4 constitutes a detailed overall study on fillers based on epoxy matrixes by McGrath *et al* [77]. The general trend is explained when fillers are added to epoxy matrixes and can be generically applied to other matrixes with similar thermoset behaviors. The amount of filler additions is dependent on the intended applications and

adjustment is made accordingly. Mechanical properties of filled polymers are usually challenging to predict exactly even though equations such as Kingery's equation has been used to predict CTE, and Halphin-Tsai [85] model to predict tensile strength, where the equation also considers the filler orientation with respect to loading directions. This is because the overall mechanical property is an interaction between factors such as volume or weight fraction of fillers, filler types, sizes, and shapes as well as the distribution and interfacial adhesion between the fillers and matrix. This complex overlay of relationship thus requires many assumptions of ideality or the neglect of some material properties.

2.4.2 Alumina

Aluminum oxide, also known as Alumina (Al_2O_3), is one of the most common filler for a great variety of microelectronic applications due to its relatively low cost and favorable mechanical properties of such as high strength and good electrical properties. Figure 2-10 shows the alumina fillers which are being used in the investigation. This comprises of angular fillers largely.

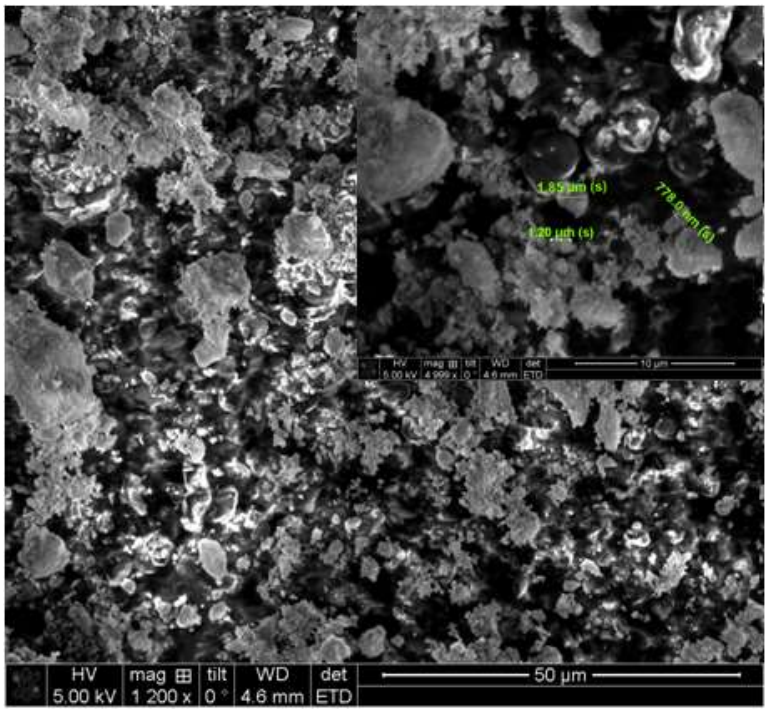

Figure 2- 10 SEM image of alumina particles.

From Table 2-3, aluminum oxide possesses high modulus of 385 GPa. On top of that, it also has a relatively low CTE of 6.6 ppm/°C and low thermal conductivity of 36 W/m-K.

Hence, it was chosen to improve the properties of the polymer matrix. In the form of alumina trihydrate [86], alumina can become a great fire retardant and helps greatly to suppress combustion.

2.4.3 Silica

Figure 2-11 shows the SEM image of silica particles which are used in the investigations for this thesis. The particles are largely angular and similar in shape to alumina.

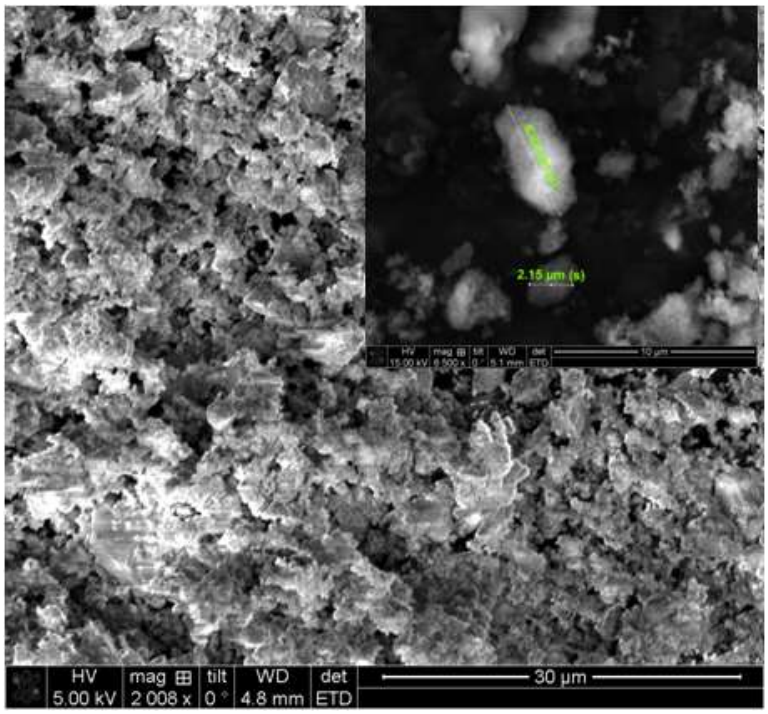

Figure 2- 11 SEM image of silica particle.

Silica particles have been the most widely used fillers for strengthening, reducing shrinkage upon curing, decreasing thermal coefficient and improving thermal conductivity of epoxy matrix. It is one of the lowest CTE fillers with values of 0.5 ppm/°C and can help to significantly reduce CTE of electronic epoxies at high loading concentrations. A low thermal conductivity of 1.5 W/m-K means that silica is slightly lower in terms of thermal conductivity but this can be enhanced with additions of materials such as aluminum nitride. Because silica exhibits hydrophilicity on its surface by nature, the OH groups may affect overall material dielectric constant and moisture adsorption[87]. It is also shown by Bertelli *et al.* [88] that silica in the form of hydrated silica helps to increase fire retardancy like alumina[89].

2.5 Effect of moisture diffusion and adsorption in polymeric composites for microelectronics packaging

Moisture adsorption and diffusion is a major concern in the field of microelectronics packaging and has been thoroughly researched for epoxy based encapsulation through both experiments and theoretical modelling [90-95]. Generally, hygro-mechanical stress arises when different materials have different rates of moisture absorption. Similar to CTE effect, this stress can be very detrimental as it imposes a strain on top of thermal strain which can cause electronic packages to fail quickly. Kitano *et al.* [96] suggested that moisture gain does not solely determine package cracking as interfacial adsorption hysteresis can be equally important.

Depending on the type of moisture exposure and the environmental impact, many literatures have documented the corrosion effects to some extent. Pecht *et al.* [97] proposed a model to predict moisture induced corrosions. Van Gils *et al.* [98] came up with virtual qualification methods which combine numerical predictions with experimental measurements to avert moisture induced failure in encapsulated packages. Many industrial standards exist to govern the routines of packaging including IPC/JEDEC J-STD-020D.1 [99] for moisture/reflow sensitivity (MSL) classification for non-hermetic surface mount device, J-STD-033B.1 [99] which deals with the handling, packaging and shipping for such devices. In moisture testing, MSL level 1(85°C/85%RH for 168 hours), MSL level 2 (85°C/60%RH at 168 hours) and MSL level 3 (30°C/60%RH for 168 hours) are commonly adopted to soak and qualify electronic materials ready for production. Stringent test specifications have also helped to identify problematic products and prevent failures such as popcorn defects induced by moisture expansion in packages. Concurrently, such specifications also help to detect early onsets of corrosion. However, all such failure modes, are unknown for PN as it has never been studied as an electronic material.

For most electronic packaging polymers, the main modes of diffusion mechanisms are:

i. Bulk diffusion [100,101]
ii. Wicking along the interface [102-105]

iii. Capillary action associated with micro-cracking [106]
iv. Channels formed by the addition of fillers [107,108] in polymer composites

Most of the mechanisms such as wicking, capillary action and channels take place slowly but humidity tests using accelerated test conditions can be used to observe advance deterioration or effects of moisture absorption at high concentrations. Elevated temperature of 85°C such as that adopted in JEDEC (J-STD-020D) moisture sensitivity level 1 (MSL level 1) converts most of the water, at 85% relative humidity (RH) to vapor state accelerating the moisture absorptions and thus accelerate changes within the polymers which would otherwise incur significantly longer test times.

JEDEC (J-STD-033C) provides the storage reference for semiconductor products storage as shown in Table 2-6.

Table 2- 6 Floor life at 30°C based on J-STD-033C

MSL	Floor life	Moisture relative humidity
1	Unlimited	85%RH
2	1 year	60% RH
2a	4 weeks	
3	168 hours	
4	72 hours	
5	48 hours	
5a	24 hours	
6	Bake before use and reflow	

2.6 Summary of literature in relation to thesis

Based on the questions raised in the previous sections, this thesis aims to study and develop a low melting temperature polymer which after curing, can be used as a high temperature potting material or encapsulant. A deeper understanding on the effects of curing parameters such as ramping rate and peak cure temperature on the mechanical properties of the material will be performed.

Thermal degradation behavior of the polymer will be studied to understand the effects of

filler addition to the enthalpy changes with regards to polymer cross-linking. The activation energy for polymer cross-linking will also be derived through Kissinger's equation.

Thermomechanical studies are correlated with thermodynamics to study the effects of various fillers with PN to understand the behavior of the new composites formed and to explain interaction of PN with the fillers and the bond formation observed in FTIR spectroscopy. Because the chemistry has numerous pathways, DFT analysis is further used to determine if such a bond relationship may exist.

The behavior of PN in moisture condition and its corresponding properties will be studied to understand moisture absorption behavior which would affect the way PN be used in electronic applications. This is especially important in answering the effects of environmental moisture on the storage of PN. Separately, the dielectric behavior at various cure temperatures will also be studied for PN and its filled composites.

A deeper understanding in terms of bond-ability of PN in the form of a die attach material will also be performed through die bonding and using die shear test to characterize its strength. Some of the challenges faced will also be discussed.

References

[1] J. D. Cressler and H. A. Mantooth, Extreme Environment Electronics. CRC Press, 2012.

[2] S. Annas, "Advances in low temperature co-fired ceramic (LTCC) for ever increasing microelectronic applications," in Electronic Components and Technology Conference, 2003. Proceedings. 53rd, 2003, pp. 1691–1693.

[3] M. T. Sebastian and H. Jantunen, "Low loss dielectric materials for LTCC applications: a review," Int. Mater. Rev., vol. 53, no. 2, pp. 57–90, Mar. 2008.

[4] C. Q. Scrantom, "LTCC Technology: Where We are and Where We're Going," in MCM C/Mixed Technologies and Thick Film Sensors, vol. 2, W. K. Jones, K. Kurzweil, G. Harsányi, and S. Mergui, Eds. Dordrecht: Springer Netherlands, 1995, pp. 77–87.

[5] Y. Imanaka, Multilayered Low Temperature Cofired Ceramics (LTCC) Technology. Boston, MA : Springer Science Business Media, Inc, 2005.

[6] “schott_db_process_htcc_ltcc_d_2012_04_30_rz.pdf.” .

[7] M. Ebert and J. Bagdahn, “Determination of residual stress in glass frit bonded MEMS by finite element analysis,” in 5th International Conference on Thermal and Mechanical Simulation and Experiments in Microelectronics and Microsystems, 2004. EuroSimE 2004. Proceedings of the, 2004, pp. 407–412.

[8] R. Knechtel, “Glass frit bonding: an universal technology for wafer level encapsulation and packaging,” Microsyst. Technol., vol. 12, pp. 63–68, Oct. 2005.

[9] N. Kinjo, M. Ogata, K. Nishi, A. Kaneda, and K. Dušek, “Epoxy Molding Compounds as Encapsulation Materials for Microelectronic Devices,” in Speciality Polymers/Polymer Physics, Springer Berlin Heidelberg, 1989, pp. 1–48.

[10] X. J. Fan, “Moisture Sensitivity of Plastic Packages of IC Devices - Springer.” [Online]. Available: http://link.springer.com.ezlibproxy1.ntu.edu.sg/book/10.1007/978-1-4419-5719-1. [Accessed: 17-May-2015].

[11] C. J. Scozzie, C. W. Tipton, W. M. DeLancey, J. M. McGarrity, and F. B. McLean, “High temperature stressing of SiC JFETs at 300/spl deg/C,” in Proceedings of 1994 IEEE International Reliability Physics Symposium, 1994, pp. 351–358.

[12] C. A. Wilkie and A. B. Morgan, Fire Retardancy of Polymeric Materials, Second Edition. CRC Press, 2009.

[13] “Coefficients of Thermal Expansion (CTE) of common Electrical Engineering / Semiconductor materials.” [Online]. Available: http://www.cleanroom.byu.edu/CTE_materials.phtml. [Accessed: 05-Jan-2015].

[14] “Aluminum Nitride | AlN | Substrate Characteristics.” [Online]. Available: http://accuratus.com/alnchar.html. [Accessed: 05-Jan-2015].

[15] L. J. Zhang et al., “Ceramic #x2014; Ceramic joining using glass frit for high temperature application,” in Electronics Packaging Technology Conference (EPTC), 2012 IEEE 14th, 2012, pp. 38–42.

[16] J. Araujo, "New Downhole Components Meet Needs for Extreme High Temperatures - 201309_ep_components_ht_downhole_tools.pdf," www.slb.com, Sep-2013. [Online]. Available: http://www.slb.com/~/media/Files/drilling/industry_articles/201309_ep_components_ht_downhole_tools.pdf. [Accessed: 06-Sep-2015].

[17] "MWD, RSS Tools Extend Operating Envelope | Exploration & Production." [Online]. Available: http://www.epmag.com/mwd-rss-tools-extend-operating-envelope-775786. [Accessed: 28-May-2015].

[18] G.-W. Lee, M. Park, J. Kim, J. I. Lee, and H. G. Yoon, "Enhanced thermal conductivity of polymer composites filled with hybrid filler," Compos. Part Appl. Sci. Manuf., vol. 37, no. 5, pp. 727–734, May 2006.

[19] C.-C. Su, C.-H. Wei, and B.-C. Li, "Thermal and Cure Kinetics of Epoxy Molding Compounds Cured with Thermal Latency Accelerators," Adv. Mater. Sci. Eng., vol. 2013, p. e391267, Feb. 2013.

[20] R. M. Perez et al., "Effect of DOP-based compounds on fire retardancy, thermal stability, and mechanical properties of DGEBA cured with 4,4′-DDS," J. Mater. Sci., vol. 41, no. 2, pp. 341–353, Jan. 2006.

[21] U. Sorathia, J. Ness, and M. Blum, "Fire safety of composites in the US Navy," Compos. Part Appl. Sci. Manuf., vol. 30, no. 5, pp. 707–713, May 1999.

[22] M. K. Kolel-Veetil et al., "Hybrid inorganic–organic poly(carborane-siloxane-arylacetylene) structural isomers with in-chain aromatics: Synthesis and properties," J. Polym. Sci. Part Polym. Chem., vol. 51, no. 12, pp. 2638–2650, Jun. 2013.

[23] M. K. Kolel-Veetil and T. M. Keller, "Polyarylacetylenes containing siloxane, silane, and carborane moieties," US8217194 B2, 10-Jul-2012.

[24] T. M. Keller, "Oxidative protection of carbon fibers with poly(carborane–siloxane–acetylene)," Carbon, vol. 40, no. 3, pp. 225–229, Mar. 2002.

[25] Y. L. Liu, C. S. Wu, K. Y. Hsu, and T. C. Chang, "Flame-retardant epoxy resins from o-cresol novolac epoxy cured with a phosphorus-containing aralkyl novolac," J. Polym. Sci. Part Polym. Chem., vol. 40, no. 14, pp. 2329–2339, Jul. 2002.

[26] D. J. Belton and E. Sullivan, “Infrared and liquid chromatographic characterization of epoxy cresol novolac-phenol formaldehyde novolac-tertiary amine resin systems,” J. Appl. Polym. Sci., vol. 31, no. 5, pp. 1309–1326, Apr. 1986.

[27] H. Ardebili and M. Pecht, *Encapsulation Technologies for Electronic Applications*. William Andrew, 2009.

[28] S. Lin-Gibson, V. Baranauskas, J. S. Riffle, and U. Sorathia, “Cresol novolac–epoxy networks: properties and processability,” Polymer, vol. 43, no. 26, pp. 7389–7398, Dec. 2002.

[29] M. Sudheer, R. Prabhu, K. Raju, and T. Bhat, “Effect of Filler Content on the Performance of Epoxy/PTW Composites,” Adv. Mater. Sci. Eng., vol. 2014, p. e970468, Apr. 2014.

[30] H. Parry and R. Hewitt, “Effect of Fillers on Epoxy Resins,” Ind. Eng. Chem., vol. 49, no. 7, pp. 1103–1104, Jul. 1957.

[31] I. Hamerton, Recent Developments in Epoxy Resins. iSmithers Rapra Publishing, 1996.

[32] T. Kamon and H. Furukawa, “Curing mechanisms and mechanical properties of cured epoxy resins,” in Epoxy Resins and Composites IV, K. Dušek, Ed. Springer Berlin Heidelberg, 1986, pp. 173–202.

[33] B. Ellis, Ed., Chemistry and Technology of Epoxy Resins. Dordrecht: Springer Netherlands, 1993.

[34] M. T. Goosey, Electronics Applications of Polymers. Elsevier Science & Technology Books, 1989.

[35] E. R. Salmon, Encapsulation of Electronic Devices and Components. CRC Press, 1986.

[36] M. Bajpai, V. Shukla, and F. Habib, “Development of a heat resistant UV-curable epoxy coating,” *Prog. Org. Coat.*, vol. 53, no. 4, pp. 239–245, Aug. 2005.

[37] S. Levchik, A. Piotrowski, E. Weil, and Q. Yao, “New developments in flame retardancy of epoxy resins,” *Polym. Degrad. Stab.*, vol. 88, no. 1, pp. 57–62, Apr. 2005.

[38] J. Artner *et al.*, "A Novel and Effective Synthetic Approach to 9,10-Dihydro-9-oxa-10-phosphaphenanthrene-10-oxide (DOPO) Derivatives," *Phosphorus Sulfur Silicon Relat. Elem.*, vol. 182, no. 9, pp. 2131–2148, Jul. 2007.

[39] J. Artner *et al.*, "A Novel DOPO-Based Diamine as Hardener and Flame Retardant for Epoxy Resin Systems," *Macromol. Mater. Eng.*, vol. 293, no. 6, pp. 503–514, Jun. 2008.

[40] M. Ciesielski, A. Schäfer, and M. Döring, "Novel efficient DOPO-based flame-retardants for PWB relevant epoxy resins with high glass transition temperatures," *Polym. Adv. Technol.*, vol. 19, no. 6, pp. 507–515, Jun. 2008.

[41] W.-L. Lee, L.-C. Liu, C.-M. Chen, and J.-S. Lin, "Syntheses and flame retarding properties of DOPO polymers, melamine polymers, and DOPO-melamine copolymers," *Polym. Adv. Technol.*, vol. 25, no. 1, pp. 36–40, Jan. 2014.

[42] P. Liu *et al.*, "Preparation, characterization and properties of a halogen-free phosphorous flame-retarded poly(butylene terephthalate) composite based on a DOPO derivative," *J. Appl. Polym. Sci.*, vol. 130, no. 2, pp. 1301–1307, Oct. 2013.

[43] K. Shree Meenakshi, E. Pradeep Jaya Sudhan, S. Ananda Kumar, and M. J. Umapathy, "Development and characterization of novel DOPO based phosphorus tetraglycidyl epoxy nanocomposites for aerospace applications," *Prog. Org. Coat.*, vol. 72, no. 3, pp. 402–409, Nov. 2011.

[44] C. Decker, "Kinetic Study and New Applications of UV Radiation Curing," *Macromol. Rapid Commun.*, vol. 23, no. 18, pp. 1067–1093, Dec. 2002.

[45] J.-W. Bae, W. Kim, S.-H. Cho, and S.-H. Lee, "The properties of AlN-filled epoxy molding compounds by the effects of filler size distribution," *J. Mater. Sci.*, vol. 35, no. 23, pp. 5907–5913, 2000.

[46] R. J. Morgan, E. Eugene Shin, B. Rosenberg, and A. Jurek, "Characterization of the cure reactions of bismaleimide composite matrices," *Polymer*, vol. 38, no. 3, pp. 639–646, Feb. 1997.

[47] S. Takeda, H. Akiyama, and H. Kakiuchi, "Synthesis and properties of bismaleimide resins containing ether bonds," *J. Appl. Polym. Sci.*, vol. 35, no. 5, pp. 1341–1350, Apr. 1988.

[48] L.-R. Bao, A. F. Yee, and C. Y.-C. Lee, "Moisture absorption and hygrothermal aging in a bismaleimide resin," *Polymer*, vol. 42, no. 17, pp. 7327–7333, Aug. 2001.

[49] J. Guofeng Bai, J. Yin, Z. Zhang, G.-Q. Lu, and J. D. van Wyk, "High-Temperature Operation of SiC Power Devices by Low-Temperature Sintered Silver Die-Attachment," *IEEE Trans. Adv. Packag.*, vol. 30, no. 3, pp. 506–510, Aug. 2007.

[50] "High-Pressure, High-Temperature Well Logging, Perforating and Testing (Oilfield Review), Schlumberger." [Online]. Available: http://www.slb.com/resources/publications/industry_articles/oilfield_review/1998/or1998sum04_hpht_welllogging.aspx. [Accessed: 09-Sep-2011].

[51] P. Hagler, P. Henson, and R. W. Johnson, "Packaging Technology for Electronic Applications in Harsh High-Temperature Environments," *IEEE Trans. Ind. Electron.*, vol. 58, no. 7, pp. 2673–2682, Jul. 2011.

[52] I. Hamerton, Ed., *Chemistry and Technology of Cyanate Ester Resins*. Dordrecht: Springer Netherlands, 1994.

[53] V. Chidambaram, E. P. J. Rong, G. C. Lip, and R. M. W. Daniel, "Cyanate Ester-Based Encapsulation Material for High-Temperature Applications," *J. Electron. Mater.*, Jul. 2013.

[54] A. Gu, "High performance bismaleimide/cyanate ester hybrid polymer networks with excellent dielectric properties," *Compos. Sci. Technol.*, vol. 66, no. 11–12, pp. 1749–1755, Sep. 2006.

[55] H. Yan, H. Wang, and J. Cheng, "Interpenetrating polymer networks from the novel bismaleimide and cyanate containing naphthalene: Cure and thermal characteristics," *Eur. Polym. J.*, vol. 45, no. 8, pp. 2383–2390, Aug. 2009.

[56] P. Musto, E. Martuscelli, G. Ragosta, P. Russo, and G. Scarinzi, "An interpenetrated system based on a tetrafunctional epoxy resin and a thermosetting bismaleimide: Structure–properties correlation," *J. Appl. Polym. Sci.*, vol. 69, no. 5, pp. 1029–1042, Aug. 1998.

[57] K. P. O. Mahesh, M. Alagar, and S. Ananda Kumar, "Mechanical, thermal and morphological behavior of bismaleimide modified polyurethane-epoxy IPN matrices," *Polym. Adv. Technol.*, vol. 14, no. 2, pp. 137–146, Feb. 2003.

[58] L. Ji, A. Gu, G. Liang, and L. Yuan, "Novel modification of bismaleimide–triazine resin by reactive hyperbranched polysiloxane," *J. Mater. Sci.*, vol. 45, no. 7, pp. 1859–1865, Jan. 2010.

[59] X. Zhao, H. Guo, Y. Lei, R. Zhao, J. Zhong, and X. Liu, "Effect of polyarylene ether nitriles on processing and mechanical behaviors of phthalonitrile-epoxy copolymers

and glass fiber laminated composites," *J. Appl. Polym. Sci.*, vol. 127, no. 6, pp. 4873–4878, Mar. 2013.

[60] D. D. Dominguez and T. M. Keller, "Phthalonitrile-epoxy blends: Cure behavior and copolymer properties," *J. Appl. Polym. Sci.*, vol. 110, no. 4, pp. 2504–2515, 2008.

[61] L. J. Henderson and T. M. Keller, "Synthesis and Characterization of Poly (carborane-siloxane-acetylene)," *Macromolecules*, vol. 27, no. 6, pp. 1660–1661, 1994.

[62] T. M. Keller, "Synthesis of elastomeric poly(carborane-siloxane-acetylene)s," US6967233 B2, 22-Nov-2005.

[63] T. M. Keller and L. J. Henderson, "Carborane-(siloxane or silane)-unsaturated hydrocarbon based polymers," US5272237 A, 21-Dec-1993.

[64] M. Laskoski, D. D. Dominguez, and T. M. Keller, "Synthesis and properties of a bisphenol A based phthalonitrile resin," *J. Polym. Sci. Part Polym. Chem.*, vol. 43, no. 18, pp. 4136–4143, 2005.

[65] P. Selvakumar, K. Padmini, M. Sarojadevi, and M. F. Leelavathy, "Synthesis, Characterization and Thermal Properties of Imide-Containing Phthalonitrile Polymers," *J. Macromol. Sci. Part A*, vol. 47, no. 1, pp. 76–88, Nov. 2009.

[66] M. L. Warzel and T. M. Keller, "Tensile and fracture properties of a phthalonitrile polymer," *Polymer*, vol. 34, no. 3, pp. 663–666, 1993.

[67] M. Liu, "Aromatic heterocyclic resin : precursor for carbon materials and high temperature foams.," Thesis, 2012.

[68] T. M. Keller and J. R. Griffith, "The synthesis of highly fluorinated phthalonitrile resins and cure studies," *J. Fluor. Chem.*, vol. 13, no. 4, pp. 315–324, Apr. 1979.

[69] H. Tomoda, S. Saito, S. Ogawa, and S. Shiraishi, "Synthesis of Phthalocyanines from Phthalonitrile with Organic Strong Bases," *Chem. Lett.*, vol. 9, no. 10, pp. 1277–1280, 1980.

[70] P. J. Burchill, "On the formation and properties of a high-temperature resin from a bisphthalonitrile," *J. Polym. Sci. Part Polym. Chem.*, vol. 32, no. 1, pp. 1–8, Jan. 1994.

[71] T. M. Keller and D. D. Dominguez, "High temperature resorcinol-based phthalonitrile polymer," *Polymer*, vol. 46, no. 13, pp. 4614–4618, Jun. 2005.

[72] Z. Brunovska, R. Lyon, and H. Ishida, "Thermal properties of phthalonitrile functional polybenzoxazines," *Thermochim. Acta*, vol. 357–358, pp. 195–203, Aug. 2000.

[73] T. M. Keller, "Phthalonitrile-based high temperature resin," *J. Polym. Sci. Part Polym. Chem.*, vol. 26, no. 12, pp. 3199–3212, 1988.

[74] H. Zhou, F. Liu, B. G. Sun, and T. Zhao, "STUDY ON ONE PHTHALONITRILE RESIN SYSTEM SUITABLE FOR RTM PROCESS."

[75] M. Laskoski, D. D. Dominguez, and T. M. Keller, "Alkyne-containing phthalonitrile resins: Controlling mechanical properties by selective curing," *J. Polym. Sci. Part Polym. Chem.*, vol. 51, no. 22, pp. 4774–4778, Nov. 2013.

[76] S.-Y. Fu, X.-Q. Feng, B. Lauke, and Y.-W. Mai, "Effects of particle size, particle/matrix interface adhesion and particle loading on mechanical properties of particulate–polymer composites," *Compos. Part B Eng.*, vol. 39, no. 6, pp. 933–961, Sep. 2008.

[77] L. McGrath, *Effect of Fillers and Filler Interface on Fracture Toughness of Epoxy-alumina Composites*. ProQuest, 2009.

[78] B. J. Cardwell and A. F. Yee, "Toughening of epoxies through thermoplastic crack bridging," *J. Mater. Sci.*, vol. 33, no. 22, pp. 5473–5484, 1998.

[79] P. Dittanet and R. A. Pearson, "Effect of bimodal particle size distributions on the toughening mechanisms in silica nanoparticle filled epoxy resin," *Polymer*, vol. 54, no. 7, pp. 1832–1845, Mar. 2013.

[80] K. C. Radford, "The mechanical properties of an epoxy resin with a second phase dispersion," *J. Mater. Sci.*, vol. 6, no. 10, pp. 1286–1291, Oct. 1971.

[81] Y. L. Liang and R. A. Pearson, "Toughening mechanisms in epoxy–silica nanocomposites (ESNs)," *Polymer*, vol. 50, no. 20, pp. 4895–4905, Sep. 2009.

[82] X.-L. Xie, Y.-W. Mai, and X.-P. Zhou, "Dispersion and alignment of carbon nanotubes in polymer matrix: A review," *Mater. Sci. Eng. R Rep.*, vol. 49, no. 4, pp. 89–112, May 2005.

[83] Y. Xu, D. D. L. Chung, and C. Mroz, "Thermally conducting aluminum nitride polymer-matrix composites," *Compos. Part Appl. Sci. Manuf.*, vol. 32, no. 12, pp. 1749–1757, Dec. 2001.

[84] M. Hodgin and R. H. Estes, "Advanced boron nitride epoxy formulations excel in thermal management applications," in *NEPCON WEST*, 1999, pp. 359–366.

[85] T. H. Hsieh, A. J. Kinloch, K. Masania, A. C. Taylor, and S. Sprenger, "The mechanisms and mechanics of the toughening of epoxy polymers modified with silica nanoparticles," *Polymer*, vol. 51, no. 26, pp. 6284–6294, Dec. 2010.

[86] X. Zhang, F. Guo, J. Chen, G. Wang, and H. Liu, "Investigation of interfacial modification for flame retardant ethylene vinyl acetate copolymer/alumina trihydrate nanocomposites," *Polym. Degrad. Stab.*, vol. 87, no. 3, pp. 411–418, Mar. 2005.

[87] T. J. Wooster, S. Abrol, J. M. Hey, and D. R. MacFarlane, "Thermal, mechanical, and conductivity properties of cyanate ester composites," *Compos. Part Appl. Sci. Manuf.*, vol. 35, no. 1, pp. 75–82, Jan. 2004.

[88] G. Bertelli, G. Camino, E. Marchetti, L. Costa, E. Casorati, and R. Locatelli, "Parameters affecting fire retardant effectiveness in intumescent systems," *Polym. Degrad. Stab.*, vol. 25, no. 2–4, pp. 277–292, 1989.

[89] X. Almeras *et al.*, "Effect of fillers on the fire retardancy of intumescent polypropylene compounds," *Polym. Degrad. Stab.*, vol. 82, no. 2, pp. 325–331, 2003.

[90] E. H. Wong, S. W. Koh, K. H. Lee, and R. Rajoo, "Comprehensive treatment of moisture induced failure-recent advances," *IEEE Trans. Electron. Packag. Manuf.*, vol. 25, no. 3, pp. 223–230, Jul. 2002.

[91] A. A. O. Tay and T. Y. Lin, "The impact of moisture diffusion during solder reflow on package reliability," in *Electronic Components and Technology Conference, 1999. 1999 Proceedings. 49th*, 1999, pp. 830–836.

[92] T. Y. Tee and Z. Zhong, "Integrated vapor pressure, hygroswelling, and thermo-mechanical stress modeling of QFN package during reflow with interfacial fracture mechanics analysis," *Microelectron. Reliab.*, vol. 44, no. 1, pp. 105–114, Jan. 2004.

[93] J. E. Galloway and B. M. Miles, "Moisture absorption and desorption predictions for plastic ball grid array packages," *IEEE Trans. Compon. Packag. Manuf. Technol. Part A*, vol. 20, no. 3, pp. 274–279, 1997.

[94] X. J. Fan, G. Q. Zhang, and L. J. Ernst, "A micro-mechanics approach in polymeric material failures in microelectronic packaging," in *Proceedings of the Third International Conference on Thermal and Mechanical Simulation in Micro-Electronics (EuroSimE)*, 2002, pp. 154–164.

[95] X. Fan, G. Q. Zhang, W. van Driel, and L. J. Ernst, "Analytical solution for moisture-induced interface delamination in electronic packaging," presented at the Electronic Components and Technology Conference, 2003. Proceedings. 53rd, 2003, pp. 733–738.

[96] M. Kitano, A. Nishimura, S. Kawai, and K. Nishi, "Analysis of package cracking during reflow soldering process," in *Reliability Physics Symposium 1988. 26th Annual Proceedings., International*, 1988, pp. 90–95.

[97] M. Pecht, "A model for moisture induced corrosion failures in microelectronic packages," *IEEE Trans. Compon. Hybrids Manuf. Technol.*, vol. 13, no. 2, pp. 383–389, Jun. 1990.

[98] M. A. J. van Gils *et al.*, "Virtual qualification of moisture induced failures of advanced packages," *Microelectron. Reliab.*, vol. 47, no. 2–3, pp. 273–279, Feb. 2007.

[99] "Home | JEDEC." [Online]. Available: http://www.jedec.org/. [Accessed: 09-Sep-2015].

[100] C. L. Soles and A. F. Yee, "A discussion of the molecular mechanisms of moisture transport in epoxy resins," *J. Polym. Sci. Part B Polym. Phys.*, vol. 38, no. 5, pp. 792–802, Mar. 2000.

[101] M. R. VanLandingham, R. R. Dagastine, R. F. Eduljee, R. L. McCullough, and J. W. Gillespie Jr, "Characterization of nanoscale property variations in polymer composite systems: 1. Experimental results," *Compos. Part Appl. Sci. Manuf.*, vol. 30, no. 1, pp. 75–83, Jan. 1999.

[102] H. B. Fan, E. K. L. Chan, C. K. Y. Wong, and M. M. F. Yuen, "Investigation of moisture diffusion in electronic packages by molecular dynamics simulation," *J. Adhes. Sci. Technol.*, vol. 20, no. 16, pp. 1937–1947, Jan. 2006.

[103] M. R. Bowditch, "The durability of adhesive joints in the presence of water," *Int. J. Adhes. Adhes.*, vol. 16, no. 2, pp. 73–79, May 1996.

[104] M. P. Zanni-Deffarges and M. E. R. Shanahan, "Diffusion of water into an epoxy adhesive: comparison between bulk behaviour and adhesive joints," *Int. J. Adhes. Adhes.*, vol. 15, no. 3, pp. 137–142, Jul. 1995.

[105] J. Comyn, C. L. Groves, and R. W. Saville, "Durability in high humidity of glass-to-lead alloy joints bonded with an epoxide adhesive," *Int. J. Adhes. Adhes.*, vol. 14, no. 1, pp. 15–20, Jan. 1994.

[106] Y. J. Weitsman and Y.-J. Guo, "A correlation between fluid-induced damage and anomalous fluid sorption in polymeric composites," *Compos. Sci. Technol.*, vol. 62, no. 6, pp. 889–908, May 2002.

[107] H. Lu, K. Yu, Y. Liu, and J. Leng, "Sensing and actuating capabilities of a shape memory polymer composite integrated with hybrid filler," *Smart Mater. Struct.*, vol. 19, no. 6, p. 065014, Jun. 2010.

[108] M. Uschitsky and E. Suhir, "Moisture Diffusion in Epoxy Molding Compounds Filled With Particles," *J. Electron. Packag.*, vol. 123, no. 1, pp. 47–51, Mar. 2001.

Chapter 3

Experimental Methodology

This chapter outlines the synthesis process of phthalonitrile (PN) and describes the approach to obtain modified PN. The steps involved in the blending and reaction synthesis of PN monomers with fillers are discussed and details are provided. The analysis of the new products and evaluation on the use of PN as a microelectronic packaging material are discussed. This chapter includes the initial evaluation of neat resorcinol based PN, followed by a study of the material with fillers included. The processability of the material within the 180°C to 360°C application regime is discussed in detail. This temperature regime is based on high temperature harsh environment (HTHE) operations such as logging while drilling (LWD) and measurement while drilling (MWD). The chapter also proceeds to explain the techniques employed for PN evaluation first as a bulk material and subsequently in a series of tests which mimic the high temperature and high pressure environment.

3.1 Overview of experimental approach

Figure 3-1 shows the experimental approach where the monomer is first synthesized and then converted to pre-polymer blends consisting of high temperature fillers. The bulk characteristics of the developed encapsulation material are first evaluated through various mechanical and chemical analysis techniques, and then tested for its application properties such as bond strength and moisture adsorption test. Although many techniques have been utilized in this research, FTIR, Density Functional Theory (DFT) simulation results are important for identification and matching of bonds formed. HPHT test is also crucial as it helps to prove the successful integration of the developed PN composite as a harsh environment electronics encapsulation material.

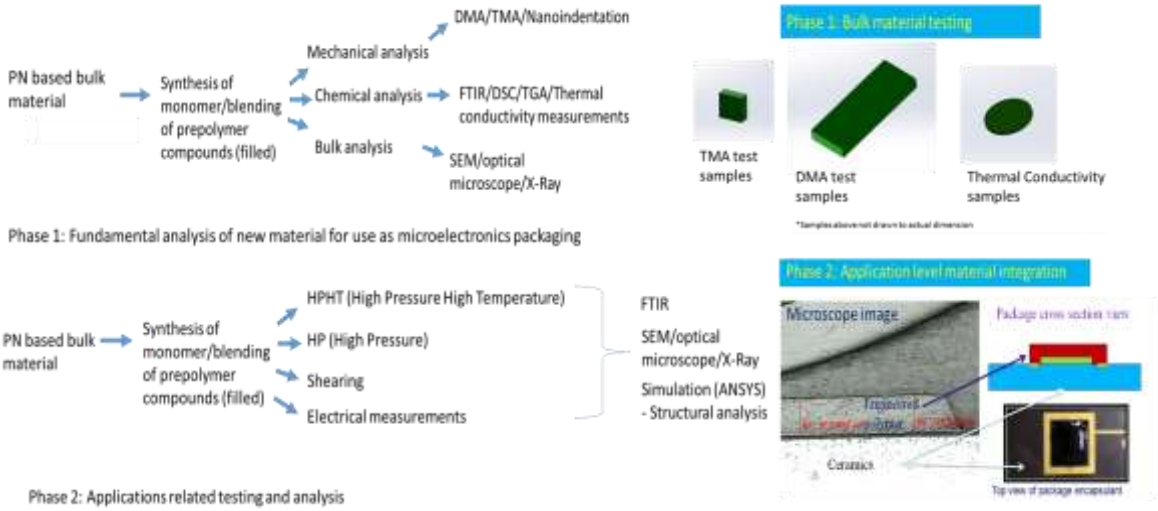

Figure 3- 1 Process flow of resorcinol based phthalonitrile analyses.

3.2 Materials

The objective of the synthesis development in this research is to create Class I [1] ready PN analogous to that of epoxy classes. Class 2 [2] ready preforms are also developed and would essentially consist of the PN in solid pressed form with fillers loaded. In this project, laboratory synthesized resorcinol-based phthalonitrile (bis(3,4-dicyanophenoxy)benzene) was used for sample fabrication. Resorcinol (Sigma Aldrich), anhydrous potassium carbonate (K_2CO_3; Sigma Aldrich), 4-nitropthalonitrile (Tee Hai Chemicals), and anhydrous dimethyl sulfoxide (DMSO; Sigma Aldrich) were used to synthesize phthalonitrile monomer.

A catalyst, 1,4-bis(4-aminophenoxy)benzene, was used during the mixture of phthalonitrile monomer and the fillers. Commercially available fillers were procured and mixed according to the weight ratios required. These include silica (Sigma Aldrich < 5 μm), and alumina (Sigma Aldrich < 5 μm), and both types are angular fillers. To keep the particles water free, the particles were kept at a temperature of 90°C to reduce contact with moisture until they are ready for use. Boron nitride was also evaluated in this experiment but the filler ratio did not go higher than 5 weight percent due to a high resultant viscosity and processability issues, the results are not discussed in the thesis.

3.3 Sample Preparation

Referring to the process flow in Figure 3-2, sample preparations of the PN involves mixing resorcinol, 4-nitrophthalonitrile, and potassium carbonate according to a molar ratio of 1:2:3. DMSO was used as the solvent although DMF could also be used instead. The constituents were then mixed and stirred continuously under nitrogen ambient at room temperature for 24 hours.

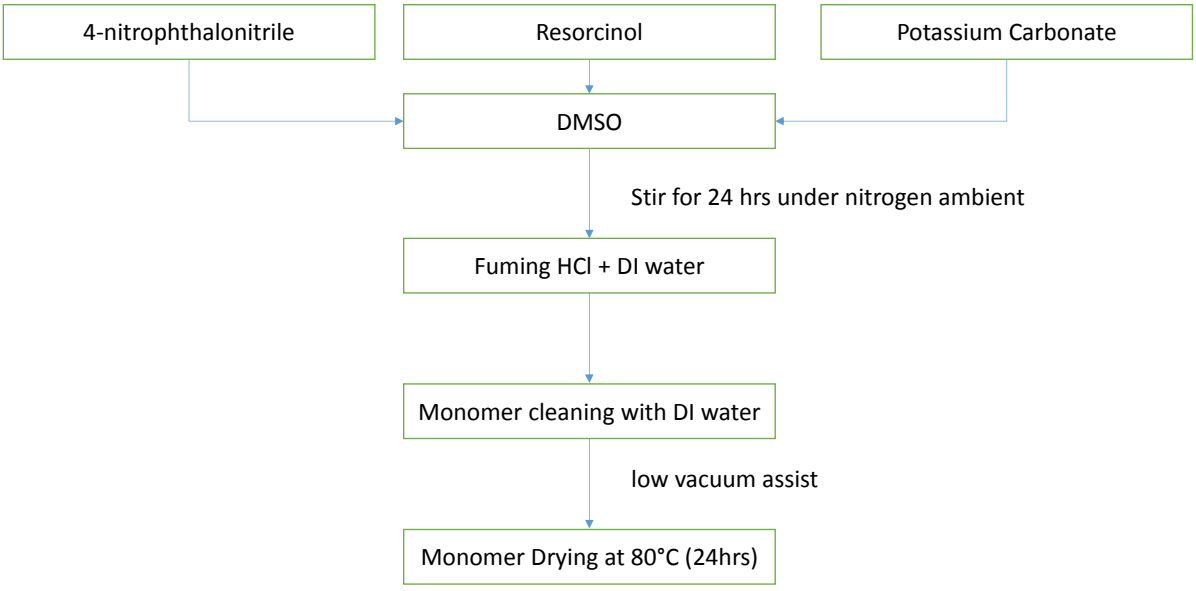

Figure 3- 2 Synthesis of unfilled monomer.

The end product of the synthesis shown in Figure 3-2 yields a pale yellow precipitate product as shown in Figure 3-3 after monomer drying which can then be filtered off by vacuum-assisted filtration. This monomer precipitates were then dried at 80°C for 12 hours to obtain a dry yellowish white powder.

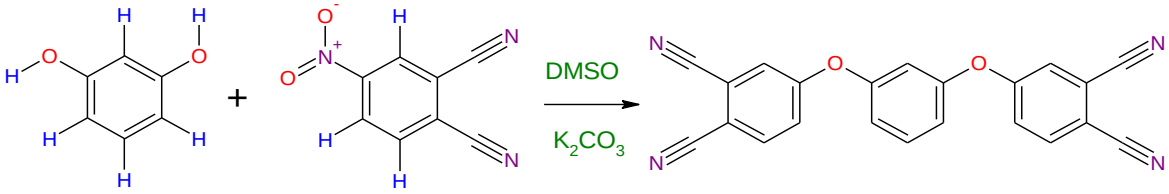

Figure 3- 3 Chemical reaction of phthalonitrile Monomer Synthesis.

Using the product shown in Figure 3-3, the monomer is further melted to form neat PN upon solidification or the encapsulant with the addition of silica or alumina fillers into the melted blend as shown in Figure 3-4 process flow.

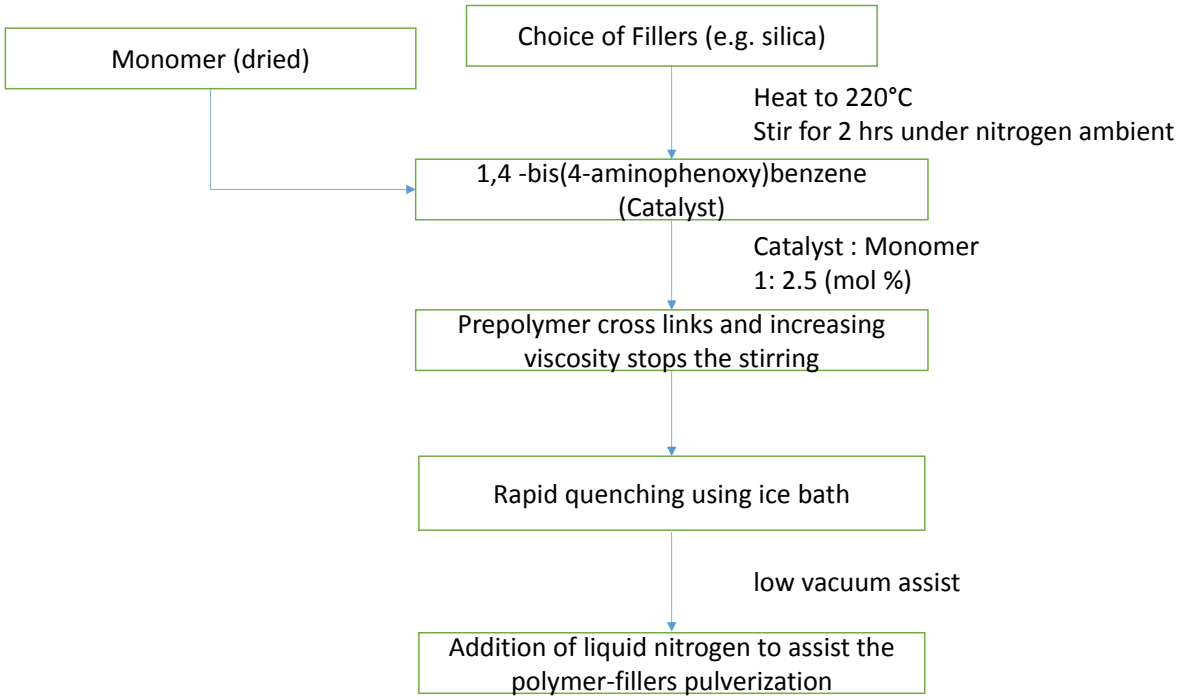

Figure 3- 4 Synthesis of filled polymer.

A subsequent step to convert the monomer to its prepolymer state was required to keep the monomer ready for use as a prepolymer. Both monomer and fillers were added to a 3-necked round bottom flask at the desired ratios and raised to a temperature of 220°C for over 2 hours. The mixture was then quenched using ice cold water and small pieces of the prepolymer were removed. 1, 4-bis (4-aminophenoxy) benzene (APB), which acted as a catalyst, was grinded together with the prepolymer into fine powder. The powder mixture was treated to the required temperatures to form the desired shape under standard

conditions from resin molding or vacuum assisted vacuum molding.

To form a good material composite, the monomer powder was melted and then stirred mechanically at high speed for a period of 24 hours at 220°C. Subsequent heating are performed at temperatures of 250°C, 280°C, 320°C and 360°C which coincides with the curing temperature. Further details can be found in Appendix A section A1.1. When APB is not added, no increase in viscosity is detected even with 24 hours of stirring. Once it had cooled down, the mixture formed a dark green crystal with a good spread of fillers within the matrix. The reaction pathway for the complete product of filled composites would be discussed in Chapter 4.

3.4 Characterization of PN and its composite properties

3.4.1 Scanning Electron Microscopy (SEM) characterization

Surface morphologies of the bulk sample as well as voids and filler surfaces were characterized using FEI Nova 600i or JEOL 6360 scanning electron microscope (SEM) at an accelerating voltage 5 kV. Samples were mounted onto a carbon tape prior to sputter deposition of a thin layer of carbon for about 30 seconds. This helps to minimize sample charging during SEM characterization. In addition, copper tapes would be mounted at the edges of the sample at high magnifications of 10 000× to minimize further charging.

3.4.2 Fourier Transform Infrared (FTIR) Spectroscopy

Fourier Transform Infrared (FTIR) Spectroscopy is an analysis technique used to determine the chemical composition of a sample with respect to its bond signatures. Here, the FTIR Perkin Elmer Instruments Spectrum GX was used for observing the peak information for different filler types as well as for their different contents. To observe the effect of the curing temperature on the FTIR results, three samples of the same filler type were cured at three different curing stages: 180 °C, 250 °C and 360 °C. The samples used were flat and their thickness was less than 1.5 mm.

To further understand the effects of filler concentrations on the chemical bonding of the matrix, different samples of various filler concentrations were measured using FTIR to check for bond changes post curing. The measurements were performed at room

temperature, using a spectral resolution of 2 cm^{-1} and 20 times of scan. Transmittance of the samples, represented by the peaks occurring from 400 to 4000 cm^{-1}, were also analyzed.

3.4.3 Dynamic Mechanical Analysis (DMA)

Dynamic mechanical analysis measures a material's mechanical behavior, such as stiffness and damping, as a function of time, temperature, and frequency. Hence, a DMA Q800 instrument was employed to acquire the storage modulus (G') and loss modulus (G'') of the samples upon subjected to an applied force. Single cantilever geometry was used and the samples (flat surface and of dimensions 30 mm × 15 mm × 3 mm) were heated in air, from room temperature to 400°C, with a heating rate of 10 °C/min. The storage modulus of the samples at various temperatures (room temperature, 100°C, 200°C, and 300°C) was measured. This measurement provides a good perspective of the material physical properties at high temperatures and is a good reference especially because the fabricated DMA test samples are of comparable sizes to the industrial standards of encapsulation.

3.4.4 Thermomechanical Analyzer (TMA)

TMA 2940 was used to measure the coefficient of thermal expansion (CTE) variations at different temperatures, which are at 50°C, 100°C, 200°C and 300°C. Measurements were performed in inert nitrogen gas (N_2) ambient where test samples were heated at a rate of 10°C/min from room temperature to 300 °C. Samples comprising of neat PN and various filler concentrations were tested.

3.4.5 Thermogravimetry Analyzer (TGA)

TGA Q500 from TA Instruments was used for this analysis, where sample mass loss was measured as a function of temperature or time. Samples were heated under air or inert N_2 conditions, at a rate of 10°C/min in from room temperature to 900˚C, and any weight changes were denoted alongside with onset of decomposition temperatures. For degradation studies, the rate is varied in steps of 10°C/min to 20°C/min in steps of 5°C/min. This is important especially when PN and the filled compositions are to be

developed for harsh environment functions.

3.4.6 Thermal Conductivity

The Linseis XFA 500 was used to measure the specific heat capacity, thermal diffusivity, thermal conductivity of the neat and filled PN samples which conforms to ASTM E1461-92 standards for thermal diffusivity of solids. These test samples measuring 12.7 mm by 12.7 mm in squares or circles were heated at a rate of 5 °C/min, up to 300 °C in a vacuum environment. Measurements were recorded in the temperature range of 50°C to 300 °C at 50 °C intervals. A laser shot was made for each sample measurement and the short energy pulse was deposited on one side of the sample while the resulting temperature rise was measured on the opposite face using a sensitive detector.
Parker's relationship [3] was utilized to calculate the thermal diffusivity as shown in Equation (3-1).

$$\alpha = 0.1388 \frac{L^2}{t_{\frac{1}{2}}} \qquad \textbf{Equation 3-1}$$

Where α denotes thermal diffusivity, and L denotes sample thickness.

By measuring the thermal diffusivity and specific heat capacity of the samples, thermal conductivity could be calculated as

$$\alpha = \frac{\lambda}{pC_p} \qquad \textbf{Equation 3-2}$$

Where α denotes thermal diffusivity (m^2/s), p represents density (kg/m^3), C_p represents the specific heat capacity (J/kg-K) and λ is the thermal conductivity (W/mK).

Comparing the values of

$$\mathbf{Q = m\ C_p \Delta T\ reference = m\ C_p\ \Delta T\ sample} \qquad \textbf{Equation 3-3}$$

Where Q is the absorbed energy (J), C_p denotes sample specific heat capacity (J/kg-K) and m is the mass (kg). Sample thickness ranging from 1.0 mm to 1.5 mm were used and are recommended especially for samples which have a low specific heat capacity. Vespel™ of known thermal diffusivity, density and specific heat was used as the reference sample. The test samples were coated with graphite to improve the heat adsorption on the sample.

3.4.7 Bond shear testing

For the bond shear tests, test packages (comprising of test dies measuring 3 mm × 3 mm and bottom substrates of 5 mm × 5 mm) were sheared using a DAGE 4000 tester with a 100 kg load cell equipped with a standard flat push tip. A standard set of test conditions was used where shear speed was fixed at 50 μm/sec, tip landing speed was 300 μm/sec and a shear height of 150 μm was held at every start. When the samples were tested under hot shear condition, a bottom heater plate design was utilized and samples were heated to 250°C, held for 3 minutes before the shearing commenced. This allowed the heat to travel from the substrate to the bonding zone. For post ageing effects study, the samples were placed in an oven and dwelled at ageing temperatures of 250°C and 360°C, over 250 hrs and 500 hrs respectively before carrying out the shear tests. Shear test samples went through pre-testing X-ray inspections. Typically, no voids were observed. For those samples where small voids were detected, they were not used.

3.4.8 2D and 3D computed tomography X-ray imaging

2D and 3D computed tomography (CT) X-ray imaging were performed using Shimadzu SMX-2000 and SMX-100CT scanners with a voltage range of 70-100 kV and a current of 60-90 μA for various encapsulations. X-ray imaging is a non-destructive technique which allows observation of the metallizations within an encapsulated package, as well as possible ceramic cracks which may result after high temperature and high pressure stress exposures. Observation with rotation using the 3D CT X-ray imaging allows reconstruction of the package from the multiple images taken to accurately pinpoint regions of interest such as zone of crack initiation or propagation.

3.4.9 Nanoindentation Hysitron TI 950 TriboIndenter™

Nanoindentation is used to measure the elastic modulus of the sample. The equipment was equipped with a standard 2D transducer and a cube corner tip. Prior to experiment, the tip is calibrated with a standard fused quartz sample for the required contact depths. A load function with a 5s-2s-5s loading-holding-unloading time and a maximum load 500 μN was used for the experiment. Oliver-Pharr method [4] was used to calculate the elastic modulus of the sample over the unloading cycles. Ten indentations were

performed on each sample.

$$E_r = \frac{\sqrt{\Pi}}{2\beta} \cdot \frac{S}{\sqrt{A_c}} \qquad \textbf{Equation 3-4}$$

Where S is the contact stiffness, β is a dimensionless correction constant and A_c is the contact area between indenter tip and contacted sample surface.

3.4.10 Flexural test

Flexural measurements were performed Instron 5567 with the 30 kN load cell in a three point bend setup. The test was performed according to ASTM D790 "Standard Test Methods for Flexural Properties of Unreinforced & Reinforced Plastics & Electrical Insulating Materials", with the deflection rate set to 0.5 mm/min. The specimens were loaded until failure or until maximum load of 30 kN was reached. Specimens were made following the dimensions of 60 mm length, 12.70 mm width and 6.30 mm thickness.

3.4.11 Tensile test

Measurements were carried out using Instron 5567 with 30 kN load in tension setup. The tensile test was conducted according to ASTM D638 Standard Test Method for Tensile Properties of Plastics, with the extension rate set at 0.5 mm/min. The specimens were loaded until failure or until maximum load of 30 kN was reached.

Dog bone samples were made according to the dimension of 75 mm overall length, with gage length of 40 mm, 10 mm width at grip and 5.5 mm width at centre portion and 4.5 mm thickness.

The stress from flexural loading follows the bending moment rule and can be explained by Equation 3-5 [5]:

$$\textbf{Flexural Stress } (\sigma_0) = 6M / (bd^2) \qquad \textbf{Equation 3-5}$$

Where, *M* is the bending moment at mid-span due to mid-span load (*P*).

The bending moment, *M* is derived from: $M = PL / 4$

Where: b = width (mm), d = depth (mm), L = length of the support span of the beam (mm).

So, flexural stress can be expressed by Equation 3-6:

$$\textbf{Flexural Stress } (\sigma_f) = 3PL / (2bd^2) \quad \textbf{Equation 3-6}$$

Flexural strain for three point bend test is thus referenced [21] by Equation 3-7:

$$\textbf{Flexural Strain } (\varepsilon_f) = 6\,Dd / L^2 \quad \textbf{Equation 3-7}$$

Where, *D* is the deflection of the centre of the beam (mm)

The modulus of elasticity or flexural modulus was referenced [21] from the formula shown in Equation 3-8:

$$\textbf{Flexural Modulus } (E_f) = L^3m / 4bd^3 \quad \textbf{Equation 3-8}$$

Where, *m* is the tangent line of the steepest straight-line part of the load-deflection curve or the gradient (slope) of the load-deflection curve.

3.4.12 Compressive test

Measurements were carried out using Instron 8516 with 100 kN load cell in compression setup. The compressive test was conducted according to ASTM D695 Standard Test Methods for Compressive Properties of Rigid Plastics. Each successive test is carried out using a displacement rate of 0.5 mm/min. The specimens were then loaded until failure or when the maximum of 100 kN was reached. Specimens were formed by square-shaped mould with dimension of 14.00 mm width and 4.50 mm thickness.

3.5 Tests on PN composites as an encapsulation material

In the development of PN as an electronic packaging material, it is important to extend the characterization tests beyond its bulk properties, that is, the properties of PN as a standalone material. The following section describes the various experiments through which PN was subjected to, to more closely match the actual operating conditions which PN might be exposed to as a HTHE encapsulation material.

This includes high temperature conditions coupled to other factors such as pressure and humidity. Test methods are designed to suit parameters fitting to environmental test standards for military electronics equipment MIL-STD-883 as well as fire and toxicity test standards MIL-STD-2031 which define the conditions for harsh environment. The same test conditions are often used for materials and devices to be qualified for oil and gas industries due to the rigorous testing criteria.

3.5.1 High Pressure High Temperature (HPHT) testing

HPHT testing was carried out in a modified hot isostatic press (HIP) unit with electrical wirings for stressing and measurements as shown in Figure 3-5. Test temperature of 250°C and 300°C was utilized with a pressure of 173 MPa (25,000 Psi) and 207 MPa (30,000 Psi), respectively. The HIP unit is capable of fully pressurizing any packages up to a temperature of 500°C with a standard deviation of±5% in temperature and pressure within the 30 cm length of the loading stage, which is firmly attached to the middle of the test chamber.

The high pressure in the chamber was achieved by using argon as the medium. Ceramic test packages which were fully encapsulated were placed onto a carrier which was then plugged securely into the chamber and subjected to the desired test conditions. In addition, the same setup can be used to conduct *in-situ* stress tests monitoring up to 18 input and output channels using parallel connections of source measurement unit (SMU)/ digital multimeter (DMM) attached to the system.

Within chamber setup is as shown in Figure 3-5b, where 4 ceramic sockets can be mounted with 24 standard dual in line packages (DIP). Current or voltage stressing can be performed in-situ with high environmental pressures up to 240 MPa and temperatures up to 500°C. After stressing, samples which had failed visual inspections such as those with cracks were then further analyzed using optical microscopy, scanning electron microscopy (SEM), and 2D or 3D computed tomography (CT) X-ray analysis.

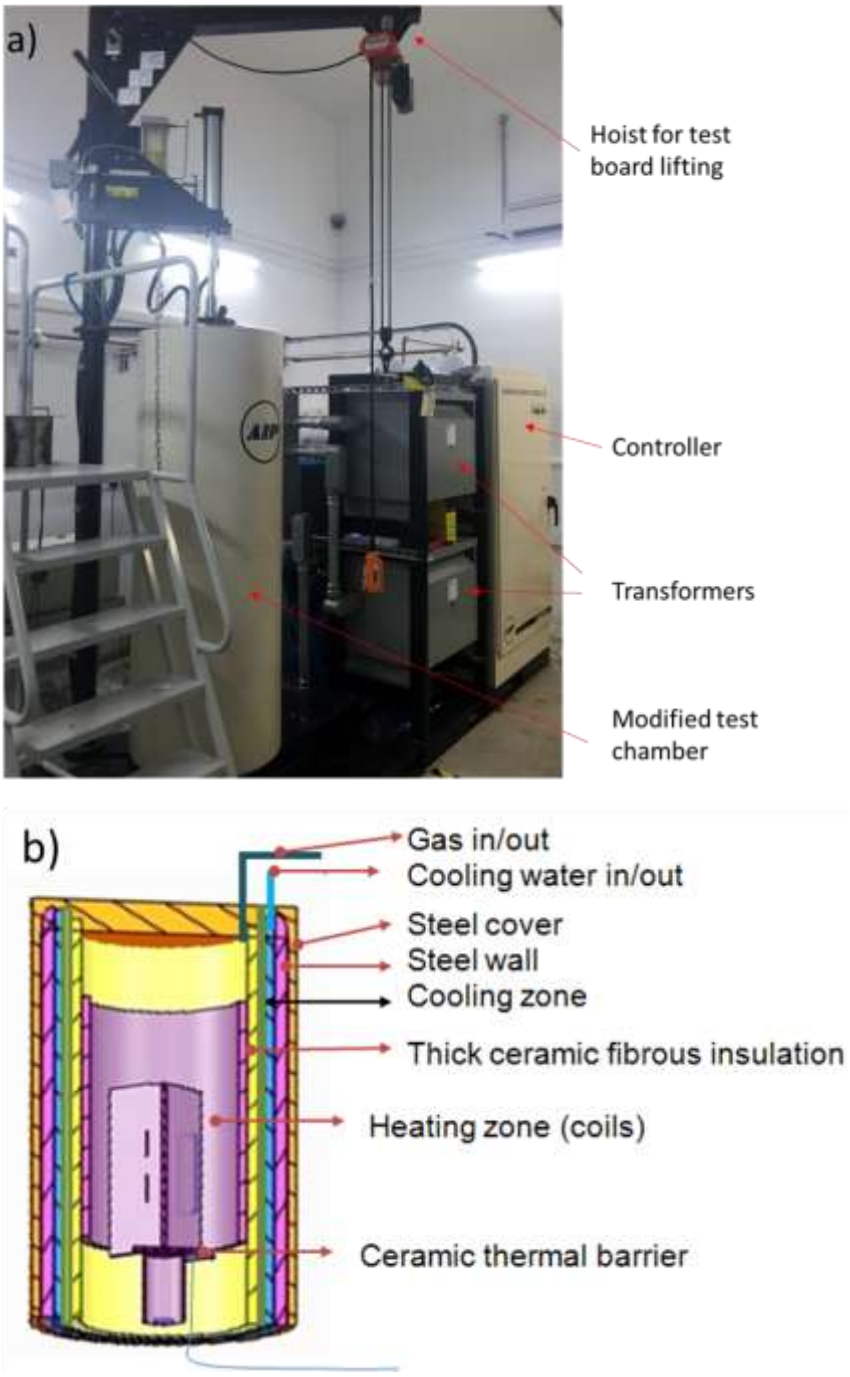

Figure 3- 5 (a) Picture of the HPHT environment tester used to characterize the PN composites as a HTHE encapsulation material (b) Interior design of the chamber setup

3.5.2 High Pressure (HP) testing

For cold isostatic press (CIP) modified high pressure (HP) tests, the test packages were wrapped in nitrile balloons and subsequently filled with deionized water that surrounded the test package as shown in Figure 3-6. This created a direct transference of stress from the environment to the package, which would press uniformly on the test package. The

package would then fracture mechanically if the surrounding pressure exceeded the maximum strength of the package material. Preferred loading is set into the controller and applied with the samples removed at each loading phase to check for signs of failure. With this setup, pressures of up to 30,000 Psi (207 MPa) could be applied.

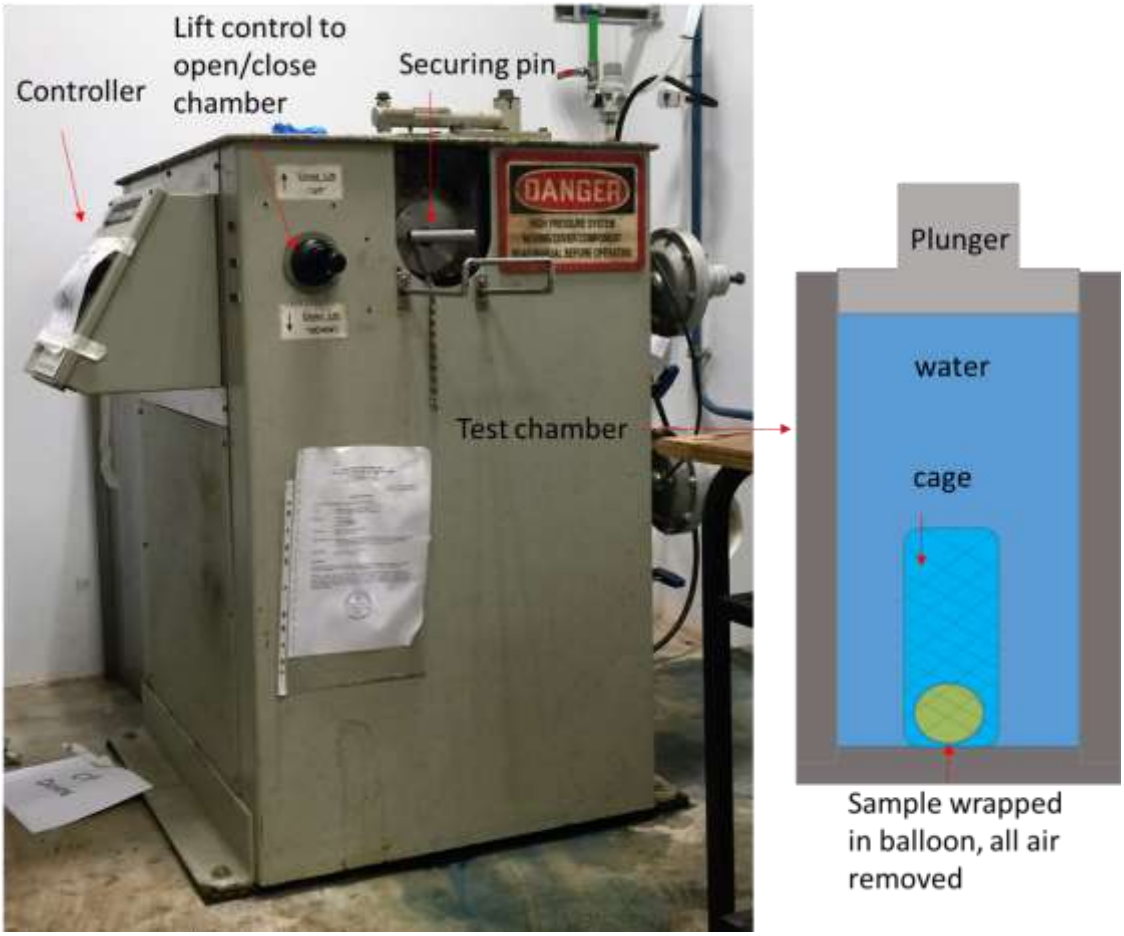

Figure 3- 6 Modified testing with CIP equipment setup.

3.5.3 Humidity testing

The behavior of PN composites in humid environment was studied by subjecting the test packages to 85% RH and 85°C (under MSL level 1 testing) using a humidity chamber manufactured by Sanwood™. The ramp rate was kept to 0.1%RH/min and 1°C/min and was set to automatic tuning. This helped to rapidly compensate any deviations in the system parameters during package or material stressing.

3.6 Simulation testing

In this thesis, mechanical simulation was performed through the use of multiphysics

modules to simulate effects of various mechanical and thermal test loads on the samples. Results are also correlated with selected test measurements to validate the accuracy of simulation. Structural mechanics were performed on ANSYS™ platforms with the drawing done either in Solidworks™ or in Workbench™. Structural analysis was accomplished using structural mechanics where Rankine's model was utilized for maximum principle stress calculations. This is essential for modelling on brittle materials and even for polymeric materials which do not exhibit elastic behavior prior to failure.
In the simulations, maximum principle stress theory was utilized and calculates the value where a material reaches its maximum elastic strength in simple tensile and can be represented with Equation 3-9:

$$\alpha_1 = \frac{1}{2}\left(\alpha_x - \alpha_y\right) + \frac{1}{2}\sqrt{\left(\alpha_x - \alpha_y\right)^2 + 4\,\tau_{xy}{}^2} \qquad \textbf{Equation 3-9}$$

Where α_x and α_y are maximum principle stresses in *x* and *y* directions and τ_{xy} denotes shear stress in *xy* plane.

As shown in Figure 3- 6, hybrid grid was used comprising tetrahedral and quadrilateral meshing. Quadrilateral meshing was preferred to make the meshing more structured. In addition, a fine mesh was applied to increase accuracy. However, this came with an increase in computational time. Figure 3-7a shows a tetrahedral mesh and Figure 3-7b shows a quadrilateral mesh. Figure 3-7c shows the overlay of meshing onto the actual test designs on ANSYS.

3.6.1 Gaussian09 DFT calculations

The structures and transition states of the PN monomers reactions were fully optimized using the ωB97x-D [6] density functional method together with the 6-31G** basis set. The ωB97x-D functional was chosen as this empirical functional is better suited than normal hybrid DFT methods (e.g. B3LYP) in handling kinetics, thermodynamics, and non-covalent interactions. Frequency analyses were performed on all ωB97x-D /6-31G** optimized geometries to confirm the nature of the stationary points as minima structures with all real frequencies. Single point calculations with ωB97x-D/6-311+G** based on the gas-phase ωB97x-D /6-31G* optimized geometry was taken for the relative enthalpy energies reported. All calculations were performed using the Gaussian 09 suite of programs [7].

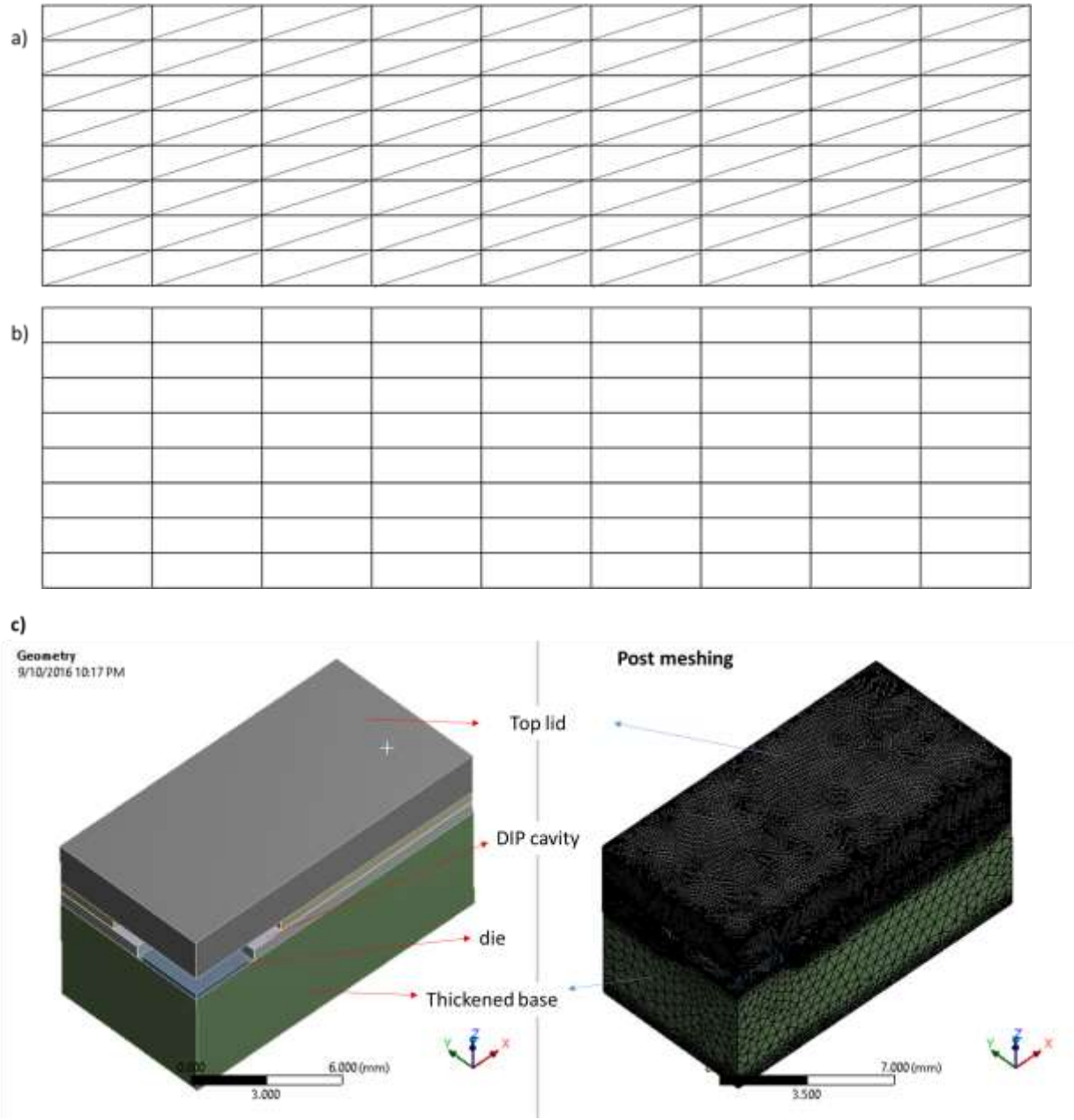

Figure 3- 7 Different types of mesh utilized in ANSYS™ **(a)** tetrahedral mesh **(b)** Quadrilateral mesh and **(c)** overlay of meshing with test sample drawing.

3.7 Curing profiles of PN systems adopted for research studies

Figure 3-8 shows the curing profile of PN based system where the curing of the PN matrix with or without fillers are treated to the same curing time mentioned.

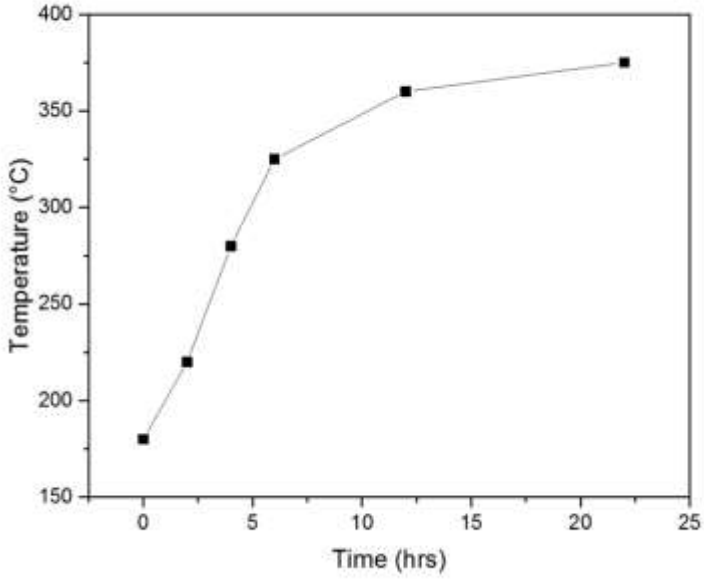

Figure 3- 8 Curing profile of PN based systems adopted.

The curing profile as shown in Figure 3-9 was adopted for the experiments in this study. A first melting temperature of about 181°C that first aims to liquefy the monomer powder. At this stage, only melting takes place and no other reactions were observed. It can be seen from the DSC curve that all the energy at 181.62°C was absorbed by the powder for melting to take place. Heating beyond this temperature without holding the temperature did not give time for the polymer to cross link as shown in Figure 3-9, where no further endotherms are observed.

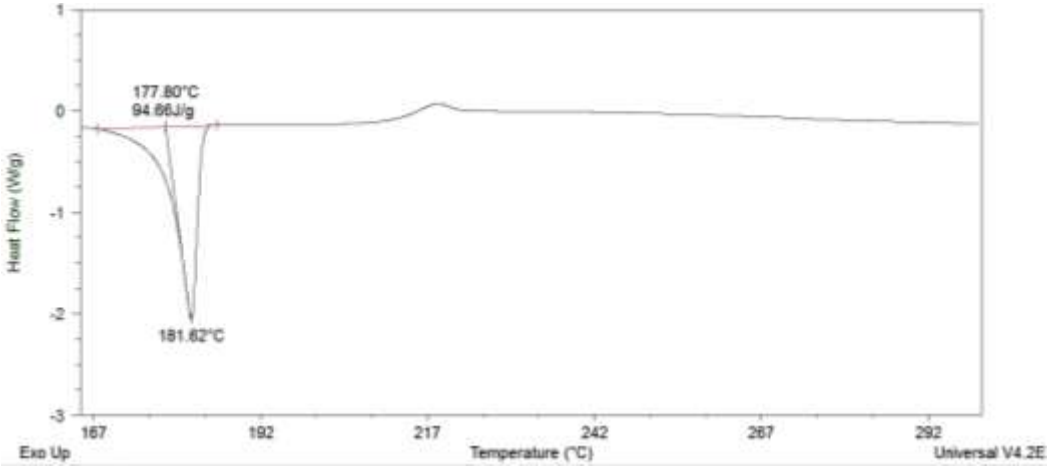

Figure 3- 9 DSC curve for neat PN without any fillers.

At 220°C, the first cross linking occurs as the monomer first starts to cross link and forms the prepolymer. At this stage, it is suitable for fillers to be mechanically blended and prolong stirring would help to keep the filler particles dispersed within the polymer matrix. The blend was then cooled from 220°C to room temperature. It could be further pulverized mechanically to form a prepolymer powder blend which is ready for use as molding compound.

Beyond 220°C, the crosslinking of triazine and phthalocyanine takes place quickly to the point where a strong bulk polymer forms, which is dark green in color. Each curing duration helps to increase the triazine and phthalocyanine cross linking tremendously and the effect is enhanced with a longer curing duration.

References

[1] M. Bajpai, V. Shukla, and F. Habib, "Development of a heat resistant UV-curable epoxy coating," *Prog. Org. Coat.*, vol. 53, no. 4, pp. 239–245, Aug. 2005.

[2] E. R. Salmon, Encapsulation of Electronic Devices and Components. CRC Press, 1986.

[3] W. J. Parker, R. J. Jenkins, C. P. Butler, and G. L. Abbott, "Flash Method of Determining Thermal Diffusivity, Heat Capacity, and Thermal Conductivity," *J. Appl. Phys.*, vol. 32, no. 9, pp. 1679–1684, Sep. 1961.

[4] Oliver, W.C. and G.M. Pharr . "An improved technique for determining hardness and elastic modulus using load and displacement sensing indentation experiment." Journal of Materials Research 7:1564-1583,1992

[5] R. Gordon and J. G. Ciallella, "Ceramic lid assembly for hermetic sealing of a semiconductor chip," US4291815 A, 29-Sep-1981.

[6] J.-D. Chai and M. Head-Gordon, "Long-range corrected hybrid density functionals with damped atom–atom dispersion corrections," *Phys. Chem. Chem. Phys.*, vol. 10, no. 44, pp. 6615–6620, 2008.

[7] M. Frisch, "Gaussian 09 Citation," 2009. [Online]. Available: http://www.gaussian.com/g_tech/g_ur/m_citation.htm. [Accessed: 07-Sep-2015].

Chapter 4

Investigation on the Thermal Degradation Behaviour and Bond Formations in PN and Fillers

Resorcinol based phthalonitrile (PN) is sensitive to its processing temperatures while its liquefying is controlled by melting temperature. Typically, the melting temperature begins at 180°C, which is much lower compared to other forms of phthalonitrile. The viscosity of PN is much lower than epoxies and has already been studied previously by Liu et. al [1]*. This study goes further to investigate the thermal behavior of PN through the addition of both silica and alumina fillers, and explores PN material suitability as a microelectronics packaging material. It provides a comprehensive research of the various thermal properties of PN and aims to reveal material properties through kinetic studies using Kissinger's equations. FTIR is also utilized to identify possible new bond formations and Gaussian09 simulations are used to explore the feasibilities of the reactions.*

4.1 Evaluation of neat and filled PN under various temperature curing using TGA

The evaluation of PN is performed based on Kissinger equations [2,3] to study the effect of various heating rates on the thermal degradation of neat and filled PN polymers. This helps to build an understanding of the activation energies involved.

4.1.1 Thermal degradation studies using TGA in air

TGA analysis was performed on samples cured to final temperature of 280°C and 360°C to monitor their weight change at dwelling temperature of 300°C and 500°C over 2 hours. As shown in Figure 4-1(a) at dwelling temperature of 300°C, more degradation was observed for PN which were cured at lower temperatures.

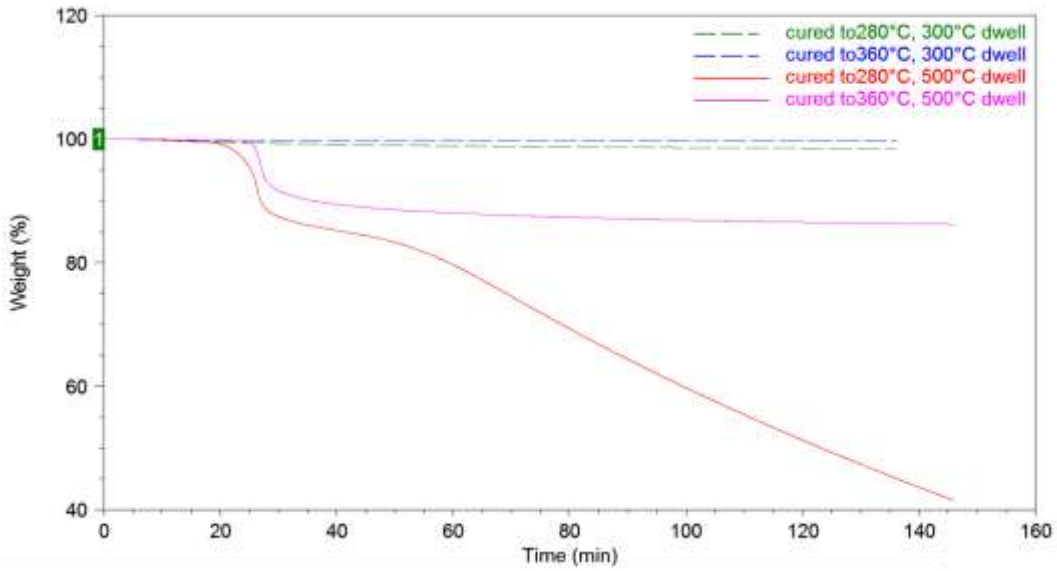

Figure 4- 1 Graph of neat PN weight % against time for 300°C and 500°C dwelling.

At longer and higher temperature curing, triazine and phthalocyanine from PN undergo a higher crosslinking which explains why the 360°C cured samples experienced a slower weight loss even at 300°C holding temperature as compared to samples cured to only 280°C. The change in weight percentage is more obvious when the dwelling environment is switched to 500°C. However, it still clearly shows that higher curing temperature of 360°C produces a structure with a higher modulus as compared to a lower curing temperature of 280°C.

4.1.2 Degradation Kinetics of neat PN

The DTGA graph as shown in Figure 4-2 represents the derivative of the TGA graph. The peak of the DTGA graph was taken to represent the maximum temperature (T_{max}) at which the energy required to degrade the polymer is reached. This is also the temperature at which maximum polymer degradation is possible.

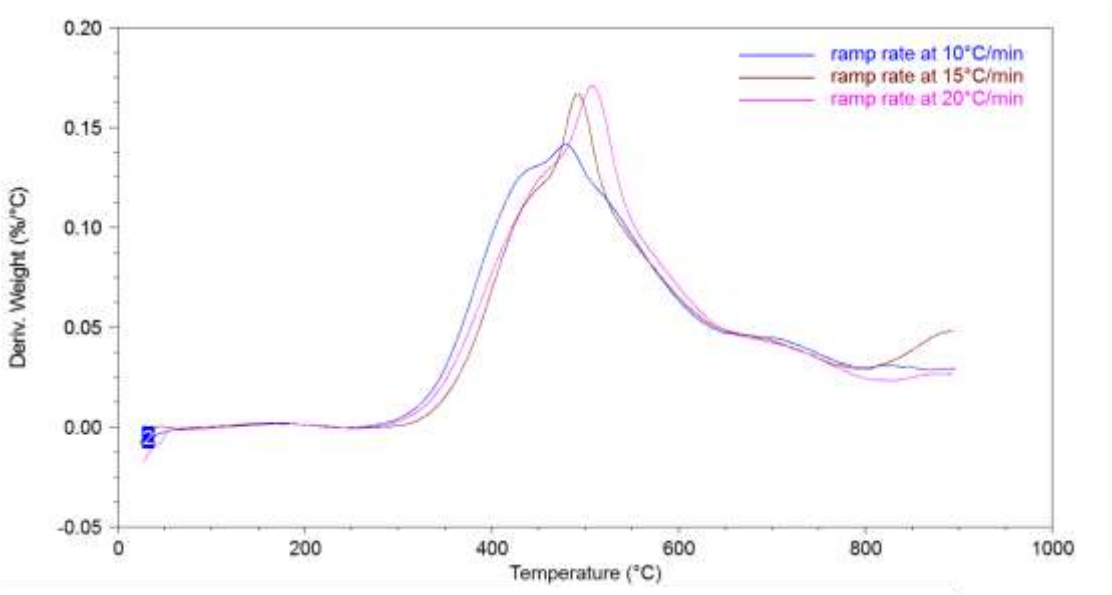

Figure 4- 2 DTGA graph 280°C cure under nitrogen gas.

From Figure 4-2, it could be seen that T_{max} shifted to a higher temperature at higher ramping rate. The temperatures of the main DTGA peaks were selected and used as T_{max} values to calculate the activation energy (E_a) by employing the Kissinger equation[31].

$$ln\frac{\alpha}{T_{max}^{2}} = \ln\left(\frac{nRAW_{max}^{n-1}}{E_a}\right) - \frac{E_a}{RT_{max}}$$

Where α is the heating rate, T_{max} is the temperature at the maximum rate of weight loss, n is the apparent reaction order, R is the universal gas constant and W_{max} is the residual weight at maximum rate of weight loss. With T_{max} values, activation energy can be found from the gradient of a plot of $ln\frac{\alpha}{T_{max}^{2}}$ vs. $\frac{1}{T_{max}}$ x 1000. Table 4-1 to Table 4-3 display the calculation leading to the derivation of activation energy of the various cured samples. The gradient ($\frac{E_a}{R}$) was fitted from the graph plotted, and E_a could be calculated correspondingly.

Table 4- 1 250°C cure Kissinger Equation values under nitrogen

	T_{max} (°C)	Y-axis ($ln\frac{\alpha}{T_{max}^2}$)	X-axis ($\frac{1}{T_{max}}$ x 1000)
10 °C/min	468.06	-9.99	2.14
15 °C/min	483.87	-9.66	2.06
20 °C/min	494.12	-9.41	2.02

Table 4- 2 280°C cure Kissinger Equation values under nitrogen

	T_{max} (°C)	Y-axis($ln\frac{\alpha}{T_{max}^2}$)	X-axis($\frac{1}{T_{max}}$ x 1000)
10 °C/min	485.56	-10.96	1.32
15 °C/min	493.02	-10.57	1.30
20 °C/min	499.22	-10.30	1.29

Table 4- 3 300°C cure Kissinger Equation values under nitrogen

	T_{max} (°C)	Y-axis($ln\frac{\alpha}{T_{max}^2}$)	X-axis($\frac{1}{T_{max}}$ x 1000)
10 °C/min	484.24	-10.06	2.07
15 °C/min	498.65	-9.72	2.01
20 °C/min	508.57	-9.47	1.97

Figure 4-3 shows the Kissinger plots of thermal degradation in nitrogen for systems with different curing temperatures. E_a and the corresponding T_{max} are summarized in Table 4-1, 4-2 and 4-3. The sample with the highest curing temperature has the highest E_a as the bonds are stronger due to more physical cross-linking, thus requiring more thermal energy to break. On the other hand, adding fillers also have the effect of lowering activation energy. From Table 4-4, lower E_a values are recorded for PN loaded with 50 weight percent fillers, with 50 weight percent alumni PN having the lowest activation energy. The lower E_a suggests that the fillers not only improve mechanical strength of the

material but also has a catalyzing effect in the reaction by lowering the energy barrier to form new polymer crosslinks.

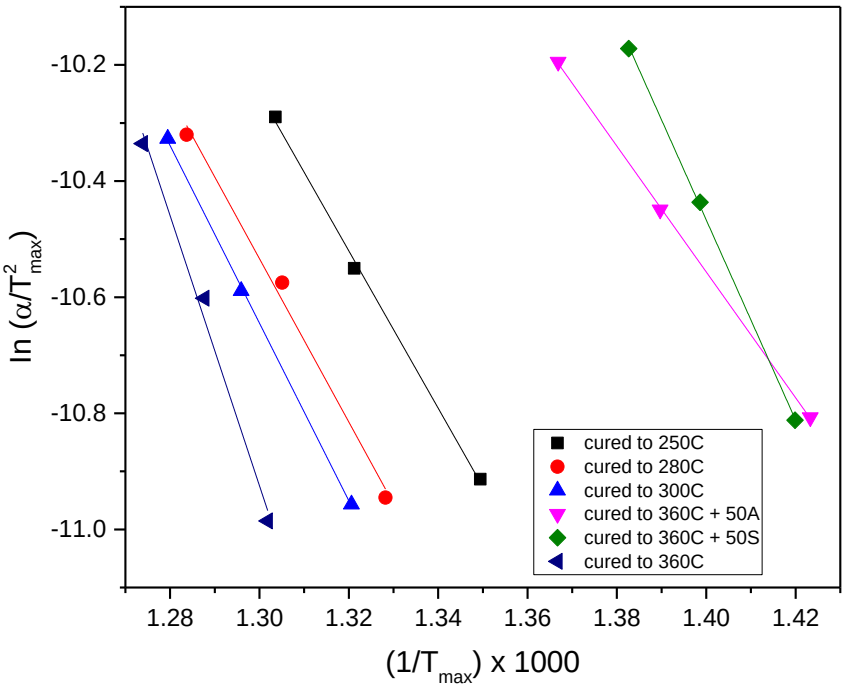

Figure 4- 3 Kissinger plots of thermal degradation in nitrogen ambient.

Table 4- 4 Summary of T_{max} and activation energy on PN and fillers in nitrogen

Nitrogen T_{max} (°C)						
	250°C cure	280°C cure	300°C cure	360°C cure	360°C+50A	360°C+50S
10°C/min	468.06	485.56	484.24	495.14	429.60	431.30
15°C/min	483.87	493.02	498.65	503.6	446.59	442.31
20°C/min	494.12	499.22	508.57	512	458.61	450.25
R^2	0.9986	0.9928	0.9996	0.9908	0.9998	0.9997
Gradient	13.54	14.064	15.29	23.255	10.832	17.229
E_a(kJ/mol)	112.62	116.94	127.13	193.36	90.01	143.06

4.1.3. TGA studies of PN with silica fillers

Figure 4-4 clearly shows that total weight loss decreases with increased weight % of fillers. Although this can be attributed to the higher weight percent of the fillers which does not degrade in TGA at the 500°C test temperature, considering that the weight percent of PN shows that the decrease in polymer weight percent decreased with higher loadings. This effect can be attributed to new interactions which lead to new bond formations between fillers and the polymer matrix. It is noteworthy that even with different amount of filler loadings, the chemical bonds in the composites should be the same. Thus, heating up to 900°C in the TGA, the decomposition pathway should be the same.

Figure 4-4 shows that weight losses are minimized with higher weight percent of fillers. The average loss for neat PN is approximately 5% and the average 5% loss applies if consideration is given only to the weight percent of PN loss only. The remaining weight for 5 weight percent loss of 10 weight percent silica filled PN should be at 95.5 weight percent remaining. But actual weight percent remaining is higher as observed in Figure 4-4 which implied that strong bonds have formed between silicon atom and polymer. Having a smaller than the average loss of neat PN implies that there are more bond interactions between the PN and fillers than the PN moieties itself.

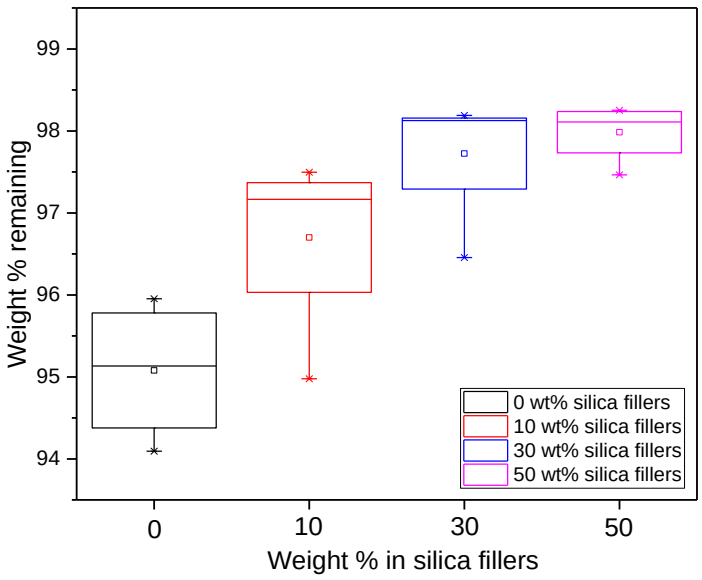

Figure 4- 4 Thermal stability of PN with different amount of silica fillers.

4.1.4 TGA studies of PN with alumina fillers

Figure 4-5 clearly shows that total weight loss decreases with increased weight percent of fillers. Although this can be attributed to a higher weight percent of fillers which does not degrade in the TGA at the 500°C test temperature, examining just the weight percent of PN shows that the net decrease in the polymer also decreased with higher loadings.

This effect can be attributed to new interactions which lead to new bond formations between fillers and polymer matrix. Figure 4-16 shows that weight losses are minimized with higher weight percent of fillers.

Higher filler loading will lead to more bonds creation between PN moieties and filler molecules. The weakest point in the filler-PN composite is still within PN polymer since it will degrade faster than the fillers. Bonding between PN and fillers may also affect thermal stability although the PN moieties interaction amongst itself is still the main contributor to the thermal stability.

An optimal amount of fillers is however required for bonding as indicated where 50 weight percent alumina loading shows little difference in the average weight percent loss from 30 weight percent alumina loading as shown in Figure 4-5.

For alumina, the viscosity of the mixture increased significantly when 50weight percent of alumina was added and this could affect the curing of PN. A similar effect has been discussed using the Eshelby Effective Inclusion Method (EIM) by Wang *et. al* [4]. Viscosity measurements for both alumina and silica fillers added can be found in Appendix A section 1.4.

Further treatise to the bond energy would be covered in section 4.4. To date, research has not been able to quantify the exact amount of triazine and phthalocyanine components formed [1] at each stage of curing, primarily due to equipment limitations.

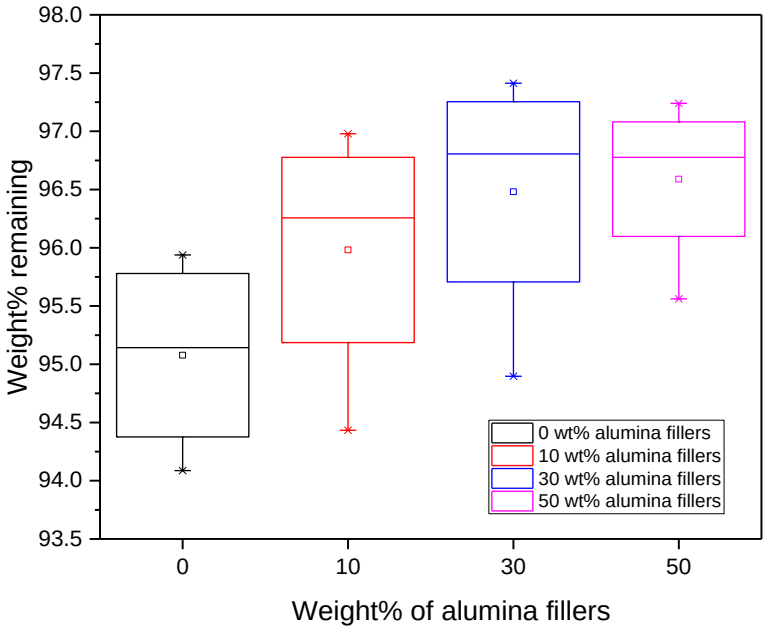

Figure 4- 5 Thermal stability of PN with different amounts of alumina fillers.

4.2. Characterization of Chemical Bonds of PN and its composites

The chemical bonds in PN and its composites with different weight percent of alumina or silica fillers were characterized using FTIR in attenuate total reflection (ATR) mode. The transmission peaks of resorcinol based phthalonitrile were evaluated to check for signs of bonding between fillers and PN after heat treatment. Samples which were cured at different temperatures are analyzed in the following sections.

4.2.1 Bond changes observed in Neat PN

For neat PN, all FTIR spectrums display transmission bands at 1008 cm^{-1} which indicates phthalocyanine, and at 1360 cm^{-1} and 1520 cm^{-1} which indicate presence of triazine ring structure. These peaks become more intensified with higher curing temperatures, due to the elevated treatment temperatures which increased the triazine quantities.

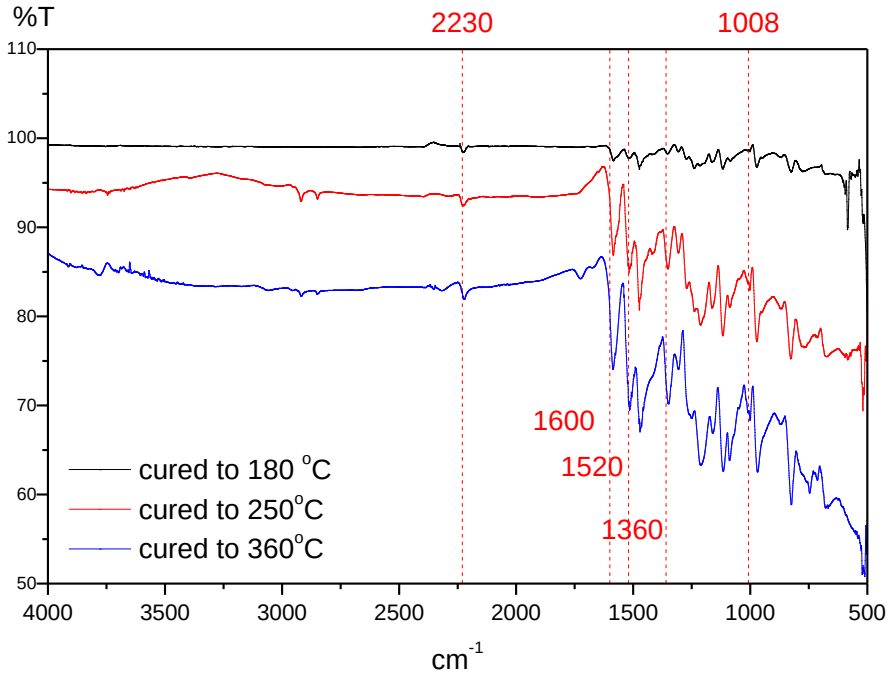

Figure 4- 6 FTIR spectrum of neat PN after curing at various temperatures.

Heating the chemical 4,4'-bis (3,4-dicyanophenoxy) biphenyl mixed with minute quantities of amidine salts or aromatic amines allows well crosslinked polytriazine to be obtained. Polytriazine is also obtained when bisphthalonitriles [5, 6] are cured along with amines. Aromatic amine or amidine salts enhances cross linking reactions amongst polymer products more readily. Based on models, self-reactions of phthalonitrile with salts or amines have also been studied in depth.

In tandem, it is proven that poly [4-(2-cyanophenyl)-1, 3, 5-triazine-2, 6-diyl-1, 2-phenylene] is generated faster with the utilization of salts. The results were mentioned by Liu *et. al* [1] where the intensity of C≡N absorption peak at 2230 cm^{-1} gradually diminished upon heat treatment [7] on neat samples of PN and without filler addition. The peak at 1600 cm^{-1} represents the aromatic structure vibration.

FTIR peaks at 1008 cm^{-1} indicated presence of phthalocyanine whereas 1360 cm^{-1} and 1520 cm^{-1} indicated the presence of triazine ring structures. These peaks can be seen to increase in intensity when curing temperature is raised from 250°C to 360°C, indicating the formation of more complex moieties. Results are also reflected in Figure 4-6 where

the relative intensity of 2230 cm^{-1} compared to the reference peak 1600 cm^{-1} decreased with increased curing. The weak peak observed at 2230 cm^{-1} for the sample post-cured up to 360°C is due to its unreacted C≡N groups [8].

4.2.2 Bond changes observed in Silica-Filled PN

Figure 4-7 shows the FTIR spectrum of different weight percent silica added to PN and treated to various high temperatures. At 10 weight percent silica as shown in Figure 4-7(a), most of the product peaks do not show up as clearly as compared to higher filler loadings despite heat treatment to high temperatures of up to 360°C. This could indicate that the amount of silica particles had not reached critical concentration levels for FTIR to pick up the vibrational or stretching energies from newly established bonds, between silica particles, triazine and phthalocyanine.

The silicon-oxygen covalent bond vibration occurs primarily in the range of 1000 cm^{-1} to 1200 cm^{-1}. Si–O–Si asymmetric stretching vibration is represented at 1055 cm^{-1}. This peak, which also exhibits the biggest change in intensity in the spectrum, describes the dense silica network where the oxygen atoms become bridges between each two silicon sites [9]. In addition, as shown in Figure 4-7(c) the symmetric stretching vibration of Si–O–Si occurs at 685 cm^{-1}.

The peak at around 825 cm^{-1} indicates the symmetric stretching vibration of Si–O bond [9]. By comparing the spectrum of neat PN with 30weight percent silica as shown in Figure 4-7(b), it can be observed that there are increases in intensity between Si (on silica) to O (on polymer structure) at 685 cm^{-1}, 800 cm^{-1} and 1055 cm^{-1}. The increase in the intensity can also be partially attributed to broken Si-O-Si structures on silica.

For prolong curing periods at high temperatures, Si-N bonds are observed to be formed. Since these bonds are not highly polarized, their characteristic peak is not sharp. For silica where the permanent bonding form resembles that of Si-N bond, an FTIR absorption peak mainly at 811 cm^{-1} is indicative that formation of Si-N bonds has occurred for all of 10, 30 and 50 weight percent of fillers.

Other peaks such as 811cm^{-1} [12] and 848 cm^{-1} up to 900 cm^{-1}[13] are also indicative of Si-N bond presence, which are clearly observable in Figure 4-7(a) and Figure 4-7(b), beyond which the overlap from Si-O bonds starts to obscure the observation.

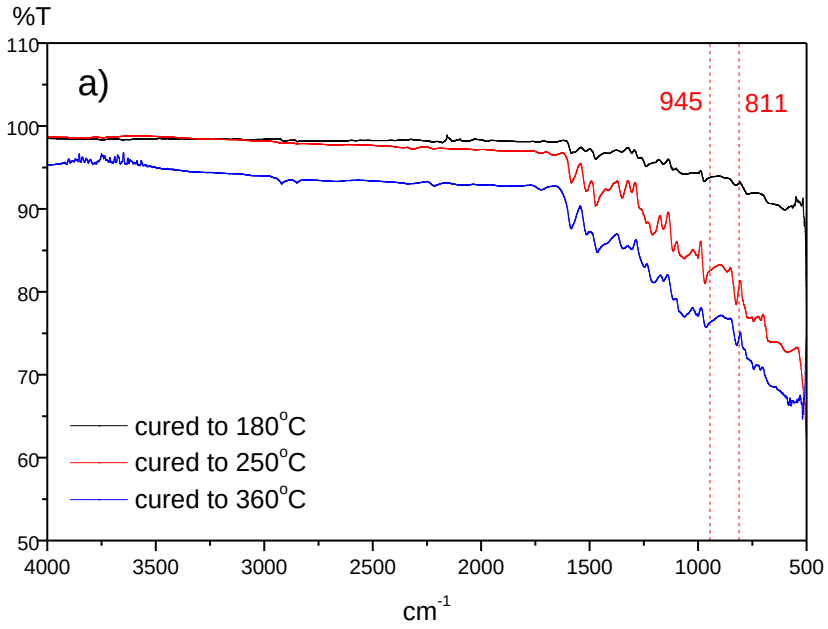

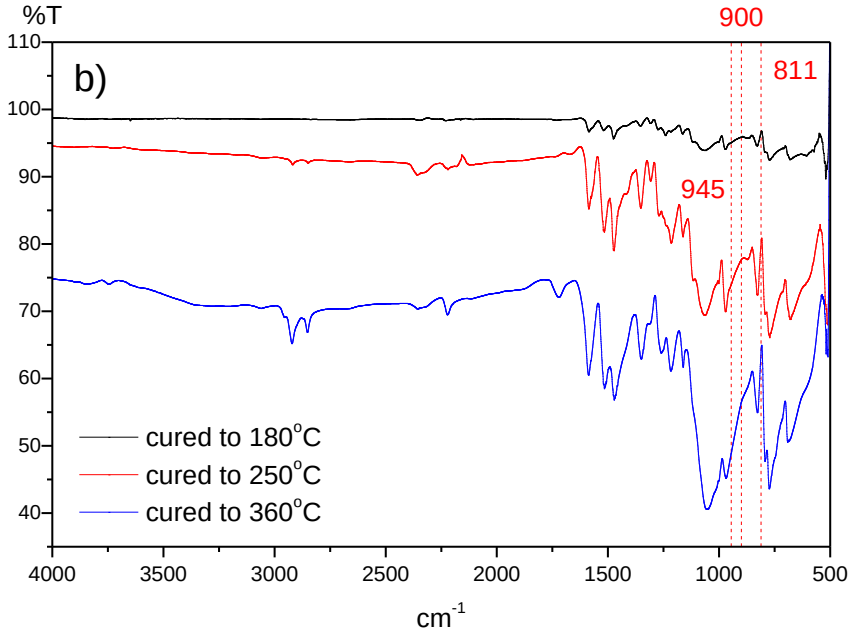

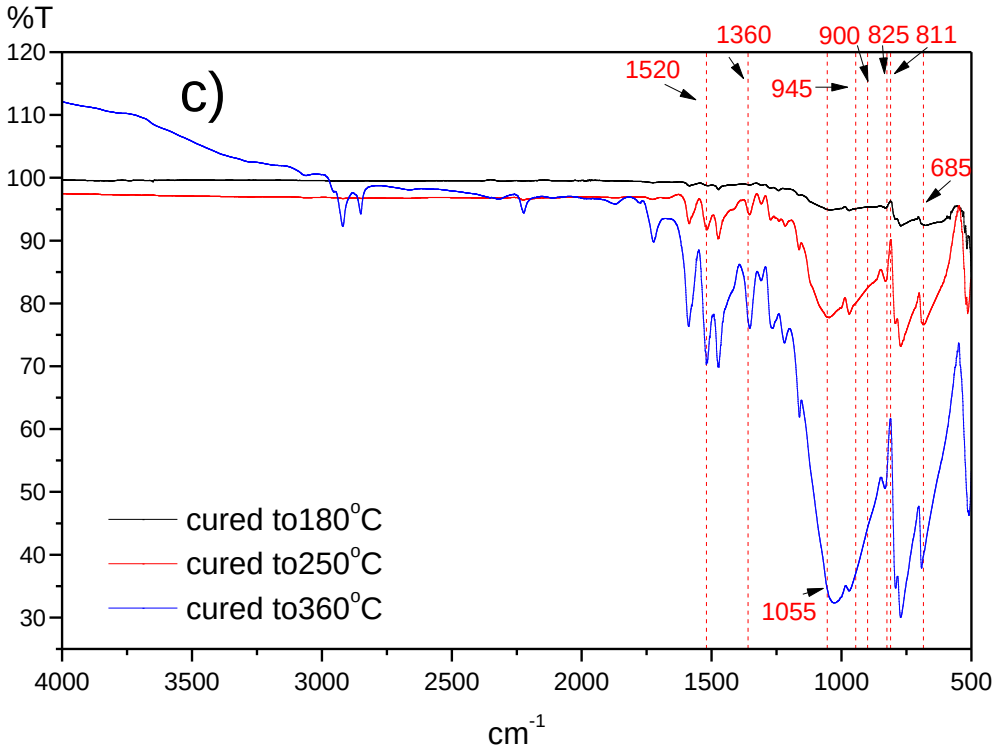

Figure 4- 7 FTIR spectrum of Phthalonitrile with different weight percent (wt %) silica at different curing temperatures **(a)** 10 wt% **(b)** 30 wt% and **(c)** 50 wt%.

4.2.3 Bond changes observed in Alumina-Filled PN

Figure 4-8a to Figure 4-8c show the FTIR results of phthalonitrile-alumina composites at different curing temperatures. The transmission peak at 580 cm^{-1} is the characteristic peak for Al–O stretching vibration in Al_2O_3 [10]. The stretching vibration of Al=O, which appears at 1350 cm^{-1} [11], overlaps with the peak at 1360 cm^{-1} (from triazine ring structure), which makes them difficult to be distinguished.

Both peaks mentioned became more intense at higher temperature treatments and with more alumina added. However, the former is more significant as it signifies that bond changes have taken place and that the bond changes could imply bonding between triazine, phthalonitrile and isoindolenine components of PN with alumina particles.

With reference to Figure 4-8(a) to Figure 4-8(c), Al-N bonds are not very infra-red (IR) sensitive, as such picking them up is more challenging, especially for the samples which

were cured at higher temperatures of 360°C. In addition, at lower filler concentrations below 10 wt%, fillers are sparsely distributed on the surface. As ATR is a reflection technique which does not penetrate deeply from the surface, this may lead to a weak or no signal detected for low filler concentration of PN. For Al-N bond, the adsorption lies between 741 cm^{-1} and 755 cm^{-1}[14]. Adsorption peaks at 665 cm^{-1} for high purity AlN films were reported by Vanbuskirk *et. al* [15].

At various percentage fillers and various curing stages, it can be observed that the Si-N and Al-N peaks increase for both silica and alumina, respectively. These results will be further verified by DFT simulations which predicted the possible Si-N bonds and Al-N bonds as shown in the next section.

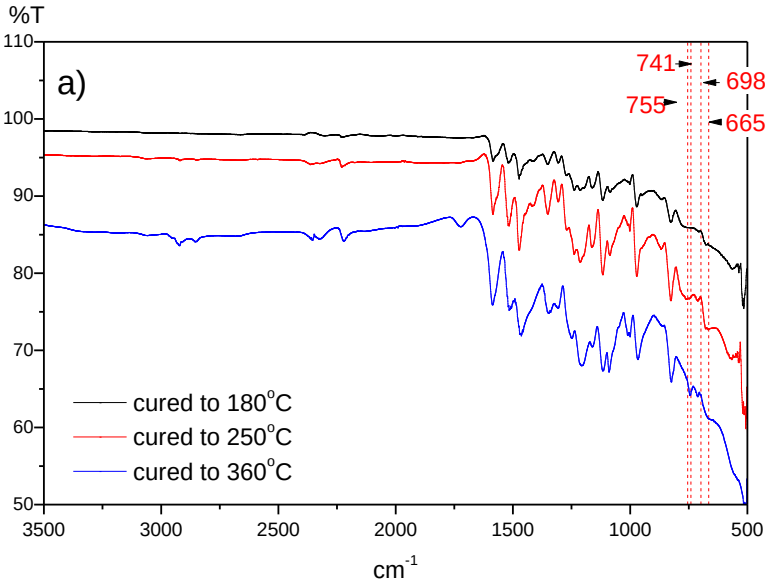
%T
a)
741
698
755
665
cured to 180°C
cured to 250°C
cured to 360°C
cm-1

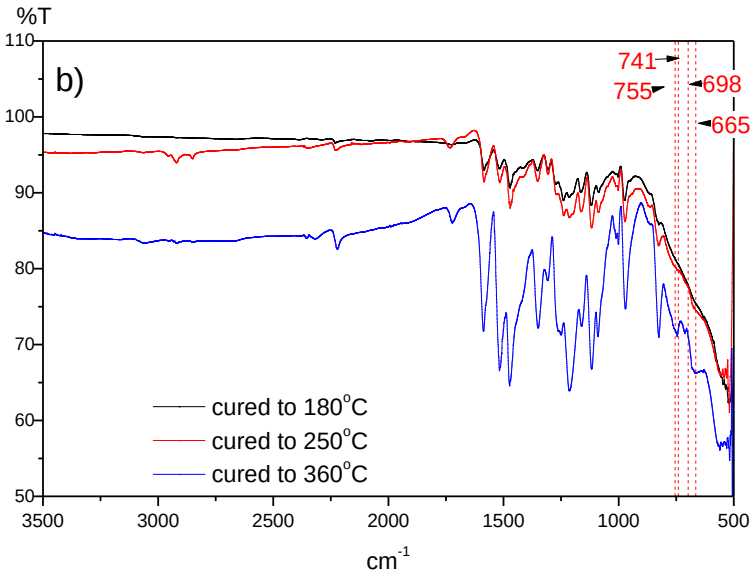
%T
b)
741
755
698
665
cured to 180°C
cured to 250°C
cured to 360°C
cm-1

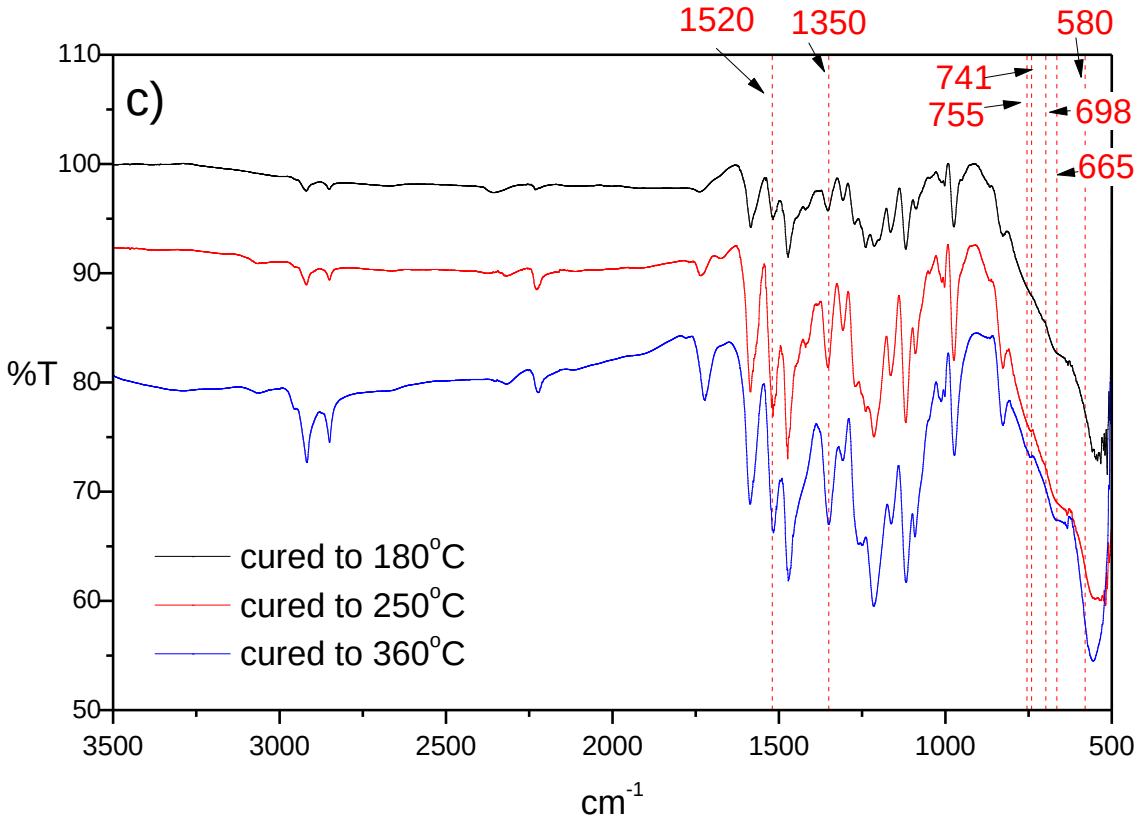

Figure 4- 8 FTIR spectrum of Phthalonitrile with different weight percent (wt%) alumina at different curing temperatures **(a)** 10 wt% **(b)** 30 wt% and **(c)** 50 wt%.

4.3 DFT calculations for thermodynamic stability of possible polymerization products in PN-filler composites

Gaussian 09 is an electronic structure program capable of modeling the molecular properties of reactive systems which include molecular energies, structures and electron densities. Using density functional theory (DFT) methods, reaction and equilibrium enthalpies are computed to predict the energetic feasibility of different reactive pathways in the polymerization as shown in Figure 4-9.

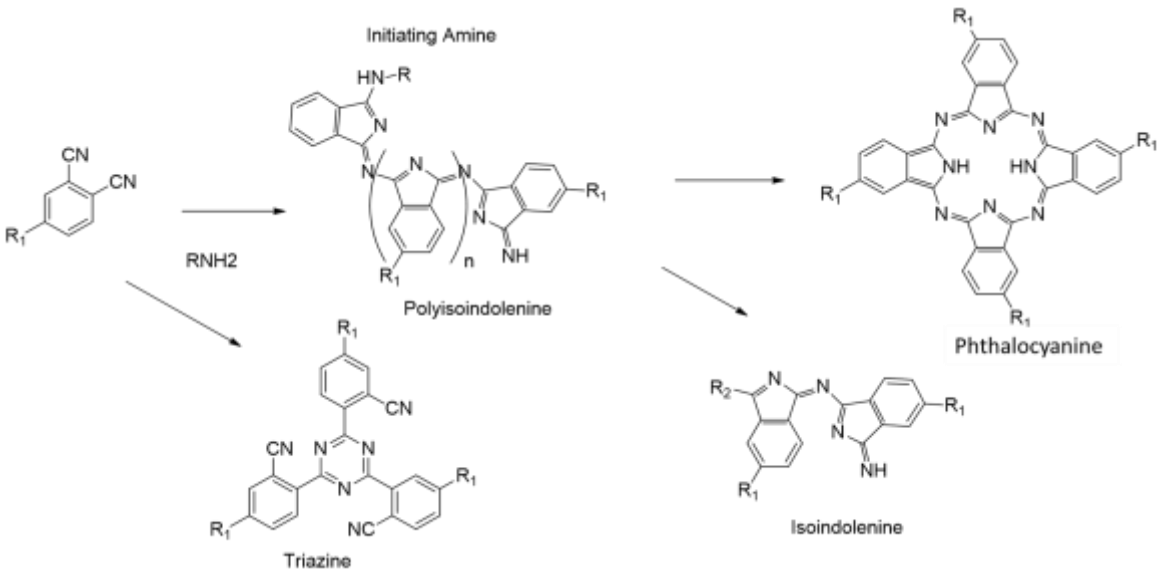

Figure 4- 9 Possible reactive pathways during polymerization of PN

When the monomers for the PN filler are subjected to high temperature, 3 different reactive mechanisms take place to produce 3 possible products; triazine, phthalocyanine and isoindolenine [16]. The polymerization is initiated with a base and propagated via two mechanisms; the formation of conjugated macromolecular chain of polyisoindolenine which then through concerted reactions forms either isoindolenine or phthalocyanine, or via the rapid cyclization of nitrile groups on the monomers to form triazine. These reacted functional groups form the building block of the polymer which can fill up nanogaps between molecules, increasing its thermal resistance [1].

The presence of these gaps was postulated by Snow *et. al* [18] through moisture absorption observations when bis(phthalonitriles) molecules were left in air. This phenomenon would be further substantiated in later sections where the nanogap size is calculated for triazine formation. The 3 different possible polymerization products will have different optimized interactions with the alumina and silica functional groups in the different type of fillers used in the experiments. Enthalpic stability of the silica and alumina adduct with the three possible products is calculated and enthalpy of formation is shown in Figure 4.11 – 4.13. A thermodynamically stable structure will possess a negative enthalpy (ΔH).

As discussed in the earlier section, chemical bonding is detected using FTIR between both the alumina and silica with the PN filler. To determine which possible polymerization products will form energetically favorable bonds with the alumina and silica, small clusters of alumina and silica were used in the calculations (Figure 4-10). Due to the critical need of water in catalyzing the bond formation between PN and the oxides, it is postulated that a condensation reaction occurs between the hydroxylated metal oxide and PN.

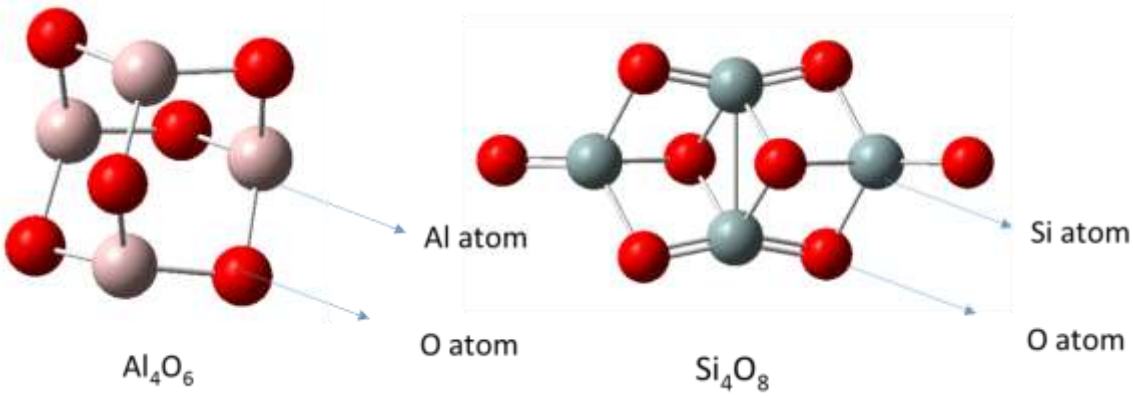

Figure 4- 10 Metal oxide cluster for Alumina and Silica.

All the optimization were performed at 453 K (180°C) as this is the minimal temperature that the monomers require to melt and start to react. Gibbs free energies can be calculated to study the thermodynamic feasibility of a reaction product.

With reference to Gibbs free energy equations where:

$$G = H - T\Delta S \qquad \textbf{Equation 4-1}$$

Where G is Gibbs free energy, H is enthalpy of the system, T is temperature measured in Kelvins (K) and S is entropy of the system. Entropic contribution (S) is small in this calculation since the calculation takes into consideration a polymeric system which differs greatly from gases or solute molecules, as such $G \approx H$.

In this case where ΔH is -163 $kJmol^{-1}$ for alumina and -108 $kJmol^{-1}$ silica particles, it is a strong indication that spontaneous reaction is possible and therefore bonding between triazine and silica or alumina particles is possible.

(a)

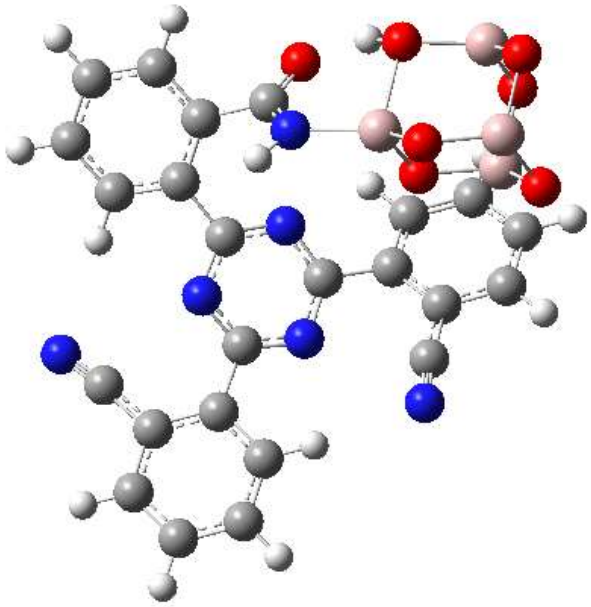

Triazine alumina adduct $\Delta H = -163$ kJmol^{-1}

(b)

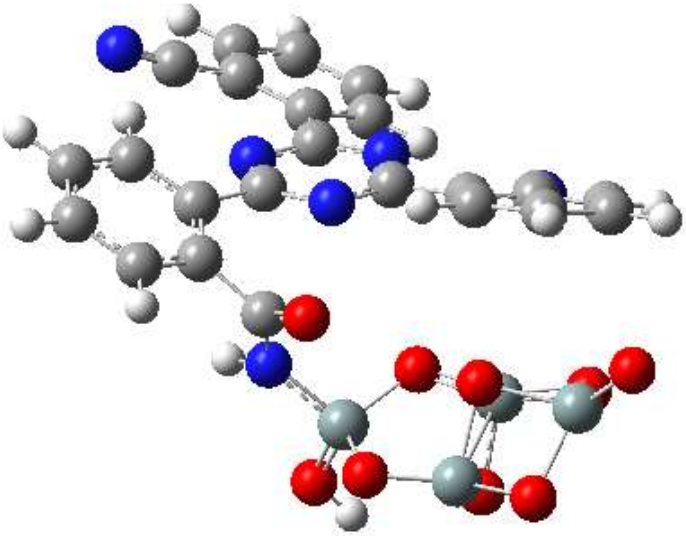

Triazine silica adduct $\Delta H = -108$ kJmol^{-1}

Figure 4- 11 Triazine adduct with (a) alumina and (b) silica.

Figure 4-11 shows the amide formation between the free nitrile group of the triazine with alumina and silica. It can be seen that both the alumina and silica will form energetically favorable products with triazine with the negative enthalpy of formation of the products.

(a)

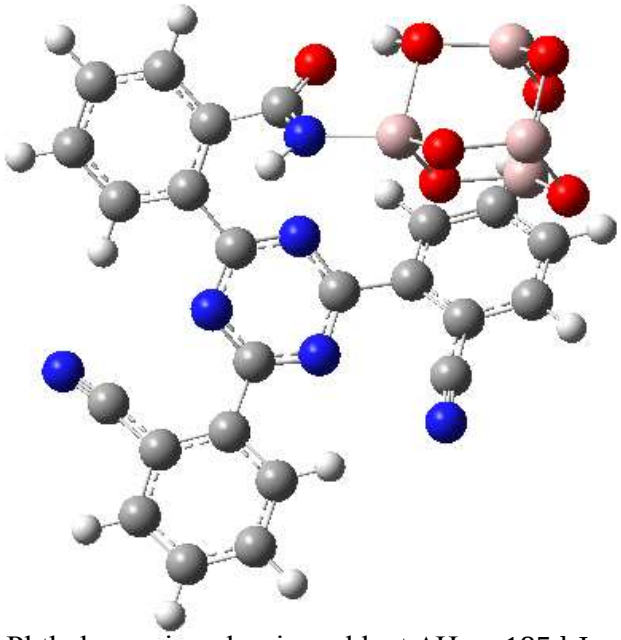

Phthalocvanine alumina adduct ΔH = -185 kJmol^{-1}

(b)

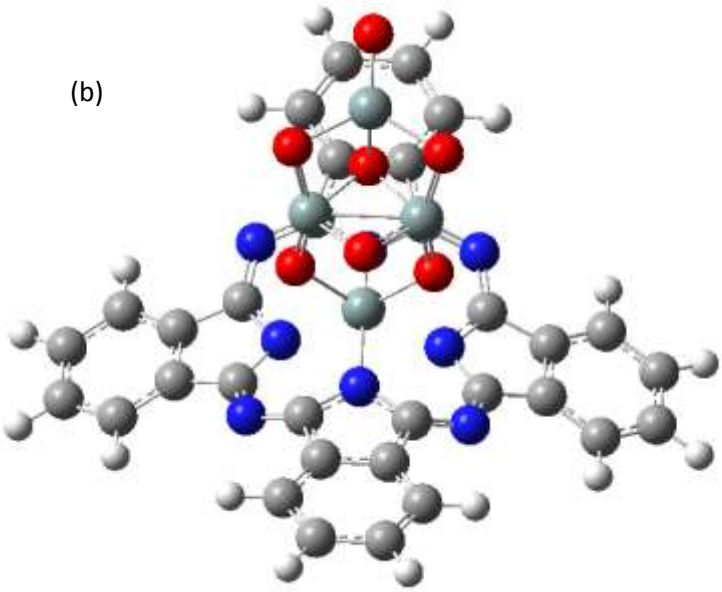

Phthalocyanine silica adduct ΔH = -122

Figure 4- 12 Phthalocyanine adduct with (a) alumina and (b) silica. Enthalpy of formation is given in kJmol-1.

Figure 4-12 shows the Phthalocyanine bonding with alumina and silica. It can be observed that energetically favorable products with alumina (-185 kJmol^{-1}) and silica (-122 kJmol^{-1}) can be formed.

(a)

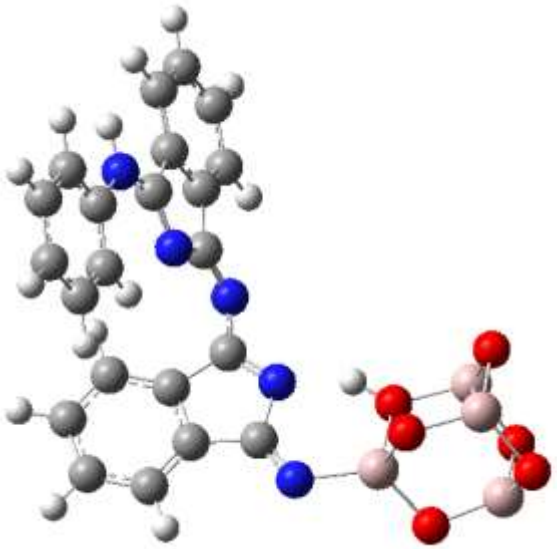

Isoindolenine silica adduct ΔH = +628 kJmol^{-1}

(b)

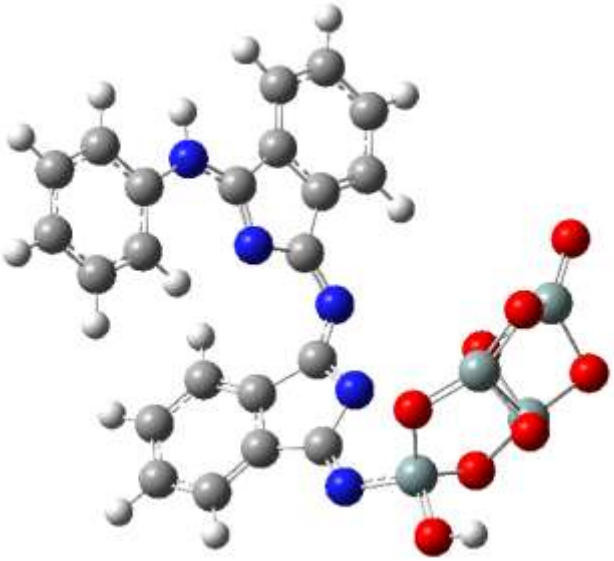

Isoindolenine silica adduct ΔH = +632 kJmol^{-1}

Figure 4- 13 Isoindolenine adduct with (a) alumina and (b) silica.

Figure 4-13 demonstrates that there will be no energetically favorable bond formation between isoindolenine/silica and isoindolenine/alumina. Both enthalpies are shown to be highly positive with values of +628kJmol^{-1} and +632 kJmol^{-1} for silica. Both results indicate the lack of stability in the reaction products, hence it is unlikely that isoindolenine will contribute to the FTIR peaks found.

As the polymerization of bisphthalonitriles constitutes in an extensive network of triazine ring formation in the early stages of curing, it is likely that most of the Si-N and Al-N [5,18] bonds determined from FTIR are from the products of triazine and fillers at temperatures above 180°C of melting temperature. Figure 4-14 summarizes the possible bonding mechanisms between silica and alumina with PN.

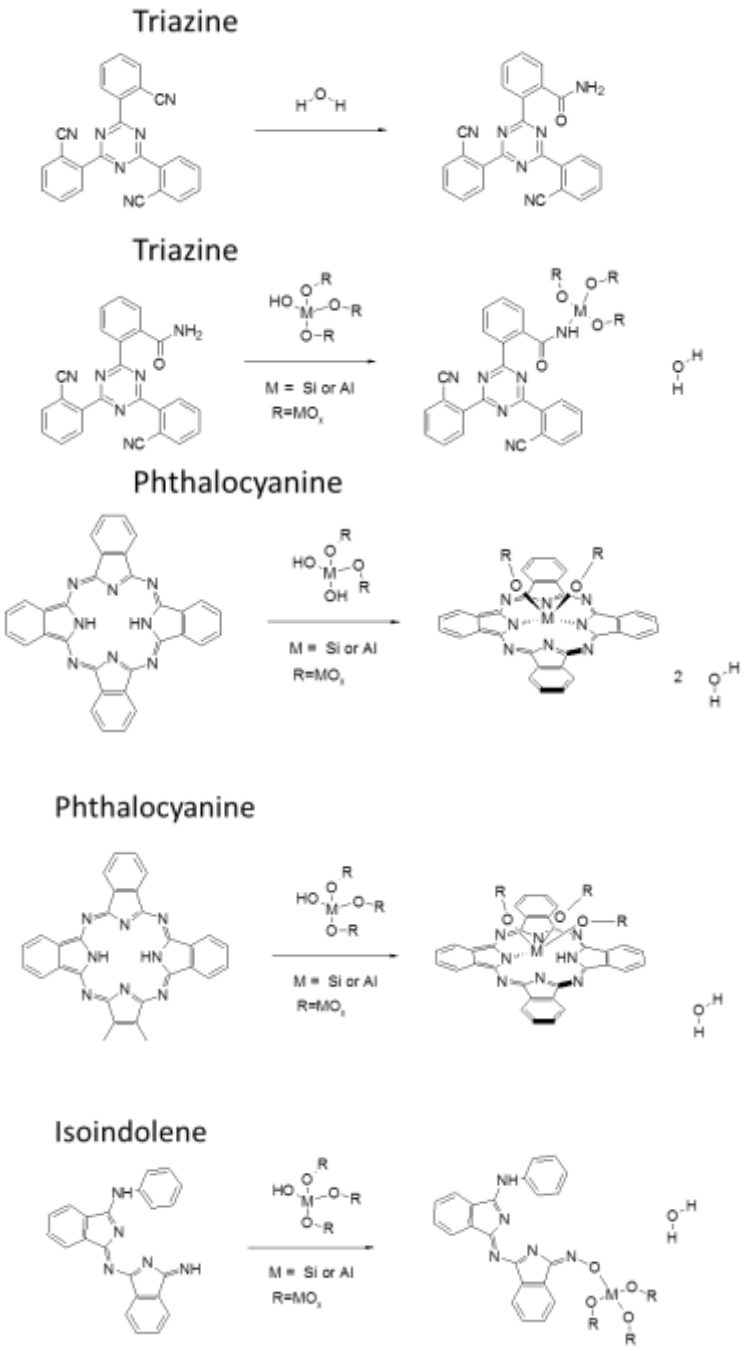

Figure 4- 14 Summary of mechanisms for bonding with oxide fillers

4.4 Summary

The use of resorcinol based PN with silica or alumina fillers as an electronics packaging materials has not been studied before. Common fillers such as silica and alumina, which are widely utilized in epoxies and accepted in current semiconductor packaging industries, were incorporated into the PN matrix. In the studies, up to 50 weight percent of fillers were added and their thermal properties were studied using TGA analysis. It is observed that the 360°C cured samples could at least survive the 300°C working environment. FTIR was further utilized to study the new bond existence between elements such as Si and Al with the N-atoms of PN. DFT calculations utilizing Gaussian09 simulations were also conducted on the molecules to study the feasibilities of bond formation between the polymer molecules such as triazine, phthalocyanine with silica and alumina. It was determined that the new Si-N and Al-N bonds observed from the FTIR measurements were likely due to the reactions between the fillers and triazine or phthalocyanine as predicted by the DFT analysis.

References

[1] M. Liu, “Aromatic heterocyclic resin : precursor for carbon materials and high temperature foams.,” Thesis, 2012.

[2] H. E. Kissinger, “Reaction kinetics in differential thermal analysis,” *Anal. Chem.*, vol. 29, no. 11, pp. 1702–1706, 1957.

[3] R. L. Blaine and H. E. Kissinger, “Homer Kissinger and the Kissinger equation,” *Thermochim. Acta*, vol. 540, pp. 1–6, Jul. 2012.

[4] K. D. Collins and M. W. Washabaugh, “The Hofmeister effect and the behaviour of water at interfaces,” Q. Rev. Biophys., vol. 18, no. 04, pp. 323–422, Nov. 1985.

[5] P. J. Burchill, “On the formation and properties of a high-temperature resin from a bisphthalonitrile,” J. Polym. Sci. Part Polym. Chem., vol. 32, no. 1, pp. 1–8, Jan. 1994.

[6] P. J. Burchill and T. M. Keller, “Curing phthalonitrile resins with acid and amine,” 5237045, 17-Aug-1993.

[7] G.-W. Lee, M. Park, J. Kim, J. I. Lee, and H. G. Yoon, “Enhanced thermal conductivity of polymer composites filled with hybrid filler,” Compos. Part Appl. Sci. Manuf., vol. 37, no. 5, pp. 727–734, May 2006.

[8] P. Hagler, P. Henson, and R. W. Johnson, "Packaging Technology for Electronic Applications in Harsh High-Temperature Environments," IEEE Trans. Ind. Electron., vol. 58, no. 7, pp. 2673–2682, Jul. 2011.

[9] U. Sorathia, J. Ness, and M. Blum, "Fire safety of composites in the US Navy," Compos. Part Appl. Sci. Manuf., vol. 30, no. 5, pp. 707–713, May 1999.

[10] L. Toma, C. Fasel, S. Lauterbach, H.-J. Kleebe, and R. Riedel, "Influence of nano-aluminum filler on the microstructure of SiOC ceramics," *J. Eur. Ceram. Soc.*, vol. 31, no. 9, pp. 1779–1789, Aug. 2011.

[11] D. C. L. Vasconcelos, E. H. M. Nunes, and W. L. Vasconcelos, "AES and FTIR characterization of sol–gel alumina films," *J. Non-Cryst. Solids*, vol. 358, no. 11, pp. 1374–1379, Jun. 2012.

[12] G. Beshkov, S. Lei, V. Lazarova, N. Nedev, and S. S. Georgiev, "IR and Raman absorption spectroscopic studies of APCVD, LPCVD and PECVD thin SiN films," *Vacuum*, vol. 69, no. 1–3, pp. 301–305, Dec. 2002.

[13] K. O. Bugaev, A. A. Zelenina, V. A. Volodin, K. O. Bugaev, A. A. Zelenina, and V. A. Volodin, "Vibrational Spectroscopy of Chemical Species in Silicon and Silicon-Rich Nitride Thin Films, Vibrational Spectroscopy of Chemical Species in Silicon and Silicon-Rich Nitride Thin Films," *Int. J. Spectrosc. Int. J. Spectrosc.*, vol. 2012, 2012, p. e281851, Oct. 2011.

[14] Nanotechnology Conference and Trade Show *et al.*, Eds., *2006 NSTI Nanotechnology Conference and Trade Show: NSTI Nanotech 2006 ; May 7 - 11, 2006, Hynes Convention Center, Boston, Massachusetts, U.S.A. ; an interdisciplinary integrative forum on nanotechnology, biotechnology and microtechnology ; [includes: 2006 NSTI Bio Nano Conference and Trade Show, Bio Nano 2006, 9th International Conference on Modeling and Simulation of Microsystems, MSM 2006, 6th International Conference on Computational Nanoscience and Technology, ICCN 2006, 2006 Workshop on Compact Modeling, WCM 2006, NSTI Nanotech Ventures 2006, 2006 TechConnect Summit ; technical proceedings]*. Boston.: NSTI, 2006.

[15] J. W. Vanbuskirk *et al.*, "FTIR and Raman Studies of the Vibration Modes in High Purity AlN Films Grown on Silicon," presented at the APS Texas Sections Fall Meeting Abstracts, 1999, p. 3604.

[16] T. M. Keller, "Synthesis and polymerization of oligomeric multiple aromatic ether-containing phthalonitriles," US5464926 A, 07-Nov-1995.

[17] A. W. Snow, J. R. Griffith, and N. P. Marullo, "Syntheses and characterization of heteroatom-bridged metal-free phthalocyanine network polymers and model compounds," *Macromolecules*, vol. 17, no. 8, pp. 1614–1624, Aug. 1984.

[18] J. A. Hinkley, "Network structure in bisphthalonitrile polymers," *J. Appl. Polym. Sci.*, vol. 29, no. 11, pp. 3339–3347, 1984.

Chapter 5

Evaluation of PN Composites Properties as an Electronics Packaging Material

This chapter investigates the effects of filler additions to "neat" PN, specifically to the properties relevant as an electronics packaging material. Characterization is performed on neat PN and their corresponding behavior is tested with addition of different weight percent of silica/alumina fillers. Various properties such as coefficient of thermal expansion (CTE), compressive strength, elastic modulus, flexural strength and tensile strength are characterized. Testing is also conducted where PN and its filled components are subjected to environmental conditions such as moisture and heat. A treatment is also provided to evaluate the effect of moisture on the changes in mechanical properties in the perspective of storage modulus. A discussion of the water adsorption behavior of PN is provided and this is important for PN is to be utilized as electronic packaging material. The behavior of PN under Joint Electron Device Engineering Council (JEDEC) MSL 1 conditions is compared with that of epoxy. Water absorption is measured and calculations are made to determine the exponent values derived from mass gain equations to predict Fickian or non-Fickian behavior. Through these studies, it was found that water moisture absorption takes on an anomalous behavior. Finally, the dielectric behavior of PN and its composites are measured and discussed under various cure conditions. The best dielectric properties are achieved using 360°C cured PN filled with 30 weight percent and 50 weight percent silica and these are comparable with standard EMCs on the market.

5.1 Change of thermal conductivities with respect to filler loadings

The influence of temperature variations on the thermal conductivity of PN with various filler type and different amounts is presented in Figure 5-1. Thermal conductivity of neat PN can be improved with the additions of fillers as observed both in Figure 5-1(a) and Figure 5-1(b). In addition, the conductivities improved with higher filler loading. For 50 weight percent alumina fillers addition, the thermal conductivity increased from 0.2 to 0.45 W/mK, a two-fold increment.

The increase in thermal conductivity is less for silica as the thermal conductivity is observed to increase from 0.2 W/mK to 0.34 W/mK. As both filled polymer types were cured to 360°C, both types did not go through softening or decomposition at usage temperatures of 300°C.

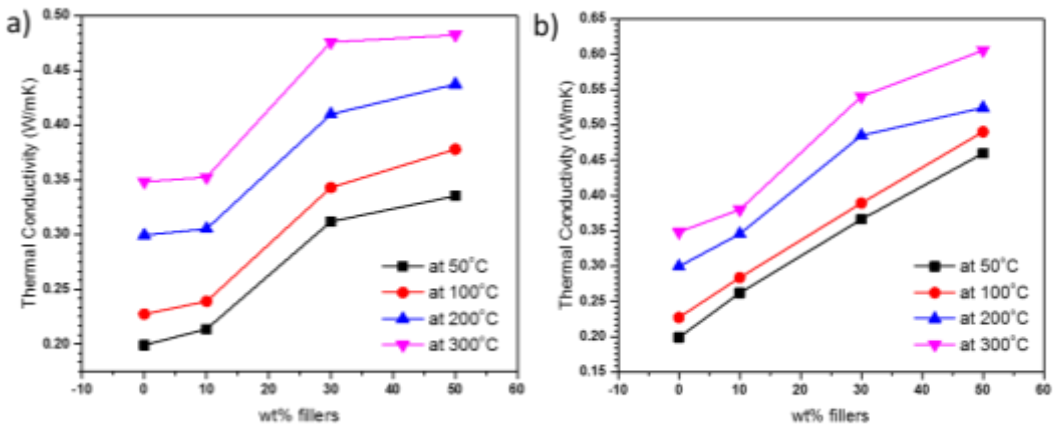

Figure 5- 1 Temperature dependence of thermal conductivity for PN with a) silica fillers b) alumina fillers

The observed increase in thermal conductivities can be attributed to the large amount of vibration and rotation experienced by the polymer molecules at higher temperatures. Neat PN polymers behave in a manner similar to epoxy with the neat PN's thermal conductivity starting at 0.2W/mK whereas the approximate thermal conductivity of thermoset polymers is typically at 0.3W/mK [1]. Similar thermal conductivity values and behavior after filler additions put PN and its composites on par with other thermoset package materials.

5.2 Coefficient of Thermal Expansion (CTE) of PN and its composites

The CTE of resorcinol based PN and its composites were characterized using TMA as shown in Figure 5-2(a). PN is a thermoset which does not go through any sharp change in CTE between 25°C and 300°C. From Figure 5-2(b), the CTE of the samples decreased significantly with filler loadings for both types of fillers. Additions of up to 50% can lower the CTE by almost half from 50 µm/m-K to 29 µm/m-K.

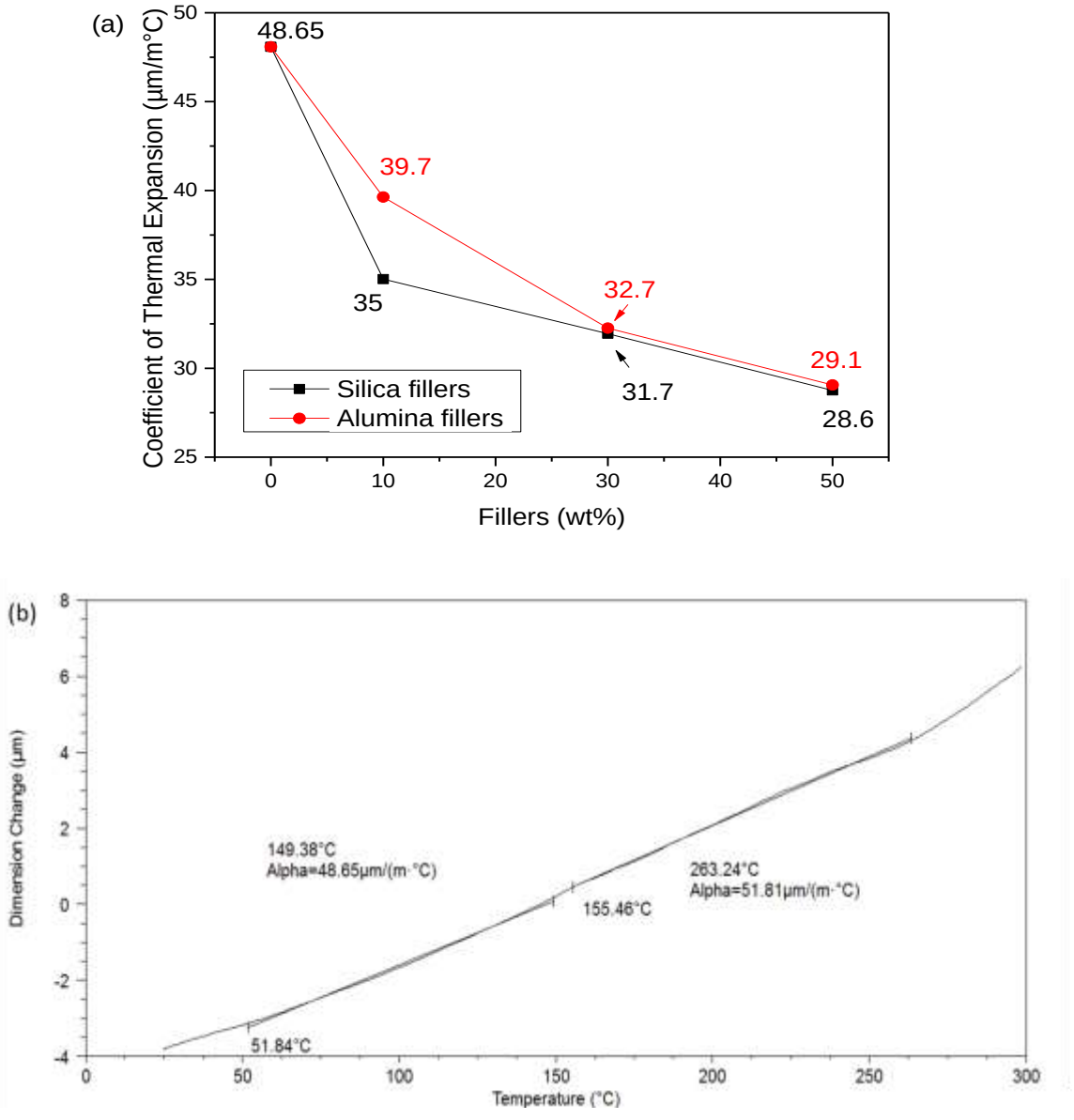

Figure 5-2(a) Example plot of neat PN CTE from room temperature to 300°C (b) Coefficient of thermal expansion (CTE) of PN with various filler loadings

It is observed that 10% of filler addition produced the sharpest improvement to the CTE. This may be correlated to enhanced polymer chain segment mobility at 10 weight percent [2], which is higher compared to 30 weight percent and 50 weight percent fillers where the same volume is now replaced by filler particles. However, the sharper non-linear decrease of CTE values departed from conditions of isostress in compliance to the mixture rule.

This may be due to the influence of shape of fillers, bonding and interaction with matrix, which needs to be further devised and studied. Nevertheless, the fillers significantly lower the thermal expansion mismatch when PN is to be placed over chips, bond wires or onto the surface of substrates, thus improving its thermo-mechanical properties.

5.3 Compression strength

The compressive strength of PN and its composites were characterized using Instron tester 8516 as described in chapter 3. Figure 5-3 shows the compressive strength of PN with different filler type and amount. Alphabets ‘A’ and ‘S’ represent Alumina and Silica filler types with the weight percent loading represented by the numbers in front of A or S.

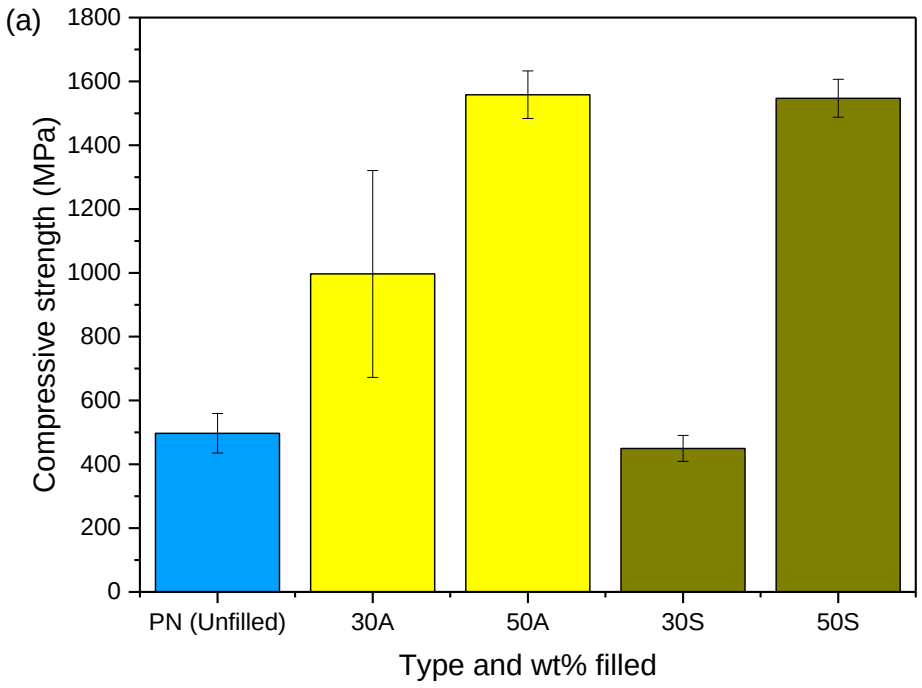

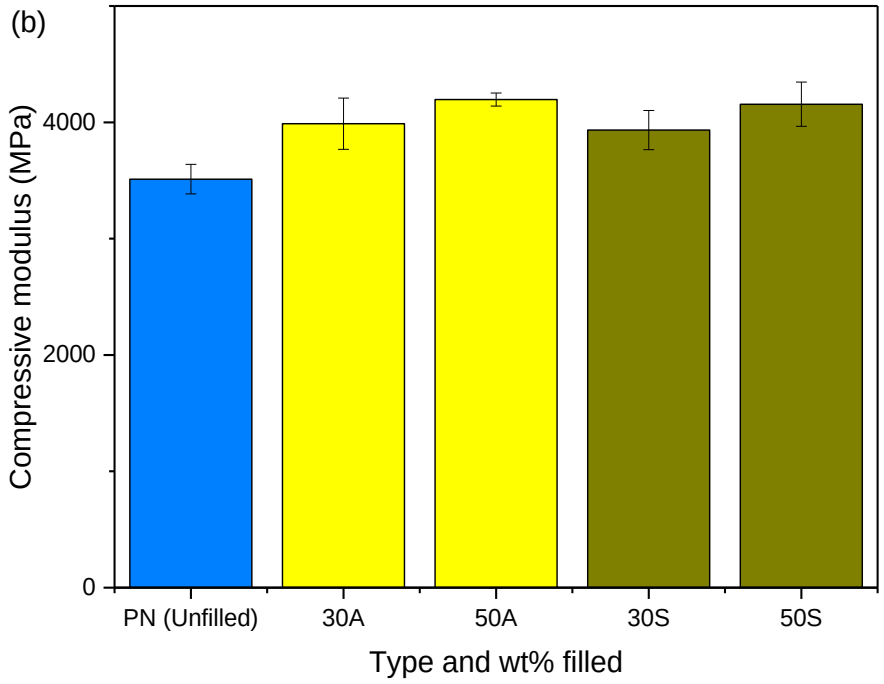

Figure 5- 3 Compositional dependence of filler additions on the (a) compressive strength (b) compressive modulus.

It can be observed that the compressive strength increases with the loading of fillers. The compressive strength of the PN composites improved proportionally with the addition of fillers, with a compressive modulus of 4 GPa at 50% alumina/silica loading. These values are much higher than commercial epoxies where the compressive strength typically ranges around 170 MPa – 207 MPa [3-6], even for heavily modified glass filled epoxies. It can also be observed that alumina filled polymers are stronger than silica filled ones. This is because the composite strength is also dependent on the compressive strength of the fillers. Since silica has a lower compressive strength (1.6 GPa [7]) than alumina (2.6 GPa [8]), a lower strength of silica filled PN is expected. The trend of compressive strength increase can be predicted with the rule of mixtures where the upper bound of iso-strain condition is given in the equation.

$$E_{composite} = E_{matrix}V_{matrix} + E_{fillers}V_{fillers} \qquad \textbf{Equation 5-1}$$

Here, *E* denotes modulus and *V* denotes volume fraction and can be derived knowing both the weight and density of matrix and fillers. The lower bound is an iso-stress condition which is described by the following equation.

$$E_{composite} = \frac{EmatrixEfillers}{\text{EfillersVmatrix} + \text{EmatrixVfillers}} \qquad \textbf{Equation 5-2}$$

The actual modulus depends strongly on the adhesion and stress transference between the matrix and fillers as discussed in Chapter 2 and are under conditions of ideality.

5.4 Elastic modulus

The elastic modulus of PN cured to different temperatures were obtained through nanoindentation with cube corner tips as described in Chapter 3. With reference to Figure 5-4(b), it is observed that the elastic modulus of neat PN is ~8 GPa and increases to ≥ 12 GPa with approximately 50 weight percent filler loading (for both silica and alumina filler type). Alumina filled polymer matrix composite (PMC) produced a slightly larger elastic modulus than silica filled ones. Since highly randomized zones on the specimen was selected for test during nanoindentation, the effects of irregularities and surface abnormalities are negligible, hence the higher modulus observed for all the PN and the various weight percent filled composites.

In addition, because of the largely defect free measurements, it can be observed that the moduli obtained from nanoindentation are larger than that derived from bulk sample tensile testing which would be shown in section 4.5.5. Rodriguez *et. al* [9] also observed a high correlation in the elastic moduli obtained from nanoindentation and the tensile tests where differences were only observed for steel where significant plastic deformation occurred.

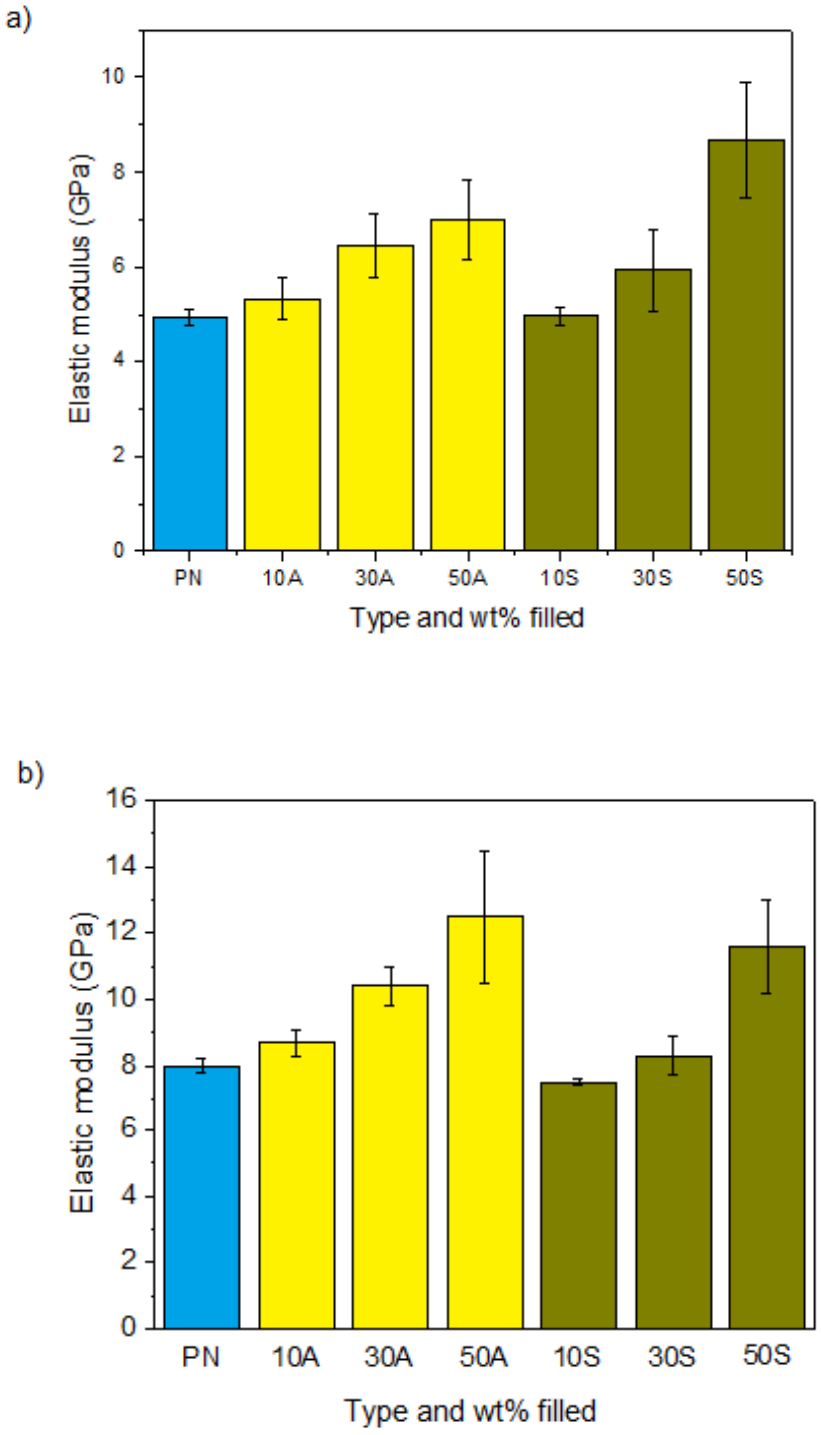

Figure 5- 4 (a) Compositional dependence of filler additions on the elastic modulus properties for samples processed to 320°C (where A, S and P abbreviate alumina filler, silica filler and neat PN, respectively, and 10, 30 and 50 denotes 10wt%, 30wt% and 50wt% %, respectively) **(b)** Compositional dependence of filler additions on the elastic modulus properties for samples processed to 360°C.

Comparing Figure 5-4(a) and 5-4(b), the effects of curing temperature on the elastic moduli can be observed with the following trends:

1) Alumina filled PN has higher elastic modulus as compared to silica filled PN with similar amount of weighted fillers added

2) The elastic modulus is higher with higher curing temperature due to more cross linking of triazine, phthalocyanine and isoindolenine

3) The elastic modulus increases with increasing amount of fillers added

5.5 Flexural strength

With reference to Figure 5-5(b), it can be observed that the increase in flexural modulus with increasing filler weight percent is likely contributed by the intrinsic stiffness of the filler particles. This may also be attributed to the effect of chain mobility restriction of the polymer matrix with the addition of rigid fillers [10]. Another observation is that the phthalonitrile polymers filled with alumina show higher average flexural modulus as compared to those filled with silica, especially those with up to 50 weight percent fillers. This is due to the higher modulus of alumina (375 GPa [8]) as compared to silica (E = 74.8 GPa [7]).

The modulus depends on the average structure and the load-bearing capability of the fillers integrated polymer whereas the strength is related to the weakest route for crack propagation. The parameters which determine the strength are more complex as explained by Selvin *et. al* [11]. It depends on the size, shape and filler type, as well as modulus, and is also affected by the adhesion between filler particles and polymer matrix which is harder to measure and quantify. According to Dittanet *et. al* [12], if the filler has poor adhesion to the matrix, load cannot be effectively transferred between filler and matrix and thus a lower strength results. This also takes into account an accumulation of size and distribution of defects such as voids within the polymer. In retrospect, as observed in Figure 5-5(a), a slightly lower flexural strength observed in 50 weight percent alumina PN is likely due to the presence of defects such as voids due to high material viscosity during the processing of the sample.

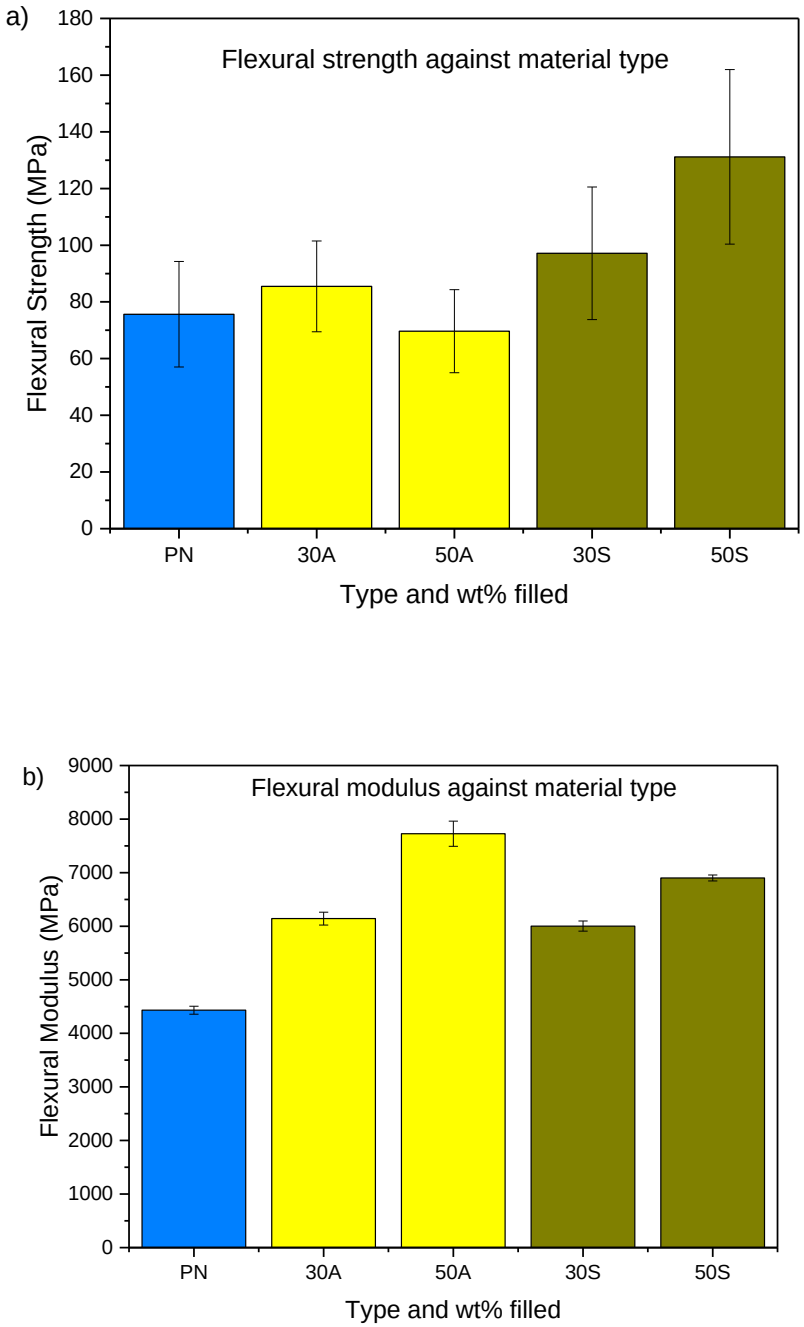

Figure 5- 5 Compositional dependence of filler additions on the (a) flexural strength (b) flexural modulus

On the contrary, Fu *et. al* [13] assumed that the modulus of elasticity is not affected by the adhesion strength between filler and matrix but strongly depends on filler quantity within the polymer matrix as the modulus of filler is typically much higher than that of the matrix.

With reference to Figure 5-5(a), the flexural strength of the filled polymers shows improvement as compared to the unfilled polymers especially for silica-filled ones. The strengthening effect could be attributed to the load being transferred between filler particles and polymer matrix due to a good filler/matrix adhesion.

5.6 Tensile strength

The compositional dependence of tensile strength of PN is shown in Figure 5-6(a). The Young modulus or the stiffness of a material measures the elastic portion of a sample [13] in accordance with standards from ASTM 638.

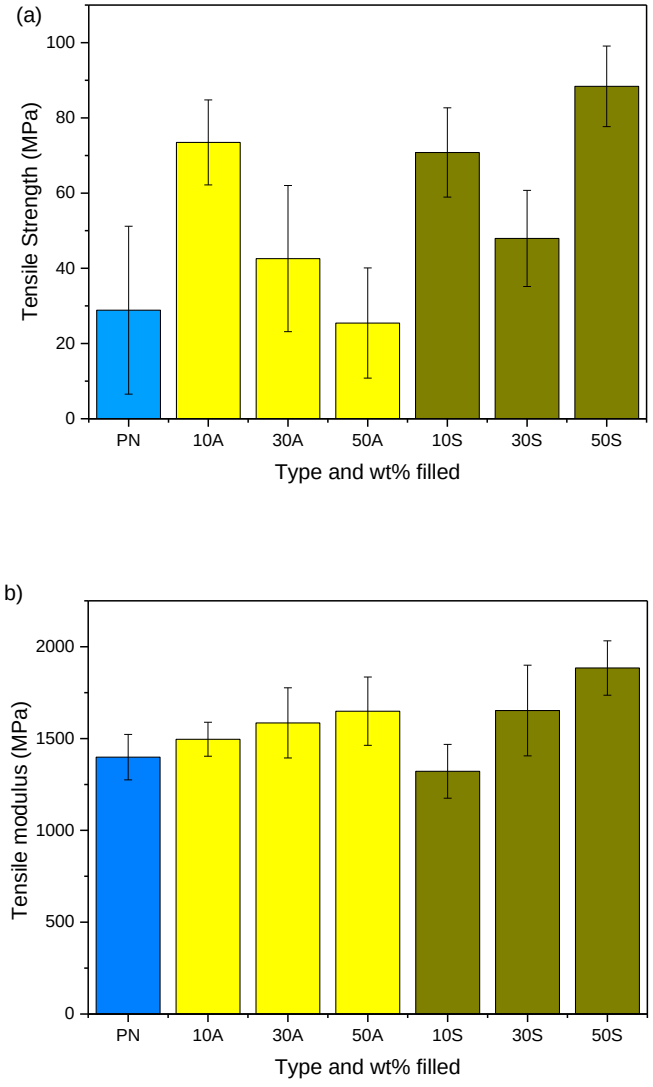

Figure 5- 6 (a) Tensile strength and **(b)** tensile modulus of PN composites as a function of filler type and weight percentage.

The increase in tensile modulus with increasing filler content is similar with the trend observed for elastic modulus that was derived from nanoindentation and flexural modulus. However, the dog bone shaped requirements on ASTM 638 may not be the most suitable sample type for testing PN due to its extremely high stiffness. As such, lower values were measured for tensile strength as compared to those obtained from flexural tests.

5.7 Moisture interaction with PN-based encapsulation

PN-based encapsulation has not been studied to date in the form of microelectronics packaging material. Its water adsorption mechanism especially in the perspective as an electronic encapsulation is largely unknown. Studies on other polymers for microelectronics packaging applications mainly focus on the material in the form of weight gain. The weight gain due to moisture uptake is the common analysis method for most composites [10], polymers [10,14] and electronic packages [15,16]. For moisture diffusion mechanism, Fan *et. al* [17] suggested that two stage mechanisms occur in both aqueous water soak through wicking and moisture diffusion such as through channeling at MSL 1 conditions, with the latter being more aggressive in terms of moisture gaining.

Water molecules which measures only 2.75 Å can travel through a wide network of extremely small gaps through the polymer. The polymerization of bisphthalonitriles constitutes in an extensive network of triazine ring formation in the early stages of curing. It is possible that most of the Si-N bonds and Al-N bonds [18, 19] are the results of measurement in Si-N and Al-N from the product of triazine and fillers at temperatures above 180°C. DFT calculations can be used to explore whether the triazine moiety from the monomers can form a cavity resulting in such gaps. As depicted in Figure 5-7, it is observed that due to the rotational freedom of the phenoxide in the representative 2 triazine polymerized system, the smallest possible cavity formed is 1.5 nm. Nano-gaps formed within polytriazine and poly(phthalocyanine) are possible channels for the diffusion of water molecules, hence the adsorption [20] observed by Snow *et al*.

DFT analysis can help to identify the possible diffusion mechanism but does not shed light to the physics of such absorption. Kim *et. al* [21] has studied the behavior of water at interfaces such as the Hofmeister effects of water [21], particularly with regards to the effects of charge transferred from the solute but this alone is inadequate to gauge the effects of water when fillers are prior exposed to moisture from humid air.

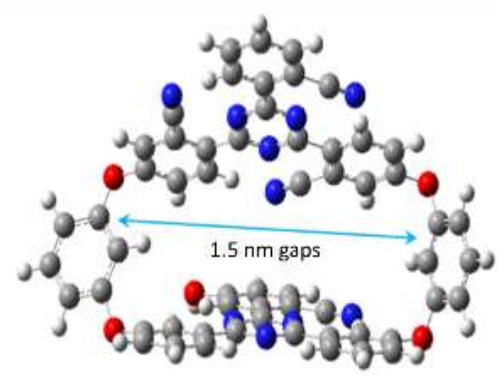

Figure 5- 7 DFT studies showing that nano-gaps exists at 1.5 nm for triazine molecules.

The following section attempts to investigate the moisture behavior of PN-based encapsulation and its absorption at higher temperatures. Previously, papers have documented the use of PN in the form of bulk composites with moisture pick up rates of 1.5% when treated in the form of amine cured bisphenol linked phthalonitrile resins [22]. More recently, other forms of bisphenol based phthalonitrile has been reported to have higher moisture absorption rates of 2.5% [23] where the moisture absorption test was completed by sample soaking in pure water at 25°C for 50 days.

The following formula is adopted in this thesis for calculation of moisture mass gain in the plastic components [24]:

$$\textbf{Mass of moisture uptake (\%)} = \frac{M(t) - M(Dry)}{M(Dry)} \times 100 \qquad \textbf{Equation 5-3}$$

Where $M(t)$ represents the weight of the sample, M_{Dry} is the dry mass of the sample before moisture preconditioning and t represents the time.

Figure 5-8 shows the graph of the weight differentials at various intervals when the samples were subjected to MSL level 1 test conditions (85°C/85%RH), up to 262 hrs.

Desorption is performed from 262 hrs onwards to monitor for moisture induced weight gain upon saturation. For all samples, mass gain was observed. This trend is similar to commercial epoxy mold compounds where Fickian type moisture gain is typically observed. In cases where non-Fickian effects were observed, Duda *et. al* [19] has created a Deborah number $(DEB)_D$ to indicate the presence of such effects and to further explore self-diffusion models without the use of diffusion data [20]. With weight percent increase in fillers, there is a decrease in water absorbed.

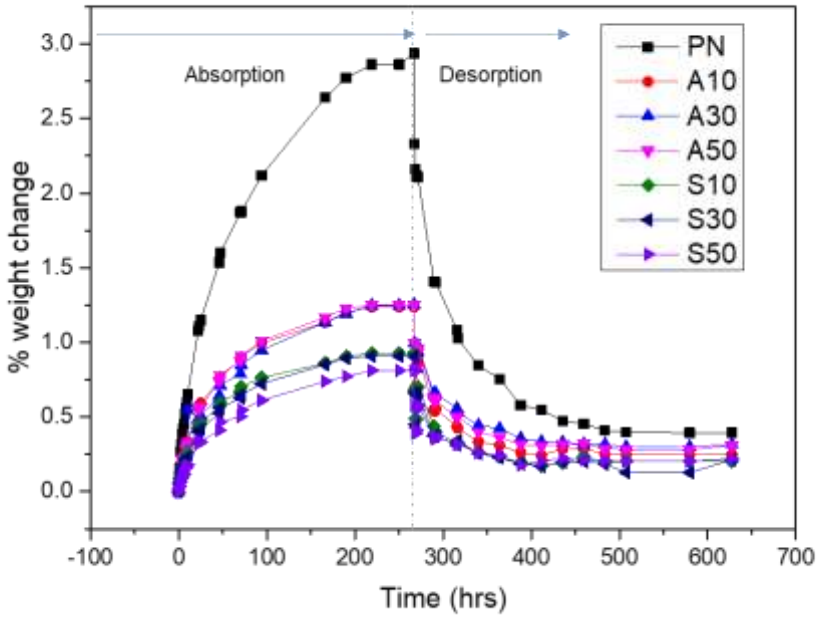

Figure 5- 8 Percentage weight change on PN-filler composites in water moisture absorption till 262 hours and desorption studies water moisture through neat PN.

As demonstrated earlier using Gaussian09, small pores as small as 1.5 nm exist in triazine in stable states and moisture may be able to travel through the pores using them as miniature pathways. The water molecules jump through the matrix in the act of a random walk akin to that described by Holck *et. al* [19].

A small amount of moisture may also diffuse through the bulk PN through mechanism such as short distance channelling. Moisture may also diffuse through the small voids which are trapped within the matrix during the curing and blending stage. As moisture

can also attach to the filler surface, some wicking may also result where the moisture travel along the interface of the particles first and subsequently into the matrix.

The investigation also identified that the mass gain of PN follows a square root function and appears to reach saturation from 214 hours onwards when exposed to MSL level 1 conditions of 85°C and 85%RH. With reference to the modified function,

$$\frac{M_t}{M_\infty} = kt^n \qquad \textbf{Equation 5-4}$$

Where M_t and M_∞ represent the amount of solvents diffused into the polymer at time t and at infinite time (equilibrium state), respectively, k is a constant related to the structure of the network and the exponent n is a number that determines the type of diffusion. The following function can be derived where,

$$\log\left(\frac{M_t}{M_\infty}\right) = \log k + n \log t \qquad \textbf{Equation 5-5}$$

The curves in Figure 5-9 can be replotted based on Equation 5-5 where the slope represents n. When the rate of diffusion is almost equal to the rate of water uptake, n has a value between 0.5 and 1.

When water moisture passes through the matrix without interaction with the polymer molecules, Fickian diffusion is expected and n is 0.5. When interaction occurs between water molecules and the polymer molecules, n goes closer to 1.

Figure 5-9 shows that water does interact with the polymer molecules as it pass through the polymer and its fillers. In fact it can be observed that even without any fillers, "neat" PN molecules also interact with the moisture which passes through. As such n is not exactly at 0.5 and is similar to the research on epoxy by Wong *et. al* [25] who observed a critical thickness above which epoxies started to exhibit anomalous diffusion. This increases distinctly also with addition of fillers. Such interactions are further substantiated by the desorption curve in Figure 5-8 where all samples retained weight from moisture absorption after more than 250 hours of desorption at 100°C.

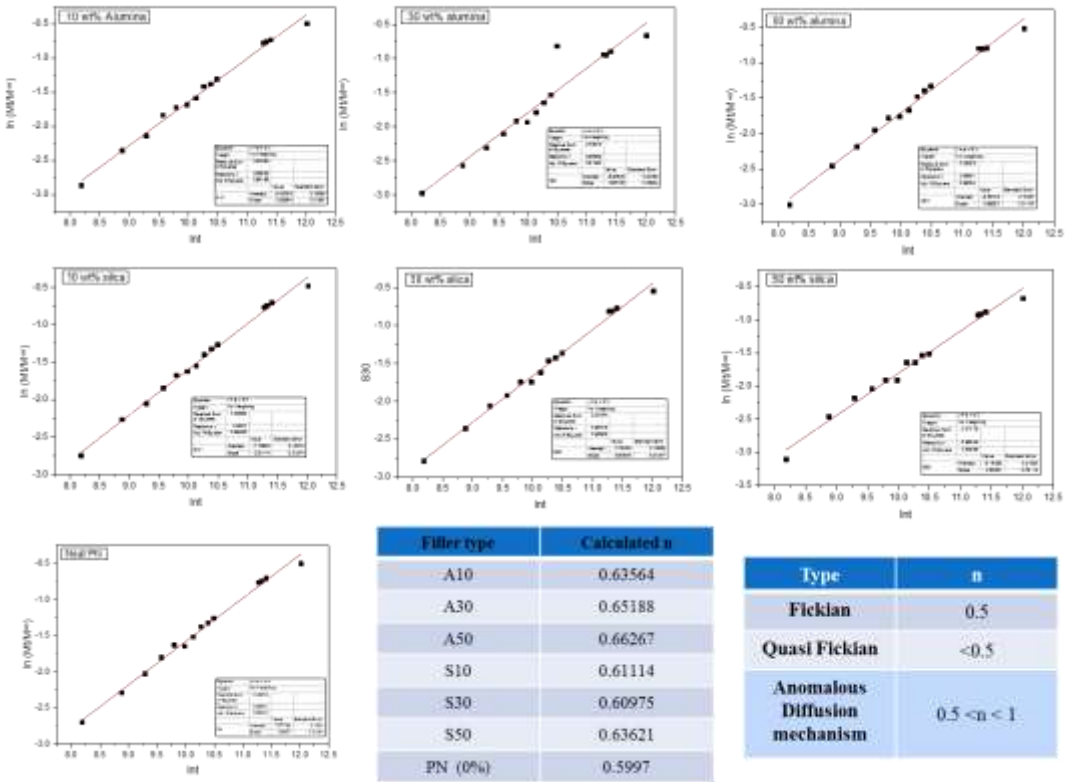

Filler type	Calculated n
A10	0.63564
A30	0.65188
A50	0.66267
S10	0.61114
S30	0.60975
S50	0.63621
PN (0%)	0.5997

Type	n
Fickian	0.5
Quasi Fickian	<0.5
Anomalous Diffusion mechanism	0.5 <n < 1

Figure 5- 9 Non-Fickian relationships of neat and filled PN.

5.8 *In-situ* DMA study on impact of humidity and temperature

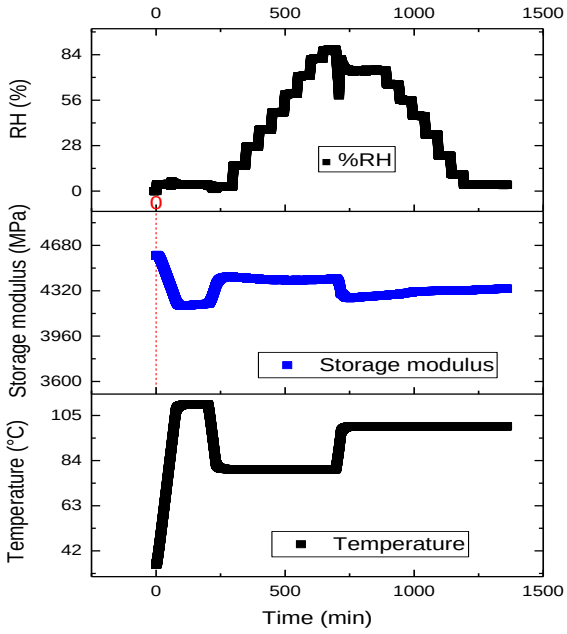

Figure 5- 10 Plot of storage modulus, temperature and RH% change with time for 50wt% alumina filled PN.

Figure 5-10 shows the temperature and relative humidity profiles during DMA measurements of the storage modulus for 50 weight percent alumina filled PN using single cantilever measurements. The temperature and humidity profiles were set as shown in Figure 5-10 and Figure 5-11 shows the corresponding changes in storage modulus of different fillers with PN.

It has been demonstrated by Deng *et. al* [26] that there is a strong correlation between mechanical data measured from Instron 5567 and DMA. In fact, the measured DMA results reflect similar trends to the test results obtained from actual bulk material flexural testing using the Instron tester. A correction factor specific to equipment and samples is recommended by Deng *et al*. Since storage modulus and flexural modulus are directly related when measured under DMA, one can simply observe the storage modulus values as indication of flexural modulus. Taking 50 weight percent alumina filled PN as reference on Figure 5-11, at constant temperature of 80°C, the humidity in the chamber was ramped stepwise upwards from 10% RH to 80% RH within 50 minutes, and a corresponding change in storage modulus is observed from 4413 MPa to 4394 MPa. This drop of 19 MPa is comparatively small and is well within the measured range of flexural modulus obtained both in DMA and on the Instron measurements as reported in Figure 5-5.

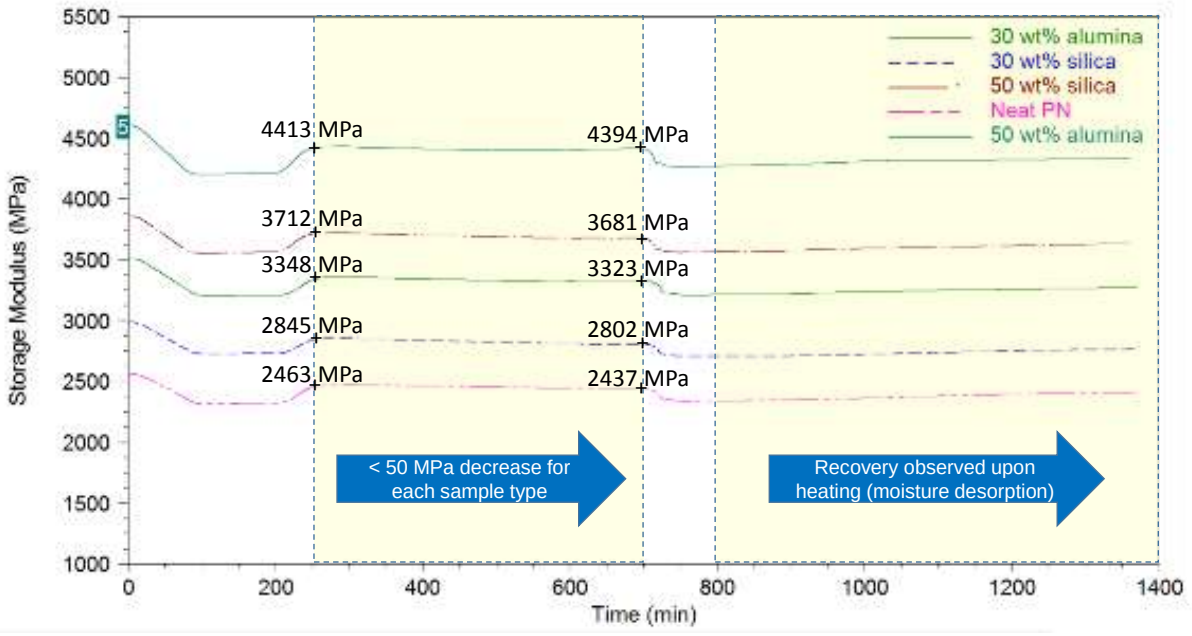

Figure 5- 11 Change in storage modulus under controlled humidity and temperature.

It can be observed that the 50A sample has the highest storage modulus, followed by 50S, 30A, 30S then neat PN. The results show little fluctuation in measured storage modulus as the samples were exposed to increasing humidity and the high modulus of the material can be retained even at high humidity.

It is observed that even when humidity was increased to about 85% RH, the modulus of PN decreased less than 50 MPa, indicated between 250 min to 700 min, for all filled samples tested in this experiment with the holding temperature of 80°C. With the highest modulus observed at 4.4 GPa for 50A, 3.6 GPa for 50S, 3.3 GPa for 30 A, 2.8 GPa for 30S and 2.4 GPa for neat PN at 85%RH /85°C condition, this 50 MPa change is well within the recovery limits of the material and thus does not constitute degradation especially when the test conditions are highly accelerated versions of what would happen at ambient working conditions.

The exposure test parameters of 85% RH and 85°C validate the performance of the PN under humidity. It also shows that the modulus of PN can be recovered by heat treatment if it has been excessively exposed to moisture from external environment. This is a property which is comparable to highly filled epoxy molding compounds.

5.9 Dielectric behaviour for PN composites

Table 5-1 shows the dielectric constant of PN composites after curing at temperatures of 280°C and 360°C. The samples were then aged at 250°C and 360°C and the values were obtained at 1 MHz measurements. The dielectric values of PMCs are directly related to the weight percent and dielectric values of the fillers added, whereby alumina has a dielectric constant of 9.8 [27] and silica has a dielectric constant of 4.2[28]. Thus, the dielectric constant of silica filled PN decreased with increasing filler weight percent while it increases for alumina filled PN.

The dielectric value of commercial glass filled epoxy mold compounds is about 4.7 at 1 MHz [29]. This shows that the dielectric constant of PN and its PMC are comparable. Thus, PN and its PMC could potentially make good substitutes for glass filled epoxies and its equivalent especially for high temperature applications.

Table 5- 1 Dielectric properties of PN at various cure temperatures (1MHz)

Curing Temperature (°C)	Material	Fill (wt %)	Dielectric constant
250°C	Silica	10	7.73
		30	7.57
		50	7.16
	Alumina	10	8.10
		30	8.53
		50	9.13
	PN	0	8.07
360°C	Silica	10	6.22
		30	5.34
		50	3.99
	Alumina	10	6.44
		30	6.76
		50	7.66
	PN	0	7.36

PN appears to have a lower dielectric constant at higher curing temperature. At lower cure temperatures, more polymer segments are available where the polar groups of such segments are free to orientate, allowing it to keep up with the changing field, hence the higher dielectric constant as observed [30]. When heated to a higher temperature, more cross-linking of poly(triazine) and poly(phthalocyanines) are formed. This effect may cause the structure to become stiffer and form more "air gaps" in between, leading to a lower dielectric constant.

5.10 Summary

PN-based composites can be tuned through filler additions to achieve the required properties to be compatible as an electronics packaging material. This includes the thermal conductivity, dielectric constant and various mechanical properties. Thermal conductivities in the range of 0.3 W/mK and dielectric constant of about 4 can be obtained for 50 weight percent silica filled PN, which are comparable to current epoxy molding compound. In addition, they have superior mechanical properties especially in terms of compression strength where it can reach 500 MPa without filler loading. This is already much higher than typical loaded epoxies with strength of up to 350 MPa. Several options such as high temperature curing and higher filler loadings can further increase the

strength. This is desirable as PN can be cured and used at above 500°C applications, filling the current gap from 300°C onwards. Moisture characterization in accelerated stress test using MSL 1 conditions has shown that cured PN experiences anomalous diffusion with no major deterioration in modulus even in strenuous operation conditions, as such is more suitable for high temperature applications as compared with its highly filled epoxy counterparts. The integration of PN-filled composites as an electronics packaging material and its evaluation in a HTHP environment will be investigated in the next chapter.

References

[1] W. D. Callister and D. G. Rethwisch, Materials Science and Engineering: An Introduction, 8th Edition. Wiley, 2009.

[2] M.-L. Sham and J.-K. Kim, "Curing behavior and residual stresses in polymeric resins used for encapsulanting electronic packages," *J. Appl. Polym. Sci.*, vol. 96, no. 1, pp. 175–182, Apr. 2005.

[3] G. Beshkov, S. Lei, V. Lazarova, N. Nedev, and S. S. Georgiev, "IR and Raman absorption spectroscopic studies of APCVD, LPCVD and PECVD thin SiN films," *Vacuum*, vol. 69, no. 1–3, pp. 301–305, Dec. 2002.

[4] K. O. Bugaev, A. A. Zelenina, V. A. Volodin, K. O. Bugaev, A. A. Zelenina, and V. A. Volodin, "Vibrational Spectroscopy of Chemical Species in Silicon and Silicon-Rich Nitride Thin Films, Vibrational Spectroscopy of Chemical Species in Silicon and Silicon-Rich Nitride Thin Films," Int. J. Spectrosc. Int. J. Spectrosc., vol. 2012, 2012, p. e281851, Oct. 2011.

[5] Nanotechnology Conference and Trade Show *et al.*, Eds., *2006 NSTI* Nanotechnology Conference and Trade Show: NSTI Nanotech 2006 ; May 7 - 11, 2006, Hynes Convention Center, Boston, Massachusetts, U.S.A. ; an interdisciplinary integrative forum on nanotechnology, biotechnology and microtechnology ; [WCM 2006, NSTI Nanotech Ventures 2006, 2006 TechConnect Summit ; technical proceedings]. Boston. NSTI, 2006.

[6] J. W. Vanbuskirk *et al.*, "FTIR and Raman Studies of the Vibration Modes in High Purity AlN Films Grown on Silicon," presented at the APS Texas Sections Fall Meeting Abstracts, 1999, p. 3604.

[7] A. W. Snow, J. R. Griffith, and N. P. Marullo, "Syntheses and characterization of heteroatom-bridged metal-free phthalocyanine network polymers and model compounds," Macromolecules, vol. 17, no. 8, pp. 1614–1624, Aug. 1984.

[8] T. M. Keller, "Synthesis and polymerization of oligomeric multiple aromatic ether-containing phthalonitriles," US5464926 A, 07-Nov-1995.

[9] M.-L. Sham and J.-K. Kim, "Curing behavior and residual stresses in polymeric resins used for encapsulanting electronic packages," *J. Appl. Polym. Sci.*, vol. 96, no. 1, pp. 175–182, Apr. 2005.

[10] C.-H. Shen and G. S. Springer, "Moisture Absorption and Desorption of Composite Materials," *J. Compos. Mater.*, vol. 10, no. 1, pp. 2–20, Jan. 1976.

[11] Y. Diamant, G. Marom, and L. J. Broutman, "The effect of network structure on moisture absorption of epoxy resins," *J. Appl. Polym. Sci.*, vol. 26, no. 9, pp. 3015–3025, Sep. 1981.

[12] P. Dittanet and R. A. Pearson, "Effect of bimodal particle size distributions on the toughening mechanisms in silica nanoparticle filled epoxy resin," *Polymer*, vol. 54, no. 7, pp. 1832–1845, Mar. 2013

[13] S.-Y. Fu, X.-Q. Feng, B. Lauke, and Y.-W. Mai, "Effects of particle size, particle/matrix interface adhesion and particle loading on mechanical properties of particulate–polymer composites," *Compos. Part B Eng.*, vol. 39, no. 6, pp. 933–961, Sep. 2008.

[14] X. J. Fan, S. W. R. Lee, and Q. Han, "Experimental investigations and model study of moisture behaviors in polymeric materials," *Microelectron. Reliab.*, vol. 49, no. 8, pp. 861–871, Aug. 2009.

[15] J. E. Galloway and B. M. Miles, "Moisture absorption and desorption predictions for plastic ball grid array packages," *IEEE Trans. Compon. Packag. Manuf. Technol. Part A*, vol. 20, no. 3, pp. 274–279, 1997.

[16] H. Ardebili, E. H. Wong, and M. Pecht, "Hygroscopic swelling and sorption characteristics of epoxy molding compounds used in electronic packaging," *IEEE Trans. Compon. Packag. Technol.*, vol. 26, no. 1, pp. 206–214, Mar. 2003.

[17] X. Fan, "Mechanics of moisture for polymers: Fundamental concepts and model study," in *International Conference on Thermal, Mechanical and Multi-Physics*

Simulation and Experiments in Microelectronics and Micro-Systems, 2008. EuroSimE 2008, 2008, pp. 1–14.

[18] P. J. Burchill, "On the formation and properties of a high-temperature resin from a bisphthalonitrile," *J. Polym. Sci. Part Polym. Chem.*, vol. 32, no. 1, pp. 1–8, Jan. 1994.

[19] O. Holck and B. Wunderle, "Microelectronics Packaging Materials: Investigating the Influence of Moisture by Molecular Dynamics Simulations - Springer," Springer, 2014, pp. 41–66.

[20] J. M. Zielinski and J. L. Duda, "Predicting polymer/solvent diffusion coefficients using free-volume theory," *AIChE J.*, vol. 38, no. 3, pp. 405–415, Mar. 1992.

[21] K. D. Collins and M. W. Washabaugh, "The Hofmeister effect and the behaviour of water at interfaces," *Q. Rev. Biophys.*, vol. 18, no. 04, pp. 323–422, Nov. 1985.

[22] T. M. Keller and T. R. Price, "Amine-Cured Bisphenol-Linked Phthalonitrile Resins," *J. Macromol. Sci. Part - Chem.*, vol. 18, no. 6, pp. 931–937, 1982.

[23] M. Laskoski, D. D. Dominguez, and T. M. Keller, "Synthesis and properties of a bisphenol A based phthalonitrile resin," *J. Polym. Sci. Part Polym. Chem.*, vol. 43, no. 18, pp. 4136–4143, 2005.

[24] C. L. Soles and A. F. Yee, "A discussion of the molecular mechanisms of moisture transport in epoxy resins," *J. Polym. Sci. Part B Polym. Phys.*, vol. 38, no. 5, pp. 792–802, Mar. 2000.

[25] T. C. Wong and L. J. Broutman, "Moisture diffusion in epoxy resins Part I. Non-Fickian sorption processes," *Polym. Eng. Sci.*, vol. 25, no. 9, pp. 521–528, Jun. 1985.

[26] S. Deng, M. Hou, and L. Ye, "Temperature-dependent elastic moduli of epoxies measured by DMA and their correlations to mechanical testing data," *Polym. Test.*, vol. 26, no. 6, pp. 803–813, Sep. 2007.

[27] "Microwaves101 | Alumina 99.5%." [Online]. Available: http://www.microwaves101.com/encyclopedias/alumina-99-5. [Accessed: 09-Sep-2015].

[28] "Properties: Silica - Silicon Dioxide (SiO2)." [Online]. Available: http://www.azom.com/properties.aspx?ArticleID=1114. [Accessed: 08-Sep-2015].

[29] "Cosmic Plastics CP7311 Epoxy Molding Compound." [Online]. Available: http://www.matweb.com/search/datasheet.aspx?MatGUID=0c7b1024ef524f9d919274ac39bdcfe1&ckck=1. [Accessed: 09-May-2013].

[30] A. Sharif *et al.*, "Pb-Free Glass Paste: A Metallization-Free Die-Attachment Solution for High-Temperature Application on Ceramic Substrates," *J. Electron. Mater.*, vol. 42, no. 8, pp. 2667–2676, Aug. 2013.

Chapter 6

Integration of PN as an encapsulant and die attach in electronics packaging*

Electronic packages are increasingly being utilized in complex and harsh applications such as deep subsea drilling, geothermal energy tapping and military applications. Owing to the high temperature and pressure demands on such packages, creating a better package requires more than just material improvements. This chapter first discusses the adaption of PN as a bonding material. In this chapter, the investigation of PN as a die attach is broadly divided into effects of fillers addition, bond stack design and thermal ageing, where bond shear results are used to characterize the behavior of PN in the form of adhesives. Next, the possibility of integrating PN as an encapsulant on a ceramic package is evaluated. The theoretical analysis is performed by using ANSYS™ simulation and then verified experimentally. An approach which combines design optimization and physical evaluation of fabricated packages provide feasible polymer lid designs for electronic packages operating in both high pressure (HP) and high pressure high temperature (HPHT) environments. It demonstrates that PN filled composites can be successfully integrated into ceramic packages for HPHT conditions.

*The content of this chapter was published in article:

E.J.R Phua, M. Liu, B. Cho, X. Hu, C.L.Gan, "Novel high temperature polymeric encapsulation material for extreme environment electronics packaging," Mater. Des., vol. 141, pp. 202–209, Mar. 2018.

6.1 Considerations for Usage of PN as Adhesive or Die Attach Material

This chapter discusses the use of PN as a die attach material broadly in the following perspectives:

- Effect of weight percent of fillers
- Effect of filler type, i.e. silica and alumina
- Effect of bond stack type, i.e. silicon/silicon, ceramic/silicon, ceramic/ceramic
- Effect of thermal aging

The adhesion and cohesion of electronics packaging encapsulant and die attach material is important, especially when it is utilized in a high temperature environment and simultaneously subjected to high mechanical stresses such as pressure. Thus, a bond stack test structure subjected to shear test will be useful to evaluate the adhesion/cohesion of the developed PN composites.

Figure 6-1 shows the test structure stack for evaluating the bond strength of PN when it is used to bond typical high temperature substrates such as ceramic (e.g. alumina) and silicon. A total of three different bond stacks are compared as shown in Figure 6-1. The corresponding CTEs are stated in Table 6-1.

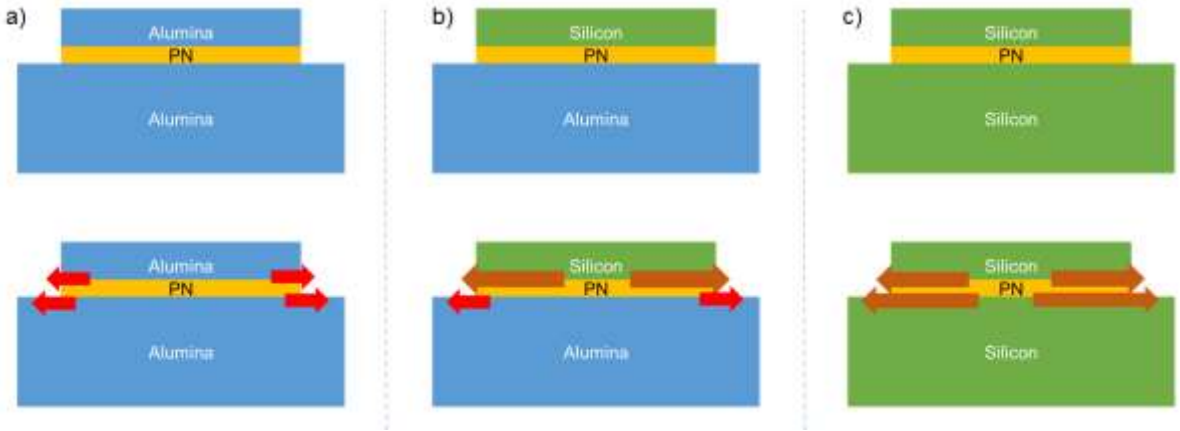

Figure 6-1 Different die and substrate stacks bonded with PN (a) alumina-alumina, (b) alumina-silicon, and (c) silicon-silicon.

Table 6- 1 CTE of different materials used in bond shear test.

Material	CTE (ppm/°C)	Thermal conductivity (W/mK)
Silicon	2.6	149
Alumina	7.2	35
Neat PN	55	0.4

6.2 Failure observations from die shear test samples

Figure 6-2 shows the optical images of sheared surfaces of different types of bond stack. Figure 6-2 (a) and Figure 6-2 (b) comprises of alumina substrate and the alumina chip respectively post bond shear test.

Following the same arrangement, Figure 6-2 (c) and Figure 6-2 (d) are alumina substrate and silicon chip respectively. Lastly, Figure 6-2 (e) and Figure 6-2 (f) are silicon substrate and silicon chip respectively.

For alumina/alumina bond stacks as shown in Figure 6-2 (a) to (c), cohesive failures are mostly observed. On the other hand, for Si/Si and alumina/Si bond stacks, mix mode failures are observed on the silicon surfaces (Figure 6-2(d) to Figure 6-2(f)).

SEM by secondary imaging was done on the surface of the phthalonitrile polymer filled with different fillers after bond shear testing. The aim is to observe the crack morphology of the fractured specimens, fillers dispersion in the phthalonitrile polymer and the adhesion between fillers and the polymer.

Good adhesion between the fillers and the matrix is one of the important criteria when modifying the properties of the filled polymer. The adhesion between the filler particles and the polymer is typically first determined by visual inspection of any particle detachment from the polymer matrix.

On alumina/alumina bond stacks, mostly cohesive failures were observed which left PN debris on both substrate top and die backside, like the failures observed in Figure 6-2(a) and (b). For Si/alumina and Si/Si stacks, mostly mixed mode failures were observed.

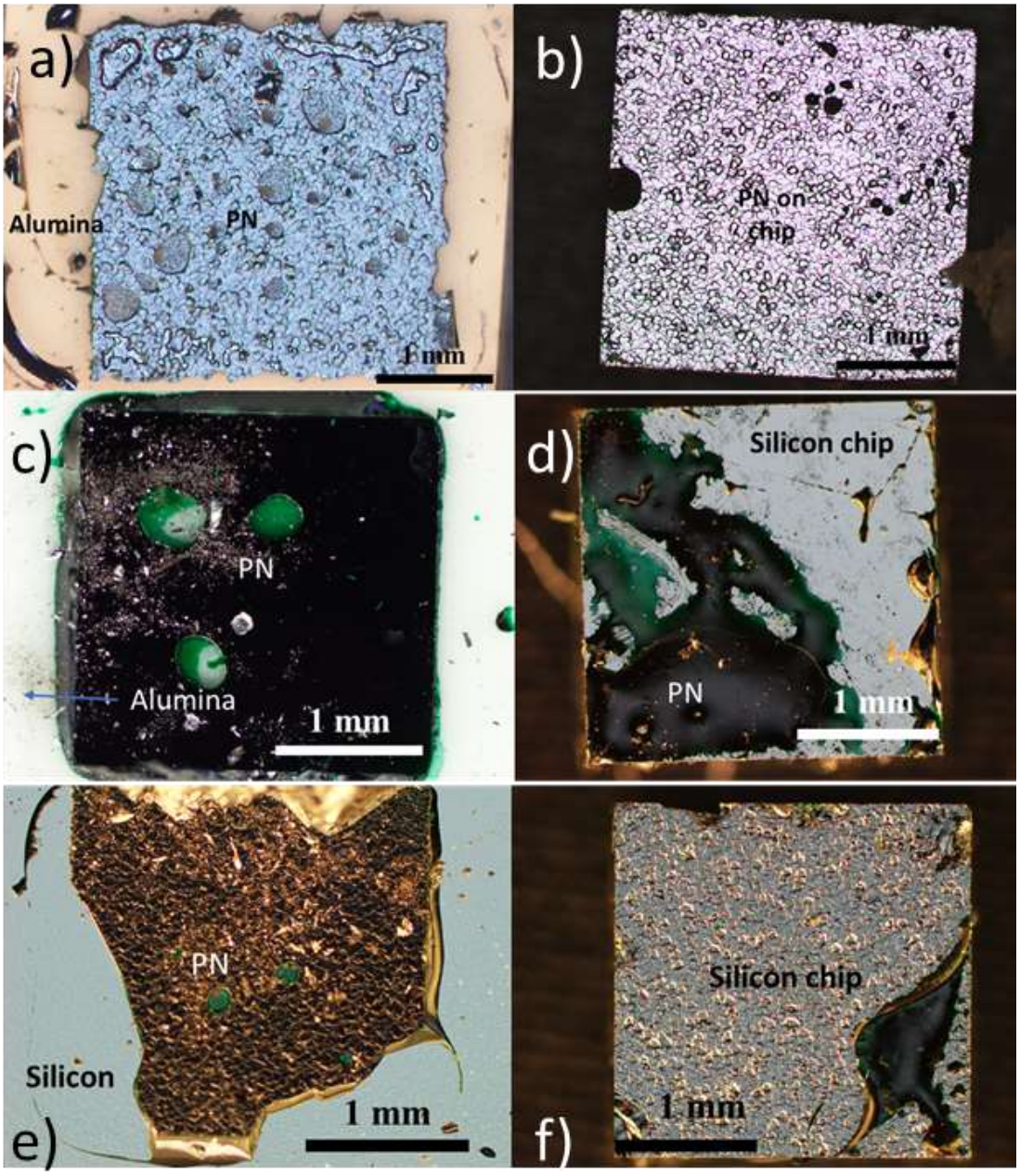

Figure 6-2 Optical images of PN mix mode failures **(a)** and **(b)** are alumina/alumina substrate and chip pair respectively, **(c)** and **(d)** are alumina/silicon substrate and chip pair respectively, **(e)** and **(f)** are silicon/silicon substrate and chip pair respectively.

Figure 6-3 and Figure 6-4 show the SEM images of PN filled with 50 weight percent silica and 50 weight percent alumina, respectively. Filler particles were observed to be well embedded within the polymer matrix for all types of fillers, which indicate that the filler particles have good adhesion to the polymer matrix.

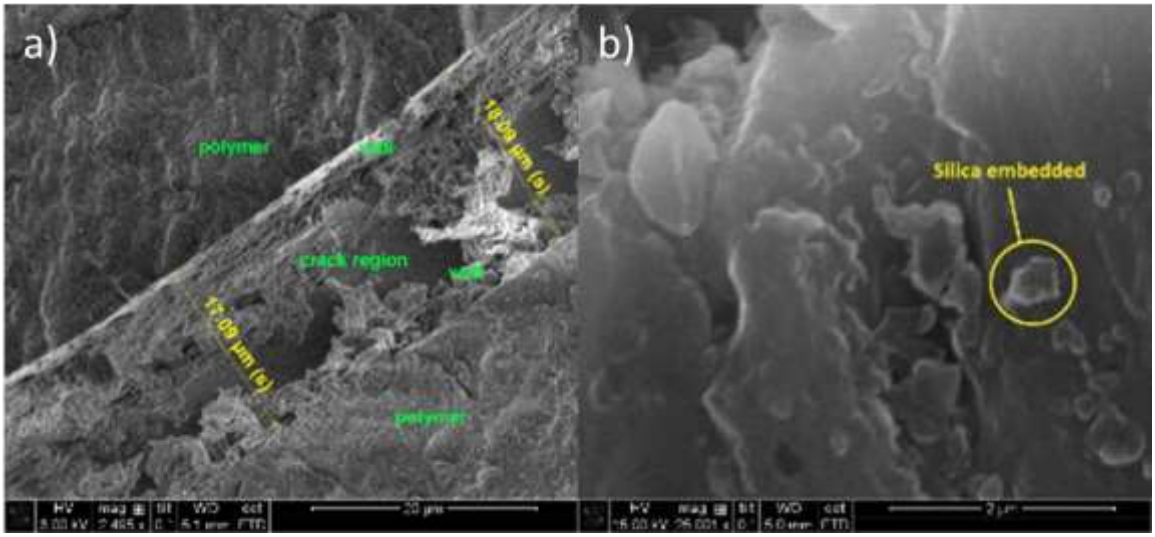

Figure 6-3 SEM images of PN filled with 50wt% silica in (a) 2500× magnification and (b) 25000× magnification.

Although some filler clusters in the polymer can be observed at sporadic locations, it did not affect the shear strength measured. The crack regions on both polymers filled with silica and alumina show faceted or clean appearance with no dimples which indicate brittle failure had occurred to the filled polymers.

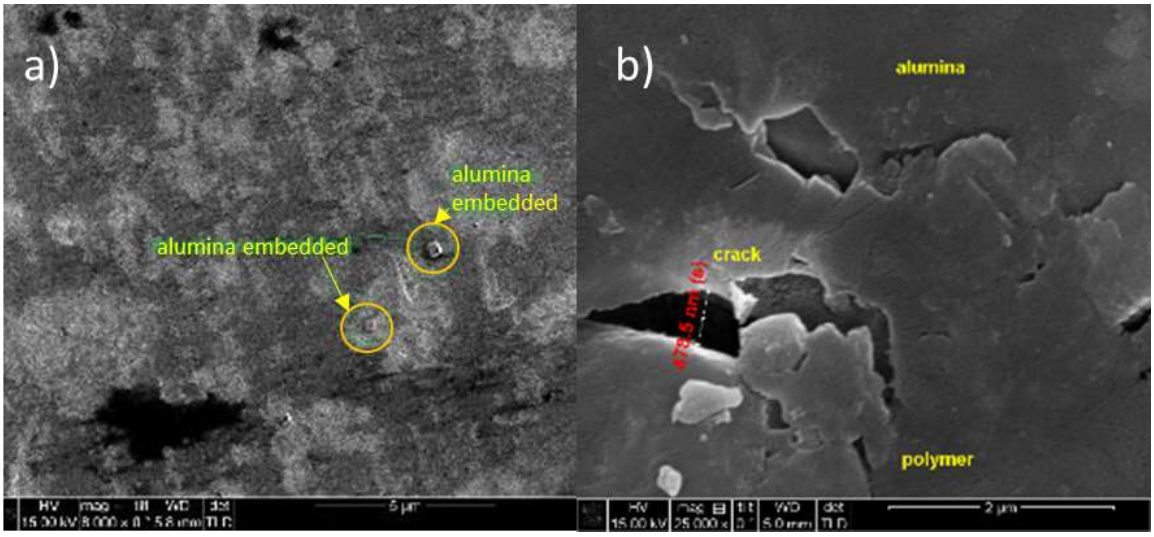

Figure 6-4 SEM images of PN filled with 50 wt% alumina in (a) 8000× magnification and (b) 25000× magnification.

Table 6-2 tabulates the overall bond shear strength of different bond stacks, fillers compositions, and also after thermal aging. These are further discussed in the following sections.

Table 6- 2 Shear strength of different stacks and filler compositions.

			No treatment	250°C/250hrs	360°C/500hrs
Stack (chip - substrate)	**Filler Type**	**Filler wt%**	**Shear strength (MPa)**	**Shear strength (MPa)**	**Shear strength (MPa)**
Alumina-Alumina	Neat PN	0	45.4 ± 6.5	78.3±5.1	14.1±3
Alumina-Alumina	Silica	30	22.2±4.4	82.6±14.6	22.6±0.7
Alumina-Alumina	Silica	50	18.6±2.8	80.9±10.2	40.5±13.7
Alumina-Alumina	Alumina	30	19.1±2.7	39±2.2	15.8±2.6
Alumina-Alumina	Alumina	50	14.3±1.2	52.8±12.9	39.8±5.0
Silicon - Alumina	Neat PN	0	10±1.36	50.3±5.2	6.97±1.3
Silicon - Alumina	Silica	30	9.58±1.61	26.4±2.6	28.1±3.8
Silicon - Alumina	Silica	50	7.63±2.04	15±2.3	20.6±3.5
Silicon - Alumina	Alumina	30	10.8±1.45	27.7±3.1	16.8±1.3
Silicon - Alumina	Alumina	50	7.05±0.56	14.3±1.8	17.4±2.5
Silicon – Silicon	Neat PN	0	15.2±2.9	57±4.8	8.61±3.9
Silicon – Silicon	Silica	30	17.3±1.9	29.4±7.8	23±5.1
Silicon – Silicon	Silica	50	15±2.1	22.5±9.1	20.4±5.6
Silicon – Silicon	Alumina	30	12.7±2.2	18±2.5	15.8±2.6
Silicon – Silicon	Alumina	50	14±2.5	20.3±5.8	20.6±3.5

6.2.1 Effect of filler percentage and types on bond shear strength

Figure 6-5 shows the shear strength of bond stacks with different types of fillers and the weight percent of each added. Initial shear strengths of PN only bonded samples are comparable or higher than samples which are filled with silica or alumina fillers. The high bond strength is largely because of the high temperature curing between individual polymer components and between surfaces of chip or substrate shown in Chapter 5.

Through Figure 6-5, it can be observed that increasing filler percentages decrease the bond shear strength regardless of the type of substrate or chip.

In all samples when the weight percent of fillers increased from 30 weight percent to 50 weight percent, bond shear strength decreased. Addition of fillers breaks the crosslinking continuity between polymeric molecules during the curing process. As the filler to triazine and filler to phthalocyanine bonds are weaker than pure polymeric bonds formed from high temperature crosslinking, lower bond shear strengths are observed when fillers are added.

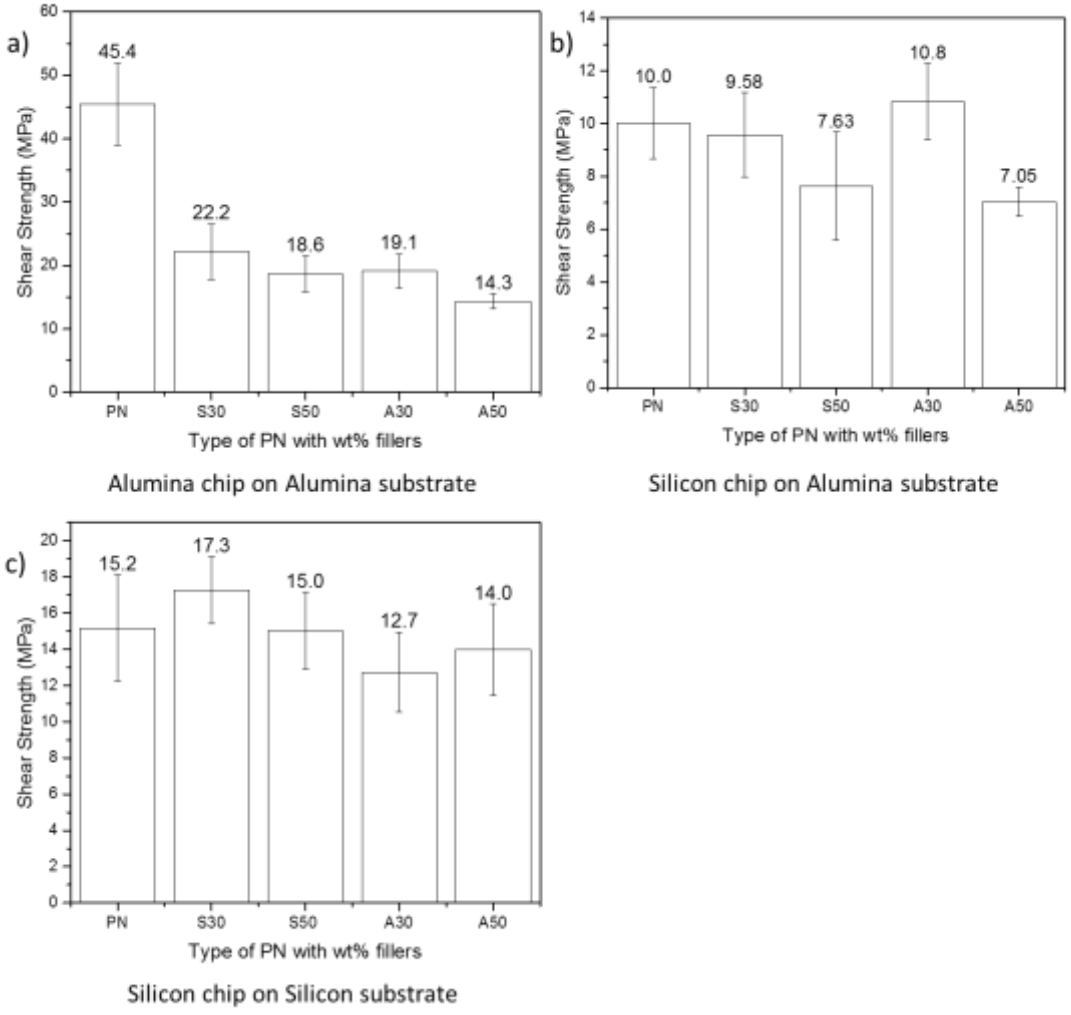

Figure 6-5 Shear strength of PN with various wt% fillers before ageing, (a) Alumina chip on Alumina substrate, (b) Silicon chip on Alumina substrate, (c) Silicon chip on Silicon substrate.

6.2.2 Effect of bond shear stack

With reference to Figure 6-6, the shear strength is highest when chip and substrate are both alumina. Bond shear strength is weaker when PN or its composites is bonded to silicon either on the chip side or substrate surface, whereby silicon-alumina bond stacks are consistently the weakest, alumina-alumina bond stack is the strongest followed by silicon-silicon stack.

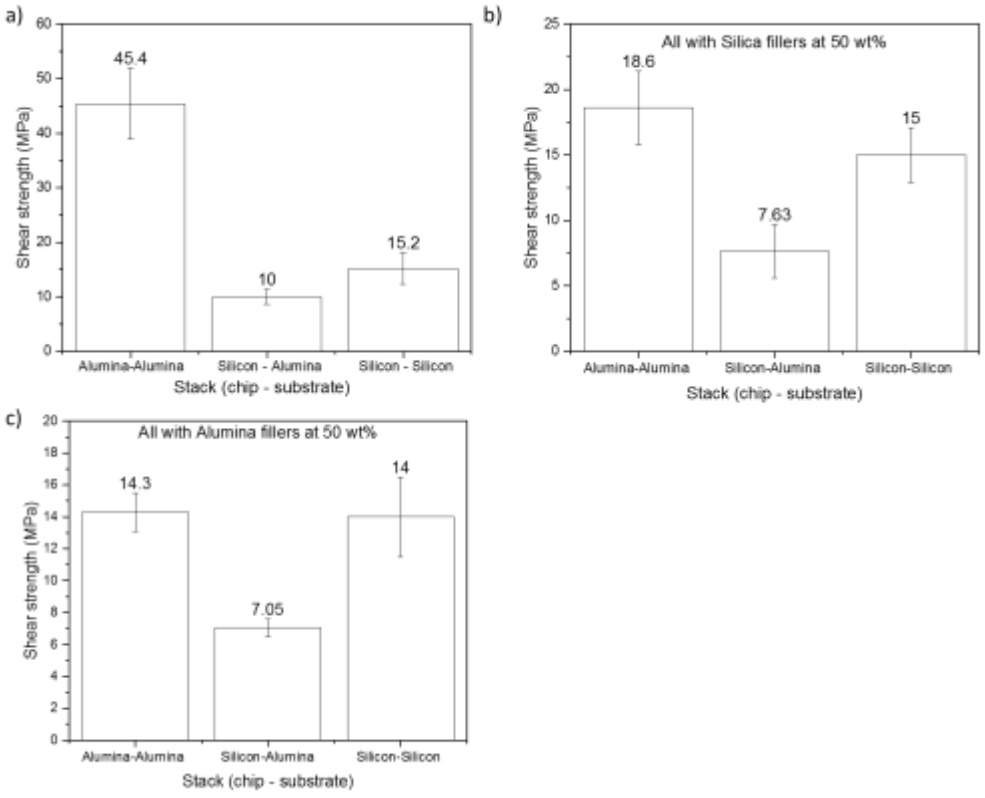

Figure 6-6 Shear strength of various bond stack with **(a)** neat PN, **(b)** 50 wt% silica filled PN and **(c)** 50 wt% alumina filled PN without thermal ageing.

This relationship is illustrated in Figure 6-7(a) through Gaussian09 where the enthalpy of absorbed phthalocyanine to silicon is only -43.3 kJ/mol and that of chemisorped phthalocyanine to silicon (Figure 6-7b) is calculated to be only -44.5 kJ/mol, which are significantly lower compared to the enthalpy of phthalocyanine to silica (-122 kJ/mol) and to alumina (-185 kJ/mol). Hence the lower tendency for bonding is observed directly through a decrease in bond shear strength when PN is bonded and cured in contact with silicon.

Referring to Figure 6-7(c), the enthalpy of triazine to silicon is a +85.4 kJ/mol. This shows that it is no longer energetically feasible for triazine to bond to silicon surface. Besides the weaker bonds between PN to silicon as compared to alumina, another possibility that may contribute to the lower bond strength of silicon/alumina stack as compared to silicon/silicon stack is the difference in CTE.

The CTE mismatch between PN and alumina is smaller as compared to between PN and silicon (see Table 6-1). Thus, a stress difference may occur between the two interfaces when PN is bonded to silicon on one side and alumina at the other, further weakening the bond shear strength. This effect is however not significant and the simulation results are provided in Appendix A.

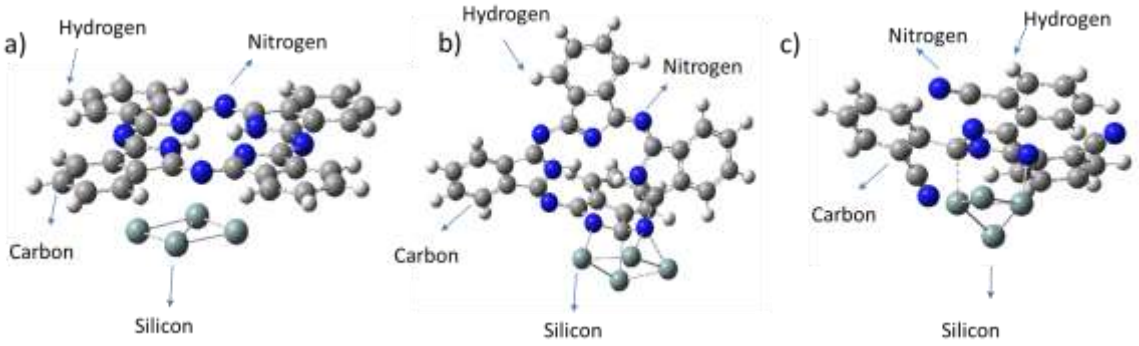

Figure 6-7 Chemical structure of (a) adsorbed phthalocyanine, (b) chemisorped phthalocyanine and (c) chemisorped Triazine to silicon for calculation of enthalpy.

Replacing neat PN with filled PN as shown in Figure 6-6 (b) and Figure 6-6 (c) proved that even with 50 weight percent of fillers added, the behavior is replicated. This shows that substrate type is also important to the bonding behavior.

6.2.3 Effect of thermal ageing on neat and filled PN samples

Figure 6-8 shows the shear strength of neat PN samples bonded in different bond stacks, before and after being subjected to 250°C/250 h and 360°C/500 h ageing tests. First, it can be observed that the shear strength of PN has increased after thermal aging at 250°C for 250 h for all samples. This is likely due to further cross-linking of the individual chains within PN during thermal aging, which has helped to raise the bond shear strength

by more than 30 MPa in the three different bond stack configurations. Even with the addition of silica or alumina fillers, the bond strength also consistently increased after the thermal aging at 250°C (Table 6-2). This shows that at an exposure temperature of 250°C, PN and its composites undergo further cross-linking, which then further toughens the material.

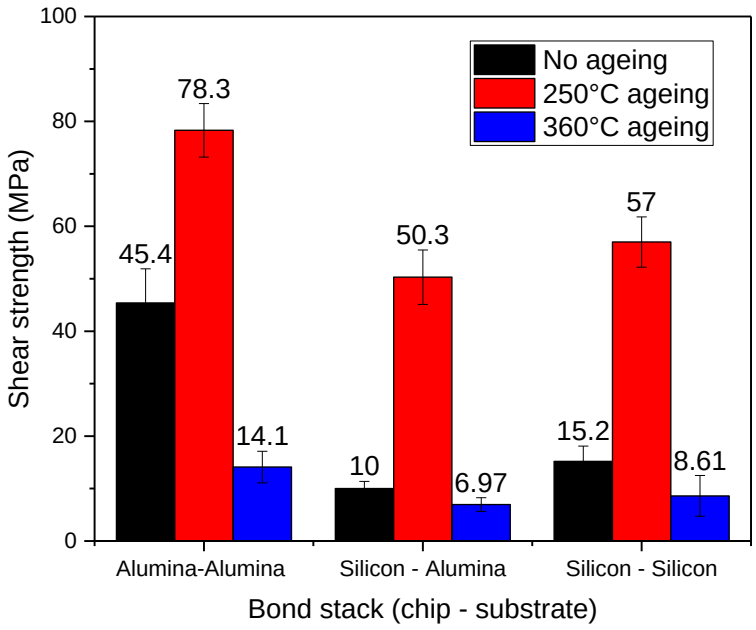

Figure 6-8 Shear strength of neat PN with various bond stacks after thermal aging.

Raising the ageing temperature to 360°C however decreases the shear strength as PN starts to degrade under prolong high temperature interaction with atmospheric oxygen, which is similar to the behavior when exposed to 500°C as explained earlier in Figure 4-1, although the degradation is slower at 360°C as compared to 500°C. Nevertheless, all the samples attained strength greater than the specification required from MIL-STD-883 Method 2019, whereby the minimal shear strength is 6.9 MPa for room temperature bond shear.

6.3 Hermetic and non-hermetic packaging in PN perspective

Presently, PN is well suited for high temperature and high mechanical performances. It is demonstrated that the mechanical strength and thermal properties are capable of that

required even in commercial HPHT operations reaching over 300°C. However, hermeticity may be an issue for specific package requirements.

Comparing the hermeticity of epoxy with PN using a helium bomb test, it was found that helium leaked at a rate of 4.6×10^{-6} atm-cc/sec when epoxy was used to bond a ceramic lid to a DIP package, whereas PN leaked at a rate of 3.5×10^{-7} atm-cc/sec. Although PN seems to have better hermeticity than epoxy, the requirement is a helium leak rate in the range of 5×10^{-8} atm-cc/sec following hermeticity specifications from MIL-STD-883G. Traditional high temperature alumina packages are used when hermetic properties are required, especially when stringent hermeticity tests specifications of MIL-STD-883 Test Method 1014 [3] are required.

Nevertheless, it is still possible for PN to be used as a high temperature encapsulants material by integrating it with the alumina packages. The results are shown in Appendix A. By injecting PN into such a package before sealing with a lid, it can reduce the thickness of alumina lids thus the overall package profile when desired. Lid designs can also be optimized to reduce the overall form factor for this integration. These results are elaborated in Appendix B. To demonstrate this proof of concept, PN encapsulated designs would be first demonstrated. This is subsequently followed by the demonstration using alumina lids injected with PN using simulation to demonstrate the substantial stress reduction when PN is injected within the package.

A further treatise on the simulation of various package designs is included in the appendix to provide an understanding on the stresses that ceramic lids typically encounter in HPHT applications and how a good encapsulation design that takes into consideration the design of the shape and size of the lid may help to mitigate these stresses. Figure 6-9 and Figure 6-10 show the simulated results for using PN encapsulant only, without a ceramic lid on top of the package. With reference to the maximum principle stress on the polymer observed, results show that neat PN would not fail where the tensile stress did not exceed the maximum tensile strength of 50 MPa at 250°C, 173

MPa test specifications, as compared with a condition of 300°C and 173 MPa where PN is expected to fail at 57 MPa.

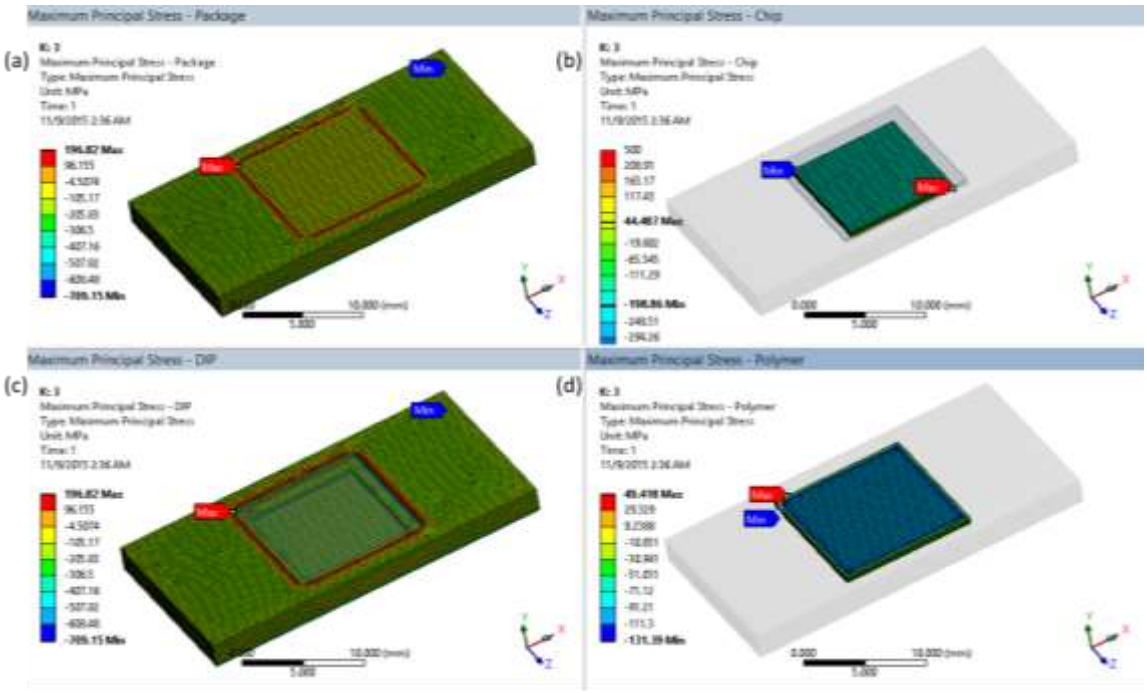

Figure 6-9 HPHT (250°C/173 MPa) induced stress studies on DIP package with neat PN encapsulant. Maximum principal stress (a) package (b) chip (c) DIP (d) polymer.

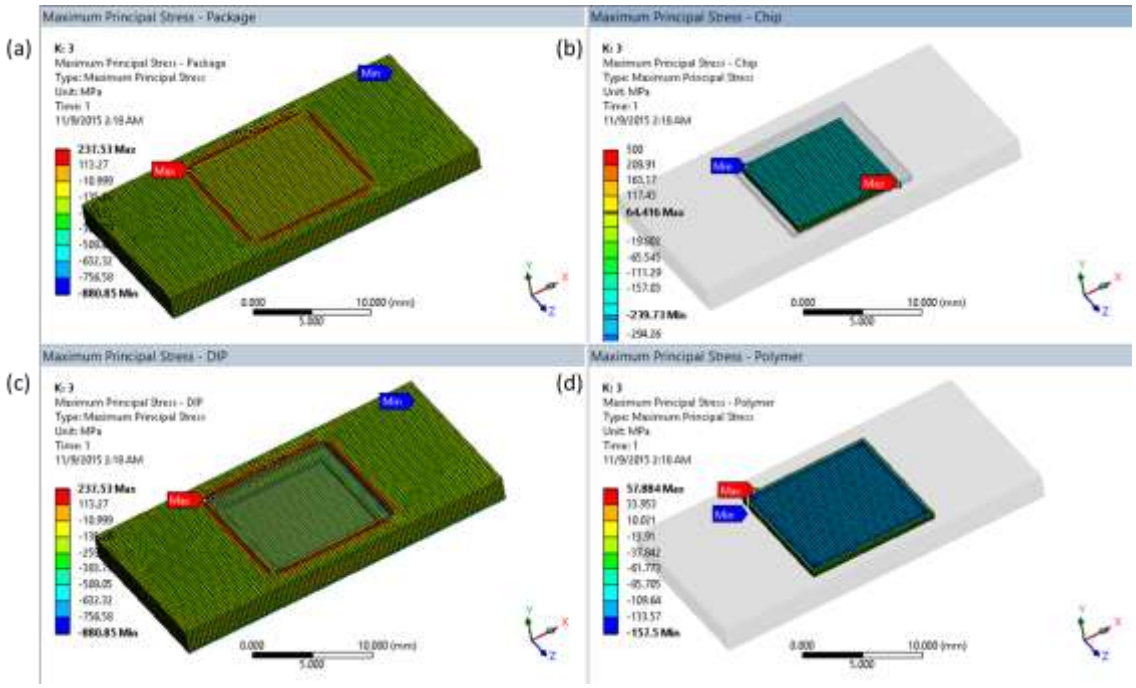

Figure 6-10 HPHT (300°C/207 MPa) induced stress studies on DIP package with neat PN encapsulant. Maximum principal stress (a) package (b) chip (c) DIP (d) polymer.

6.4 Experimental studies on PN encapsulant under HPHT

In order to verify that PN does not fail under the HPHT condition as simulated in the previous section, an experiment with the neat PN dispensed over a dummy package as a glob top encapsulation method was adopted. The package was then placed in the HPHT system with a temperature ramp rate of 10°C/min to 250°C and at a pressure of 173 MPa (25 000 Psi) for 168 hours. Natural cooling was then used for the chamber to return to room temperature. Figure 6-11 shows pictures of the package before and after the HPHT test. As shown, the sample remained intact with no visible cracks observed.

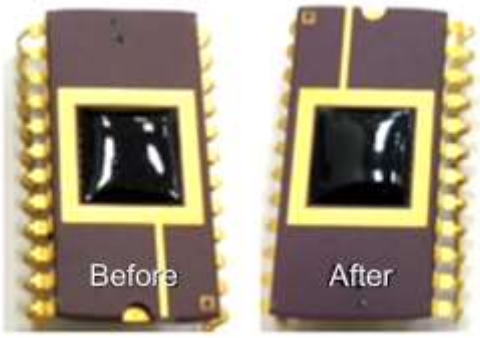

Figure 6-11 Demonstration of neat PN as a glob top encapsulation on a ceramic package in a HPHT environment (at 250°C, 173 MPa for 168 h).

Another experiment was then conducted to test the PN encapsulated package at the harsher HPHT condition, i.e. 300°C, 207 MPa. However, as shown in Figure 6-12, the high stress was not sustainable by PN where the encapsulant is observed to fracture and cracks had formed.

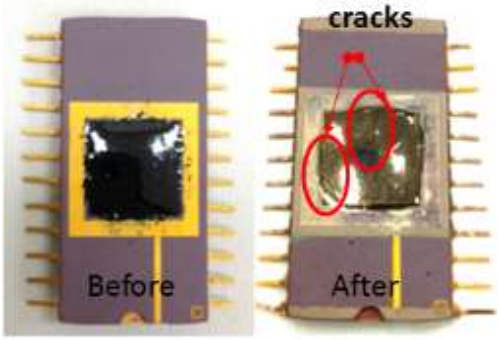

Figure 6-12 Visible crack propagation from polymer encapsulation fringe to centre of encapsulation for neat PN encapsulated DIP sample after HPHT testing at 207 MPa (30 kPsi) and 300°C.

DIP encapsulated with PN composites was then subjected to an intermediate test condition that has a higher temperature but lower pressure, i.e. 310°C and 190 MPa (equivalent to 1875 atm), for a duration of 168 hours, to test the limit of its survivability under HTHP conditions. From Figure 6-13, a crack-free surface was observed for the samples placed under a uniform pressure of 190 MPa, indicating that PN with 50 weight percent silica addition has the mechanical strength and endurance to withstand such external pressure.

This is further substantiated by simulation results as shown in Figure 6-14(d) where the stress generated on the polymer is estimated to be 13.7 MPa. This is well below the tensile stress limit of 50 MPa. No damage was observed on the sample before and after testing using both 2D and 3D computed tomography X-ray inspection.

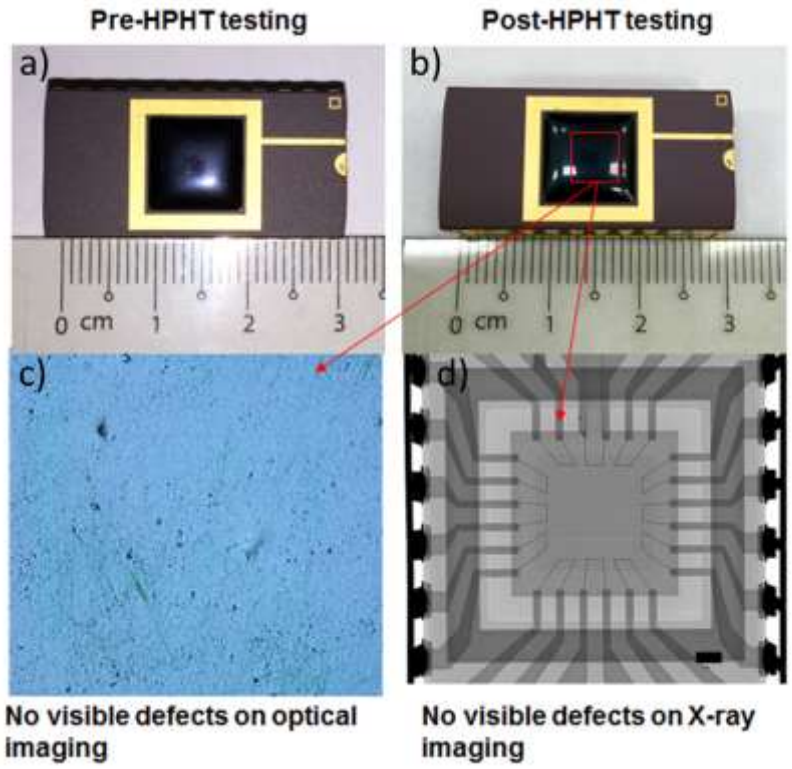

Figure 6-13 Images showing the encapsulated DIP with 50 weight percent silica (a) before and (b) after being subjected to HTHP conditions. (c) Optical imaging shows no visible cracks on the encapsulated surface. (d) X-ray imaging reveals the wire-bonds remained intact after sample was subjected to 190 MPa at 310°C.

The wire-bonds remained intact as revealed from the X-ray images, likely due to the significantly reduced CTE mismatch between the encapsulant, the substrate and the die that relieved the stresses generated by the thermal expansion which may damage the delicate wire-bonds. Pre and post-stressing sample inspections were also performed using SEM with no cracks observed under high magnifications.

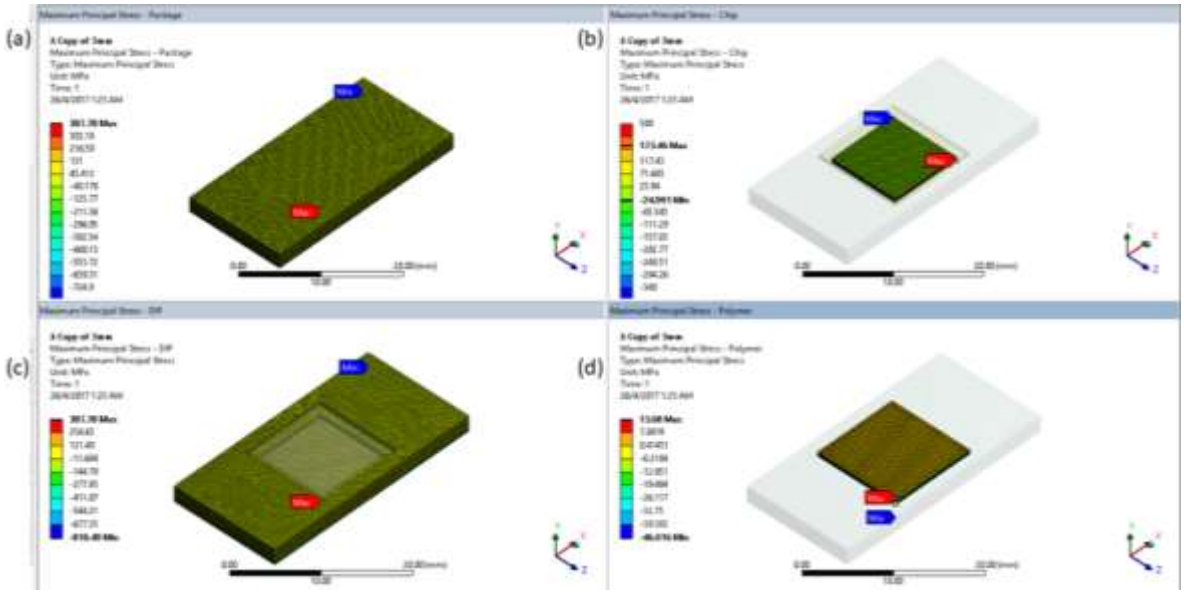

Figure 6-14 (a) HPHT (310°C/190 MPa) induced stress studies on DIP package with 50 weight percent silica filled PN encapsulant. Maximum principal stress **(a)** package **(b)** chip **(c)** DIP **(d)** polymer.

6.5 Summary

In this chapter, PN is explored to be used as a die attach and encapsulants in electronics packages for high temperature high pressure environment. PN with different weight percent of silica or alumina fillers were evaluated as a die attach through bond shear tests on different bond stack configurations. It is observed that the bond strength is weakest in a silicon/alumina stack. Based on DFT simulations, triazine and phthalocyanine do not bond well to silicon, in contrast with alumina where the enthalpy of formation is energetically favorable. Thus, PN may be more suited to be used as bonding material between alumina packages and lids. Nevertheless, the bond strength of all the configurations, including silicon/alumina, meets the minimum standard requirement even after thermal aging at 360°C for 500 hrs.

In order to improve the structural integrity for lid robustness of ceramics packages used in HPHT applications, the most typical solution is to just increase the lid package thickness. In the thesis hypothesis, it is postulated that PN may replace the ceramic lid to be used as an encapsulant instead. Through ANSYS™ simulations based on Rankine's theory, it is predicted that PN can survive in 250°C, 173 MPa condition but not 300°C, 207 MPa. To verify the results through experiments, the PN encapsulant was first successfully integrated into a ceramic package with wire-bonds, without any damage to the wire-bonds or silicon chip. The samples were then placed in the specially designed HPHT test system and stressed at the conditions for 168 hrs. The experimental results were consistent with the simulations, where cracks were observed in the 300°C, 207 MPa stressed sample, but not on the 250°C, 173 MPa sample. It was further shown that PN composites can be used in 310°C and 190 MPa environments.

Although PN and its composites are not hermetic like epoxy, it can still be used in a high temperature high pressure environment where mechanical survivability has been proven in chapter 4 and electrical functionality test results can be found in Appendix A. Package redesign can include having it function as a cavity filler which may improve the mechanical integrity of the ceramic package in the high pressure environment. Thus, increased performance and reliability of the HPHT package may be achieved with the optimal design of PN and its composites with the ceramic package, and with a proper understanding of the environmental conditions.

References

[1] "Aluminum Oxide | Al2O3 Material Properties." [Online]. Available: http://accuratus.com/alumox.html. [Accessed: 08-Oct-2015].

[2] Petersen, "Silicon as a mechanical material," *http://www.me.berkeley.edu/~lwlin/me119/papers/paper9.pdf*, May-1982. [Online]. Available: http://www.me.berkeley.edu/~lwlin/me119/papers/paper9.pdf. [Accessed: 10-Sep-2015].

[3] "MIL-STD-883 Test Methods 1004 - 1018." [Online]. Available: http://eesemi.com/milmethods.htm. [Accessed: 09-Aug-2017].

Chapter 7

Implications/Impact/Outstanding Questions

In summary, the work presented in this thesis has demonstrated that PN and its composites can serve both as an encapsulation and adhesive material for electronics packaging. This chapter discusses the implications of the research on high temperature encapsulation. It draws together the thesis works by proving the hypothesis of high temperature effects on filler-matrix of PN, which has not been evaluated previously for high temperature encapsulation on a thermomechanical and electrical basis. It also includes some reconnaissance studies of material selection for high temperature encapsulant and possible fillers. The future work regarding the exploration of PN in various facets of electronic packaging is also discussed.

7.1 Scientific significance

Many polymers such as cyanate esters, modified epoxies and toughened polyimides have been investigated to date as high temperature encapsulation material and some have shown promise. Operation demands have called for higher temperature electronics and the use of adequate packaging protection is therefore of utmost importance since the package is the first layer of protection any electronics has against the external environment. T*he first hypothesis of this thesis is to verify that the 360°C cured state of resorcinol PN and its filled moieties would be able to meet the thermal requirements of HT application.* The research hereby focuses on identification of resorcinol based PN as a low melting temperature candidate yet with high thermomechanical strengths with increased curing.

The research first explored the usage of PN as a material using TGA to study the thermal stability of using neat and filled PN to check the effects of filler (such as silica and alumina) additions. Through detailed studies of the bulk material, the properties of neat PN was first characterized and then further studied by varying between filler types and filler concentrations.

This leads to the second hypothesis which is that the addition of fillers does not weaken the PN structure but instead allows tuning of its thermal properties and mechanical properties which would help PN function in a HPHT application environment.

The addition of 50 weight percent of fillers, for both silica and alumina, was found to decrease the activation energy significantly for crosslinking reactions. This implies that the cross-linked silica and alumina coupled to post cured PN matrix has lower bond energy as compared to neat PN. Considering just neat PN, the activation energy of PN increases with curing temperature, implying that high temperature curing increases the bond strength between its moieties, and hence the increase in activation energy observed. Hence it is possible to use both neat and filled PN for various packaging purposes.

TGA tests further revealed that when samples are cured to 360°C and subjected to temperatures of 500°C for 2 hours, the decrease in weight is approximated to be 5% for neat PN. The percentage decreases and over a range when fillers are added. This indicates that PN has interacted with the fillers to gain additional stability. The decrease in weight percent loss can be correlated to the subsequent DFT results which show favourable bonding between the fillers and PN.

It is thus proven that through the first hypothesis that PN has thermal properties which are better in terms of decomposition temperatures and thermal stability, where most epoxies fully decompose above 250°C. The experiments proceeded from here to identify the type of bonds which are present between PN and its fillers which are important to its mechanical properties. This is also important to the second hypothesis which is to prove that filler addition does not cause PN or its moiety to weaken as a whole.

FTIR suggested that neat PN experiences increase in triazine at 1360 cm^{-1} and 1520 cm^{-1} and phthalocyanine at 1008 cm^{-1} as observed from the increase in FTIR intensities with curing profile. This shows active structural moieties formation at each curing profile. At this stage of formation, it is thus possible to make silica and alumina fillers bond with PN moieties through high temperature curing treatments. It is possible to form covalent bonds in the crosslinking polymer moieties through Si bonded to N of polymer moieties or Al bonded to the N of polymer moieties. This is verified through FTIR measurements where peaks at 811 cm^{-1} and 665 cm^{-1} for Si-N and Al-N bonds, respectively were detected.

DFT simulations using Gaussian09 prove that Si-N and Al-N bonds are energetically feasible between PN and silica or alumina fillers. Gaussian09 is first used to demonstrate the formation of macromolecule polyisoindolenine which then goes through concerted reactions to form phthalocyanine and then isoindolenine. The bonding of such moieties at high temperature results in formation of tiny gaps which may constitute part of the diffusion pathways for molecules such as water.

In the simulation, Gibbs free energy is being calculated and the resulting enthalpy between the moieties and filler adducts are studied. It is found that alumina has the higher enthalpy to both triazine and phthalocyanine as compared to silica. On the other hand, isoindolenine shows a positive enthalpy indicating that it is energetically infeasible for isoindolenine to bond with silica or alumina. Such correlation between the DFT to FTIR results on the possible bond formation between PN and fillers, as well as the possible formation of channels for water diffusion have not been studied previously. It is also the first time fillers which have been previously used with epoxies are studied and correlated to PN.

To understand the kinetics of the curing process, TGA studies at different ramp rates were conducted for PN cured to different temperatures as well as filled with fillers. The calculation of the activation energy as done using Kissenger's equation. Higher activation energies were obtained for PN cured to higher temperature, while the addition of fillers lower it.

It is also hypothesized that the mechanical strength of PN would increase with higher thermal cure conditions. Nanoindentation results have shown that by increasing the curing condition from 320˚C to 360˚C, the elastic modulus of PN increased 30% to 80% for filler combinations such as 30A, 50A and 50S. Compressive testing has further proven that for 360˚C cured neat PN, the measured compressive strength is 500 MPa which is much higher than most epoxy used for standard electronics packaging, whose compressive strength ranges between 6.89 to 350 MPa [1]. This is desirable especially when PN is designed to survive in not only high temperature but high pressure environment as well.

Besides high compressive strength, PN other mechanical properties such as flexural and tensile strength are comparable to state of the art epoxies. Neat PN has a stable storage modulus as shown in accelerated testing conditions, carried out under moisture MSL level 1 (85%RH/85°C) conditions where it is demonstrated that PN served as a tough material both against high heat and in moist environments where humidity can reach

85%RH. It is also investigated that PN has a recoverable modulus as reflected in the controlled DMA-RH testing. This makes it possible for PN to be used for field applications such as logging while drilling where it is possible for PN to recover modulus changes after immersion in water.

With the excellent properties observed in mechanical studies, it is hypothesized that PN can also be used in various functions such as die attach, sealant or even as a total encapsulation replacement. Bond shear analysis further shows that silicon dies can be bonded strongly to different underlying substrates such as alumina and silicon substrates with high shear strengths, especially for neat PN, which otherwise is not achievable with state of the art epoxies [2]. The mechanism of bonding is similar to how PN and its moieties would bond to silica and alumina in the filler-matrix interactions as mentioned in Chapter 4.

Neat PN has comparable and even better shear strength as compared to low temperature silver paste cured to similar temperatures of 300°C-400°C [3]. This serves as an excellent bonding alternative compared to solder paste which can be further strengthened with increased bonding temperature and curing profiles. Although addition of fillers helps to negate CTE issues, it would lead to a decrease in bond shear strength, with decreased polymer volume. Polymeric components such as triazine and phthalocyanine crosslink strongly within themselves in the polymer network. Although bonding PN to silica or alumina is possible, the bonds formed are not as strong with pure silicon due to a lower enthalpy for absorbed and chemisorped phthalocyanine to silicon calculated to be -43.3 kJ/mol and -44.5 kJ/mol in Gaussian09™ analysis. It is no longer energetically feasible for triazine to bond to silicon surfaces as indicated by an enthalpy of +85.4kJ/mol. Bond shear strength is affected by the type of failures, which can be adhesion or cohesion or mix mode failures.

Although PN is a good encapsulant which can be used to provide adequate package protection, it does not provide complete hermeticity. A proof of concept was carried out

by dispensing PN as a glob top encapsulation on a ceramic substrate. Figure 7-1 shows the process flow for PN as glob top encapsulant on DIP substrate.

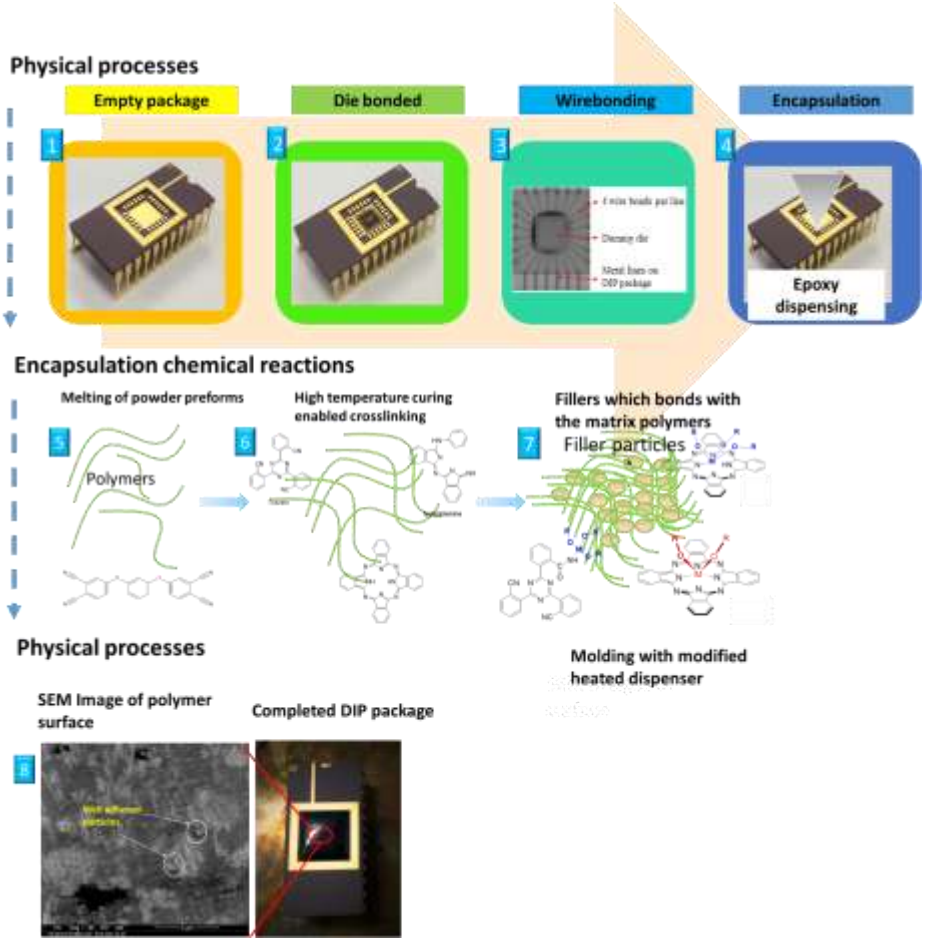

Figure 7- 1 Summary to demonstrate the processability and adaptability of PN

This novel design can make a HPHT package thinner as compared to those implemented with purely ceramic lids. Yet, PN encapsulants can take on the same extreme pressures dominated traditionally by alumina type packages. The demonstration was done by melting of PN powder or pellet and dispensing them onto a wire-bonded chip on a ceramic package. The package was also subjected to HPHT conditions for 168 hrs. It was shown that PN encapsulation package can survive conditions of 310°C, 190 MPa.

In the perspective of fabrication, it is much easier to make a dome shape PN lid as compared to making a ceramic lid with the same dome design as shown in Appendix B., The making of a dome type cavity on alumina is much more tedious as it requires high

temperature processes to form the lids into the required shapes followed by extensive drilling and polishing. This is only possible with the use of expensive tooling such diamond drill bits. Extra drill time is also to be factored into the production cost. Final processing which involves further polishing are then done to smoothen the lid surfaces to the required finishes. All these add up to increase the cost of making HPHT compliant packages.

7.2 Testing limitations

It is possible through the use of state-of-the-art commercial equipment which combines the use of simultaneous DSC-TGA (SDT) to monitor actual mass changes during endothermic and exothermic transitions. This technique is good for high temperature reactions greater than 250°C but is not sensitive for PN-filler reactions which start at a lower 180°C. It is theoretically possible to determine the bond enthalpies using modulated differential scanning calorimetry (MDSC) techniques. However, this is not adequately sensitive to pick up rapid filler to molecule bonding especially after the first melting at 180°C, to reflect and differentiate the differences in enthalpies at the various weight percent of fillers. As such, even MDSC which is a highly sensitive technique is also inadequate to differentiate clearly the enthalpy differences due to filler weight percent changes. This technique has already been utilised in the perspective of Kissenger's equation for the studying of epoxy and filler components. Transitions between filler-epoxy molecules are slower as compared to PN based encapsulants, hence can be studied with MDSC.

The use of FTIR coupled to Raman may be a good idea to explore the polymer behaviour, especially when they are bonded to various fillers. Attempts to achieve measurements using 488 nm laser was not successful as considerably less peaks were picked up as compared to FTIR. Also, the noise to signal ratio is significant enough to mask out prospective signals of interest. This however can be improved with the use of water typed objective lens which would give more stable measurements with less noise observed. But the power of the laser still caused significant damaged to the sample, thus making characterization difficult. Such limitations cannot be overcome even with the use

of water lens in a Raman setup as it is an existing equipment limitation which would require improvement.

Utilising Gaussian09 simulations, it is possible to predict reaction pathways for silica and alumina with the various PN moieties. These values tally well with the experimental observations such as during prediction of bond feasibilities using FTIR. Future experiments with different filler and more complex pathways can be conducted with the use of this software to gauge the observed products before proceeding with experimental phases. Larger scales of adduct can also be utilised to monitor for possible differences and is achievable with higher computational power.

With retrospect, it is also possible to test out the properties of environmental pressures during curing where the PN properties might be enhanced with higher engineering pressures to compact the polymer together at high temperature while curing. These studies might allow PN and cured components to be mechanically improved further by being more compact but studies would still have to be carried out with addition of fillers if thermal mismatch and thermal conductivity are of concern.

7.3 Future work

Based on initial studies, it is possible to coat PN onto metal by standard bonding techniques or by coating metal onto PN using thin film deposition processes. PN bonds strongly onto the surface of metals such as steel or copper and thus makes it an extremely good matrix for such metals. Utilizing this special bonding affinity between PN and the various metals, it is possible to fabricate PN based printed circuit boards (PCB) comparable to the low temperature glass reinforced epoxy laminate sheets (FR4). Considering the excellent thermal and mechanical properties of PN, this makes PN a very attractive candidate for high temperature performance PCBs. Essentially, this has high potential in filling the gap between high temperature and heavy ceramic and metallic boards with a polymeric high temperature alternative.

For future high temperature processing of PN, it is also possible to introduce PN into standard assembly processes such as solder masking as a high temperature substitute in the form of resorcinol based PN which has a low melting temperature of 180°C and is easily dispensed as a liquid which sets rapidly. Adopting the use of PN implied that it is still possible to leverage on existing industrial equipment previously used to process epoxies, thus making PN a complementary material for many existing semiconductor packaging processes.

References

[1] "Overview of materials for Epoxy Molding Compound." [Online]. Available: http://www.matweb.com/search/DataSheet.aspx?MatGUID=d32b84b0ef1e410596e9dda9e02429c7&ckck=1. [Accessed: 17-Mar-2016].

[2] Y. Guan, X. Chen, F. Li, and H. Gao, "Study on the curing process and shearing tests of die attachment by Ag-epoxy electrically conductive adhesive," *Int. J. Adhes. Adhes.*, vol. 30, no. 2, pp. 80–88, Mar. 2010.

[3] K. Suganuma, S. Sakamoto, N. Kagami, D. Wakuda, K.-S. Kim, and M. Nogi, "Low-temperature low-pressure die attach with hybrid silver particle paste," *Microelectron. Reliab.*, vol. 52, no. 2, pp. 375–380, Feb. 2012.

Appendix A: Auxiliary Data

A1.1 Curing parameters and related exotherms

For polymers cured without any fillers, there was no curing peak observed from the heating up to 400°C or under isothermal heating at 220°C. The resin remained as a liquid for many days at 220°C with no increase in viscosity. Figure A.1 shows the DSC thermograms which clearly show the curing peaks at 220°C and 360°C with other curing peaks in between.

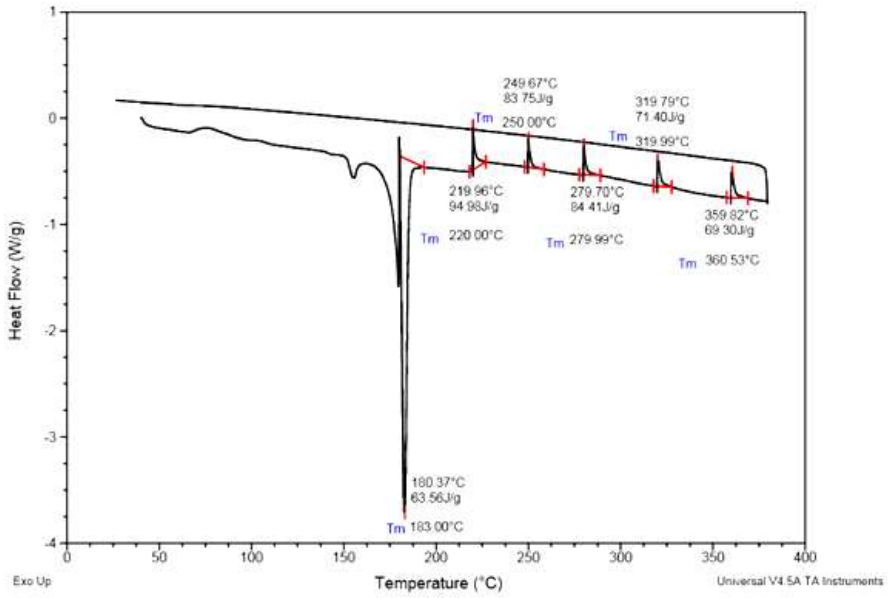

Figure A.1 Typical dynamic DSC thermograms of rPN/APB system

A1.2 Storage modulus variation against temperature

The PN polymer has higher modulus when thermally cured to higher temperatures and is supported through DMA storage modulus analysis as shown in Figure A.2.

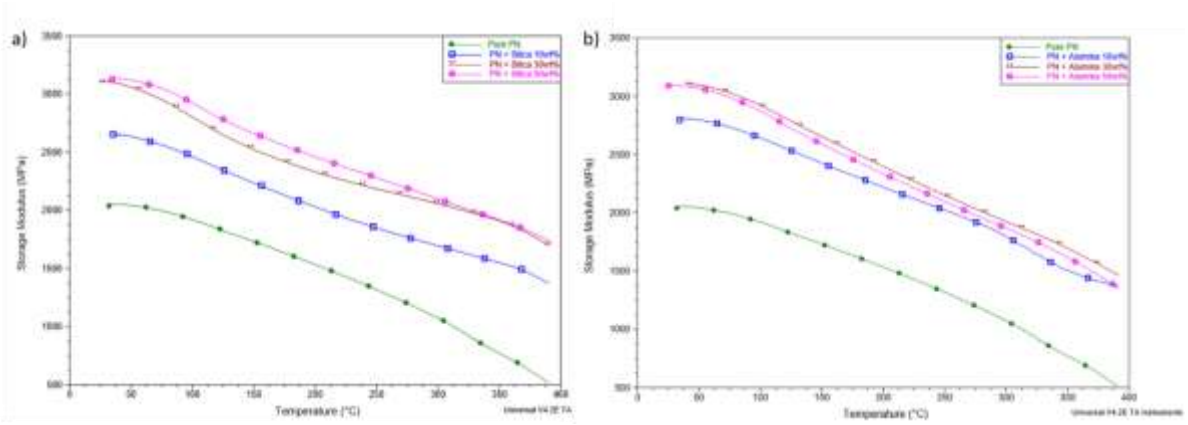

Figure A.2 DMA measurement for silica and alumina filled samples depicting stable storage modulus over temperature increases without sharp drop in modulus

A1.3 Rheometric study of rPN and its composites

A rheometric study was conducted to analyse PN and its filled composite previously and is in Figure A.3. Reference at the shear rate of 100 is typically used for molding operations. It can be observed that the viscosity of PN and its composites are below 2 Pa.s, which is relatively low compared to epoxy which ranges between 600 - 45000 Pa.s.

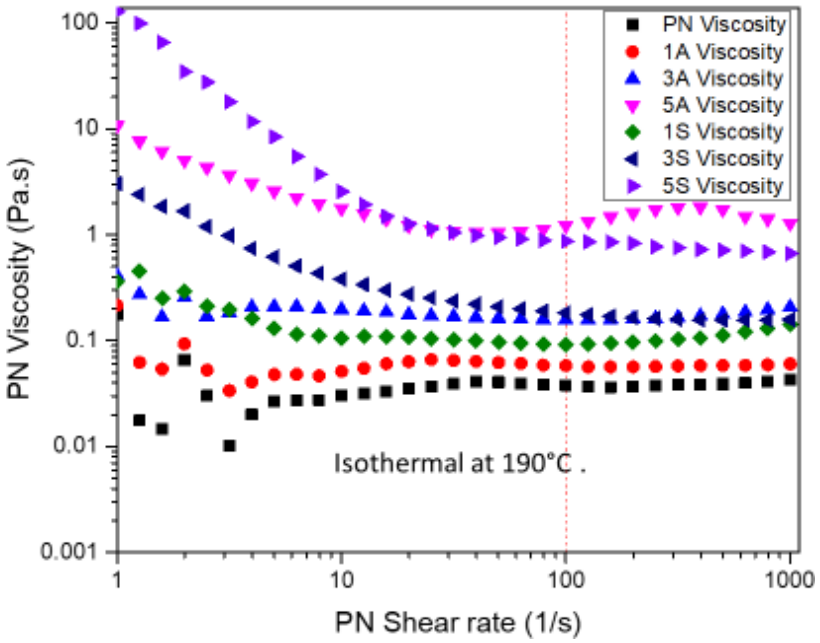

Figure A.3 Rheology data for neat PN and its filled composites

A1.4 CTE effects on stress differences

CTE accounts only partially for the stress effect experienced during temperature rise and fall. In this consideration, bond energy feasibilities accounts more for the detachment than the stress differences.

Taking reference to Figure A.4a) and Figure A.4b) whereby temperature is ramped up from room temperature to 250°C, the stress on PN (in silicon die on silicon substrate) is as observed at 0.00256 MPa and is negligible compared to the bond shear stress observed (i.e. 57 MPa). Similarly, for Al die on Al substrate, when the temperature is ramped up from room temperature to 250°C, the stress of alumina die on alumina substrate on PN is observed to be 0.00213 MPa and is also negligible compared to the bond shear stress observed (e.g. 78.3 MPa).

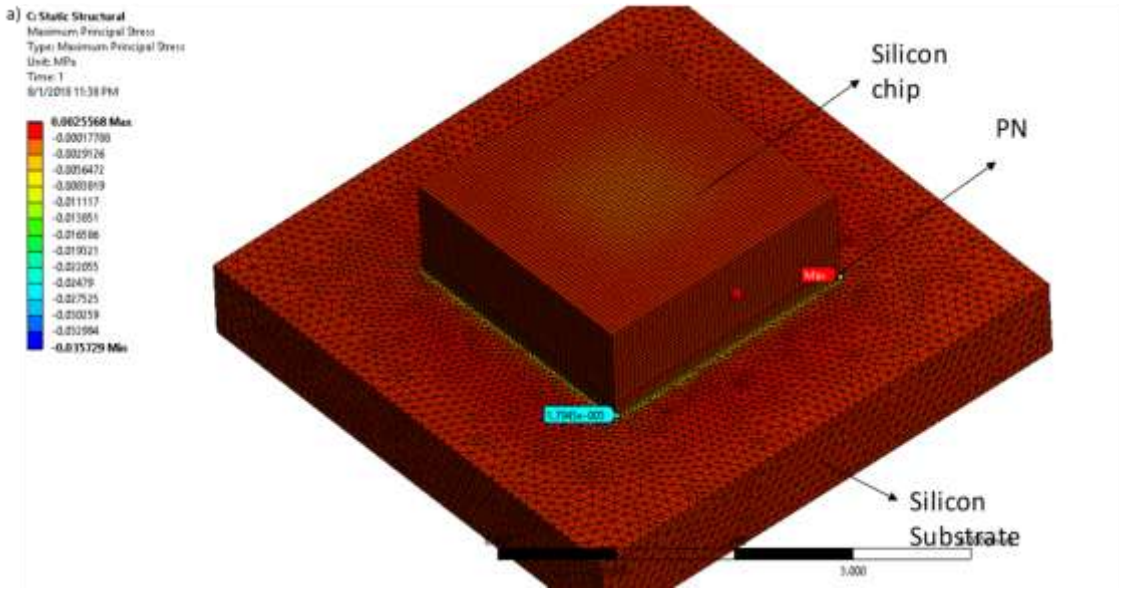

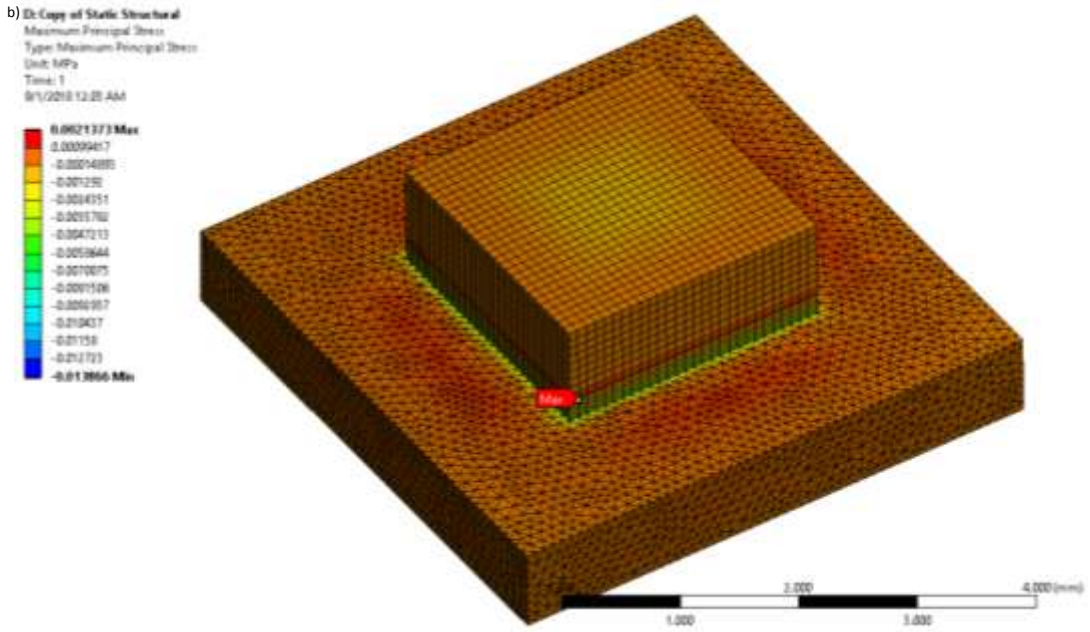

Figure A.4 a) Stress on silicon die bonded to silicon substrate **b)** Stress on alumina die bonded to alumina substrate

When encapsulation is performed using epoxy resins and cyanoacrylates and exposed to dwell temperatures of 250°C, Figure A.4 (a) – (c) depicted high resistances of 14 Ω implying that the wirebonds have been damaged. Figure A.4 (d) shows high resistance of 6Ω and is highly unstable. All PN and composites show low resistances of 0.53Ω +/- 4% deviation.

A1.5 PN survivability in HPHT environment

The reason that it is claimed that the PN composites can be used in HTHP environment is because experiments where electrical measurements of wire-bonded samples were monitored were done at temperatures of 250°C for more than 125 hrs. It has been proven that the encapsulation is tough enough to withstand the thermomechanical stresses of up to 310°C and 190 MPa. Figure A.5 shows the data for PN, 30A, 50A, 30S and 50S. All PN samples survived the 125 hrs of testing with no resistance degradation observed as compared to epoxy and cyanoacrylate in Figure A.5.

The test conditions are as follow:

A constant current stress of 0.15A was supplied with a sampling rate of 300 s set to a voltage limit of 2 V. When encapsulation is performed using epoxy resins and cyanoacrylates and exposed to dwell temperatures of 250°C, Figure A.5 (a) – (c) depicted high resistances of 14 Ω implying that the wirebonds have been damaged. Figure A.5 (d) shows high resistance of 6 Ω and is highly unstable. All PN and composites show low resistances of 0.53Ω +/- 4% deviation.

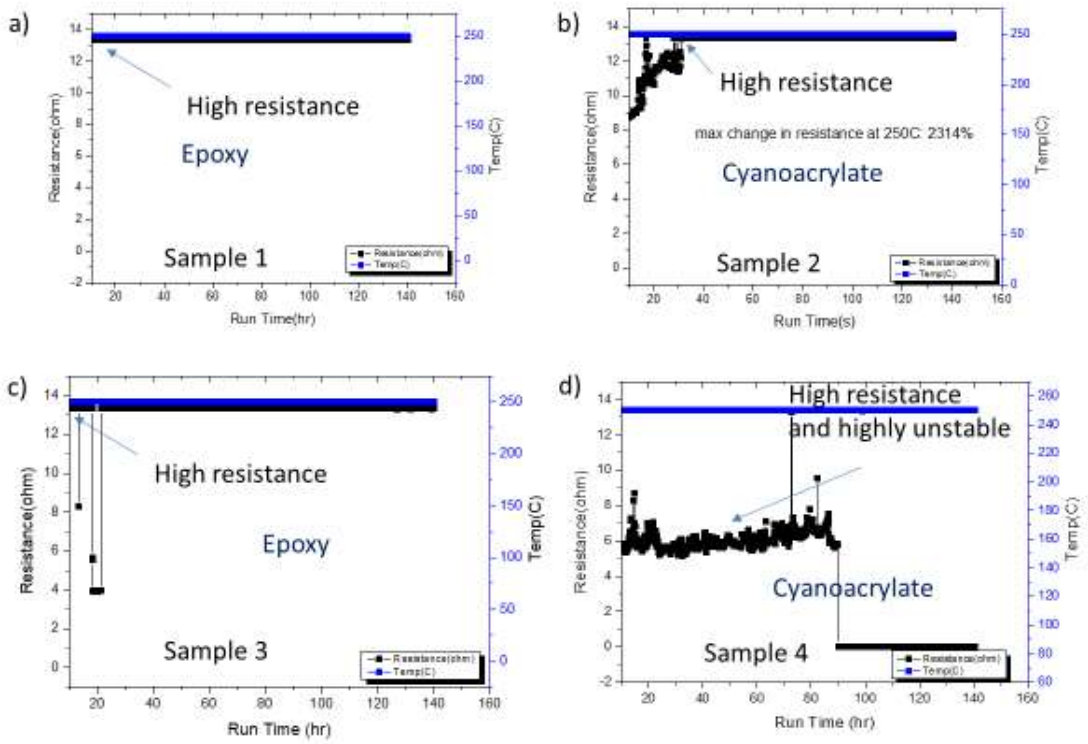

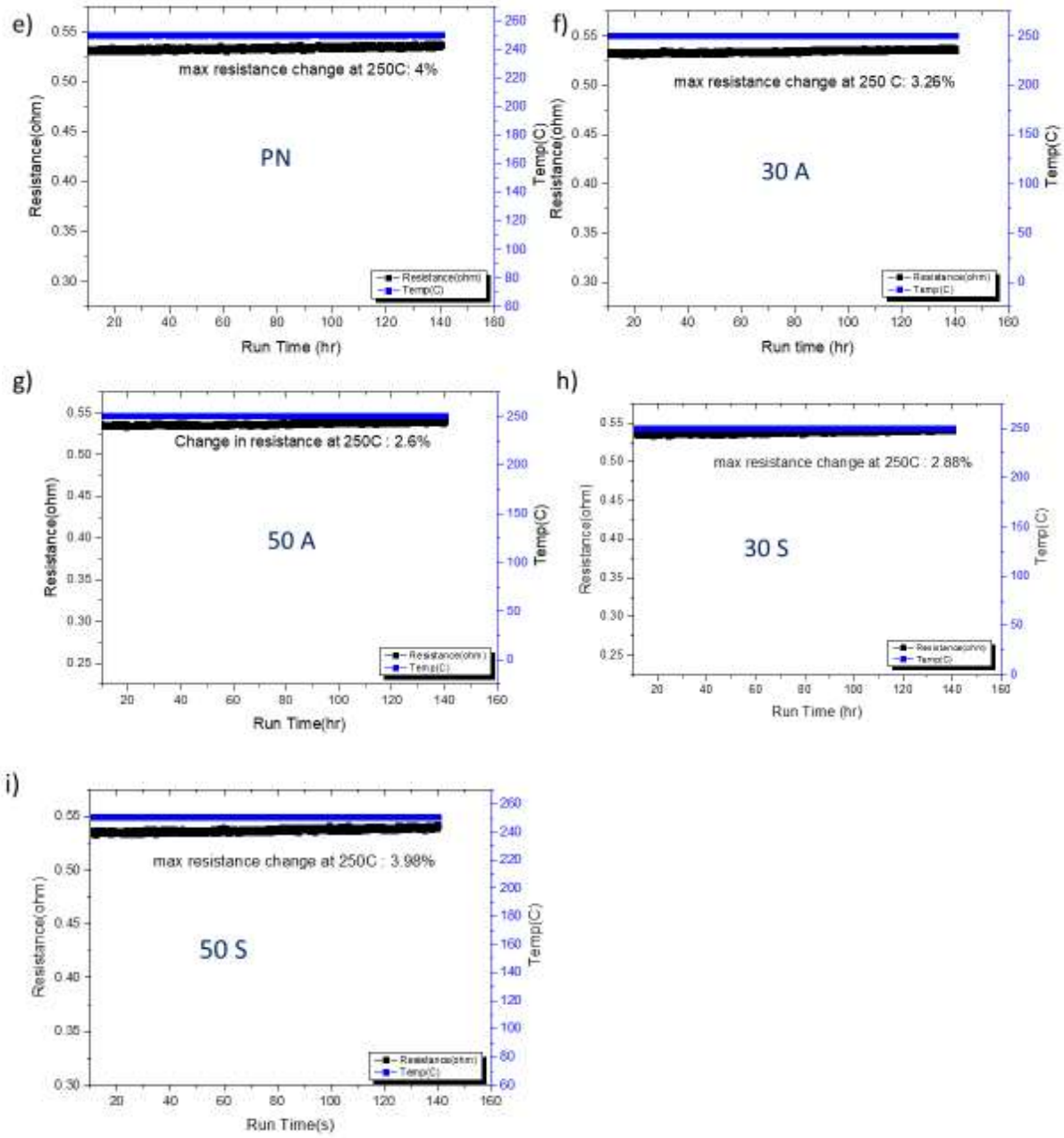

Figure A.5 Electrical stressing for various packages

A1.6 Perspective of TGA analysis

Samples were cured at 2 different temperatures: 280 °C and 360 °C under N_2 environment. Each set of samples were ramped up to 900 ^{o}C with different heating rates: 5, 10, 15 and 20 ^{o}C per minute as shown in the Figure A.6.

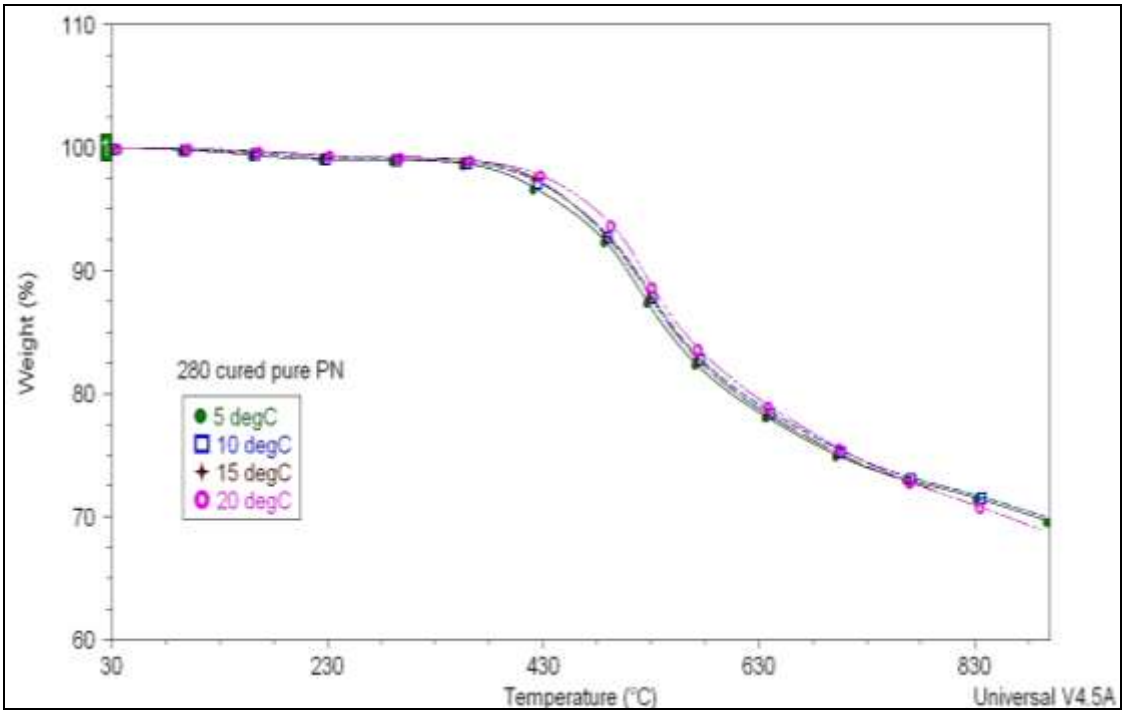

Figure A.6 TGA graph of 280 ^{o}C cured pure phthalonitrile

According to the application operating conditions, the temperature ranges from 300°C to 500 ^{o}C. Weight loss was being measured at this temperature to determine whether the polymer is able to withstand such environment. As temperature increases, the bonds in polymer start to break and polymer degrades, resulting in weight loss. 5 weight percent (wt %) loss was taken as a gauge in many studies. The results were collected from the TGA graphs and presented as follows.

Table A.1 and A.2 report the results for char yield at 500°C and temperature at 5 weight percent loss of samples cured at 280 ˚C respectively. Whereas Table and A.4 report the results for char yield at 500°C and temperature at 5 weight percent loss of samples cured at 360 ˚C respectively.

Table A.1 Char yield at 500°C under N2 (280 ˚C Cured).

280 ˚C Cured- Char yield at 500°C							
Heating rate (˚C)	**50wt% A**	**30wt% A**	**10wt% A**	**50wt% S**	**30wt% S**	**10wt% S**	**Pure PN**
5	92	93	90	94	93	91	90
10	94	94	91	96	93	92	91
15	95	94	93	96	94	93	92
20	96	96	94	97	96	94	93

TableA.2 Temperature at 5wt% loss (280 ˚C Cured)

280 ˚C Cured- Temperature at 5wt% loss							
Heating rate (˚C)	**50wt% A**	**30wt% A**	**10wt% A**	**50wt% S**	**3wt% S**	**10wt% S**	**Pure PN**
5	466	483	463	489	488	457	454
10	495	496	473	511	487	479	465
15	500	500	487	519	500	486	464
20	511	507	496	524	517	493	480

Table A.3 Char yield at 500°C under N2 (360 ˚C Cured)

360 ˚C Cured- Char yield at 500°C							
Heating rate (˚C)	**50wt% A**	**30wt% A**	**10wt% A**	**50wt% S**	**30wt% S**	**10wt% S**	**Pure PN**
5	95.6	94.9	94.4	97.5	96.5	95.0	94.1
10	96.6	97.1	96.6	98.0	98.1	97.2	94.7
15	97.0	97.5	97.0	98.2	98.1	97.5	95.6
20	97.3	96.6	95.9	98.2	98.2	97.1	96.0

Table A.4 Temperature at 5wt% loss (360 ˚C Cured)

360 ˚C Cured- Temperature at 5wt% loss							
Heating rate (˚C)	**50wt% A**	**30wt% A**	**10wt% A**	**50wt% S**	**30wt% S**	**10wt% S**	**Pure PN**
5	504	499	494	530	515	500	490
10	515	520	514	540	535	516	494
15	527	528	522	548	533	528	512
20	533	527	517	548	540	527	520

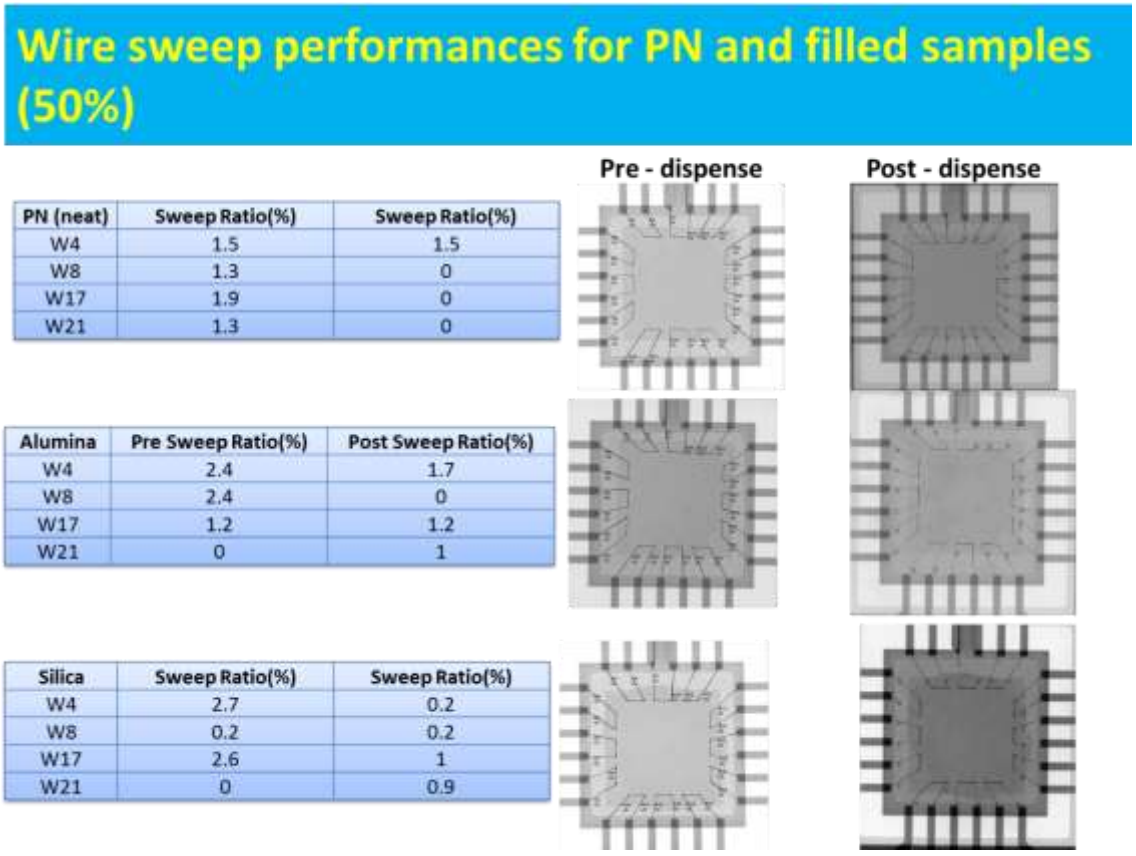

Figure A.7 Experimental verification of PN material properties post high temperature curing

As an electrical encapsulant, wire sweep may also be of concerns; Figure A.7 shows negligible changes to the wire sweeping of the PN filled samples at various temperatures. All the points are also retested for electrical connectivity post high temperature encapsulation and no open circuit measurement was found. This is an instance where a DIP package is PN filled and is checked for PN flow properties. The test also verified that the encapsulant has less viscosity despite being melted straight from a powder form. The resulting encapsulation can also withstand high temperature curing and cross link without causing any damages to the chip.

A1.8 Lid fabrication and bonding

Experiments were carried out to verify the robustness of the lid designs. Bismuth-rich glass frit was used as the bonding material between the ceramic package and the lid. Both the flat and dome cavity lids were exposed to the high pressure environment during testing. As a result, the bonding material chosen has to maintain package hermeticity

with no significant degradation in properties during the high temperature operations. A treatment profile as shown in Figure A.8 was used to achieve the hermetic sealing. All temperature ramps followed a rate of 10°C/min to allow adequate time for minimizing differential stress build up between materials. The top and bottom ceramic pieces of various thicknesses were bonded according to the simplified matrix shown in Table A.5. The first thermo-conditioning step removes the additives from the glass frit paste and the subsequent sealing step allows load placement on the lid to achieve better adhesion. This thermal profile has been reported previously by Sharif *et al.* [37][161].

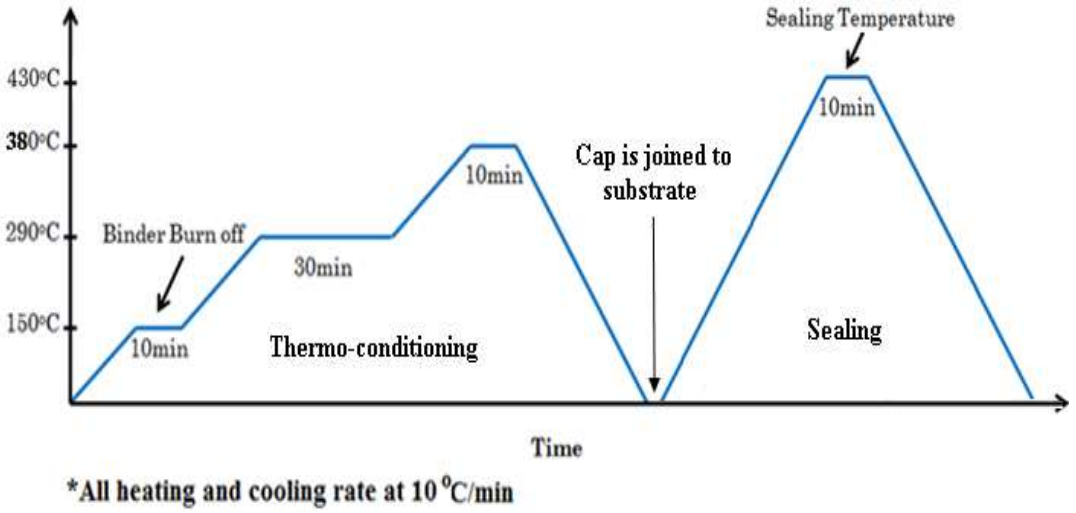

Figure A.8 Thermal profile of bonding ceramics substrate and lid with glass frit.

Table A.5 Ceramic lid and base designs for bonding

Material	Parts	Thickness
Alumina (99.5%)	Top flat lid	1-5 mm
	Bottom flat base	1-5 mm
	Dome cavity lid/base	3.2 mm (thinnest)

To prove the structural compatibility of ceramics bonded with glass frit, hermeticity tests were performed on alumina packages with dimensions of 14 mm × 14 mm × 5 mm with a die cavity of 10 mm × 10 mm × 3 mm. These pieces were then bonded to standard alumina substrates of 15 mm × 15 mm × 5 mm to demonstrate the feasibility of using glass frit as the bonding material. A bonding pressure of 0.15 MPa is recommended for optimized bonding and for residual gases to escape during the thermo-compression

bonding process. In the experiments, glass frit has been successfully used to provide hermetic sealing to ceramic pieces using this method described by Lim *et al.* [1-2].

References

[1] L. J. Zhang et al., "Ceramic-Ceramic joining using glass frit for high temperature application," in Electronics Packaging Technology Conference (EPTC), 2012 IEEE 14th, 2012, pp. 38–42.

[2] A. Sharif *et al.*, "Pb-Free Glass Paste: A Metallization-Free Die-Attachment Solution for High-Temperature Application on Ceramic Substrates," *J. Electron. Mater.*, vol. 42, no. 8, pp. 2667–2676, Aug. 2013.

Appendix B: Ceramics lid design for ruggedized electronics packaging

B1 Test samples description

Figure B-1 shows a 24-pin DIP package widely available on the market. A ceramic lid is used to encapsulate the semiconductor chip within the package cavity to protect it from the external harsh environment. Encapsulation designs can be classified broadly into hermetic or non-hermetic. Hermetic IC packages can be achieved using ceramics substrates and lids bonded with glass frits. Alternatively, they can be encased in metal and sealed via welding. On the other hand, polymer encapsulation typically produces non-hermetic packages and is unable to withstand high temperature environment, especially for 300°C and above applications.

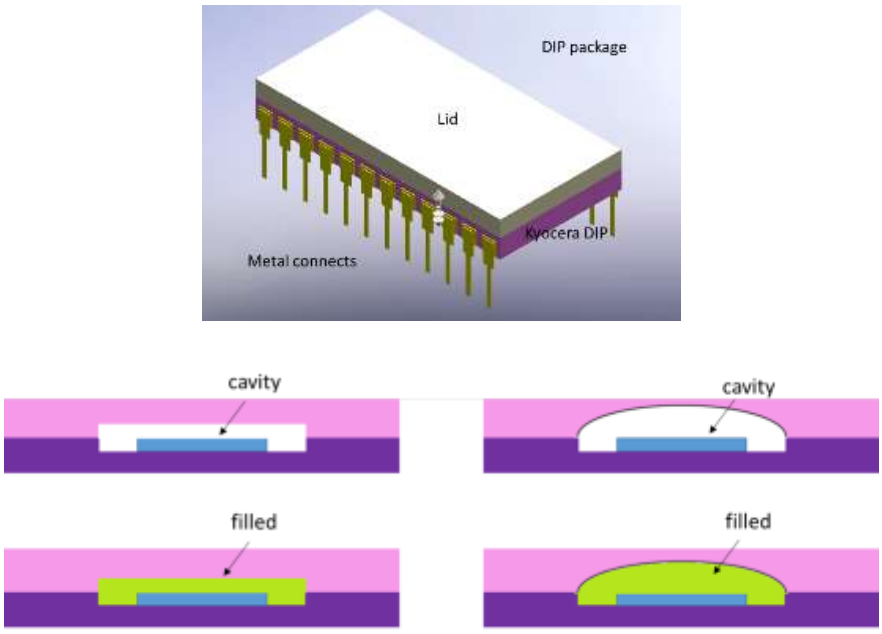

Figure B-1 Cross sectional view of different design layouts with PN fill and square or dome typed cavities for stress structural studies.

PN presents itself as an alternative polymeric material which can achieve gap fill as well as protection for the underlying chips under harsh environment. Much research is still on-going to identify good substitutes for epoxy in the high temperature regimes. In this research scope, a study on how hermetic encapsulation is achieved through design optimization of ceramic encapsulation is being discussed. Regions of weakness would be

identified on the ceramic lid designs and PN is suggested for cavity filling as it is one of the few polymers which can meet the high temperature requirements to date.

B2 Proposed designs for ceramic lid without polymer cavity fill

Two lid designs were studied using finite element analysis (FEA) based on maximum principle stress theory (Rankine's theory) in ANSYS™ software. The first design is a conventional flat lid (Fig. B-2(a)), while the second design has a dome cavity (Fig. B-2(b)) to reduce the stresses on the package with a minimum lid thickness. The lid is then attached on top of a commercial ceramic dual in-line package (DIP), with the die placed within the DIP cavity as shown in Figure B-2. A series of simulations was carried out to determine the optimized design parameters for the smallest form factor of the lid while ensuring that the maximum stress on the package did not exceed the failure stress. Further verification of the simulation results was done through fabrication of the optimized lid design and testing it under HP conditions.

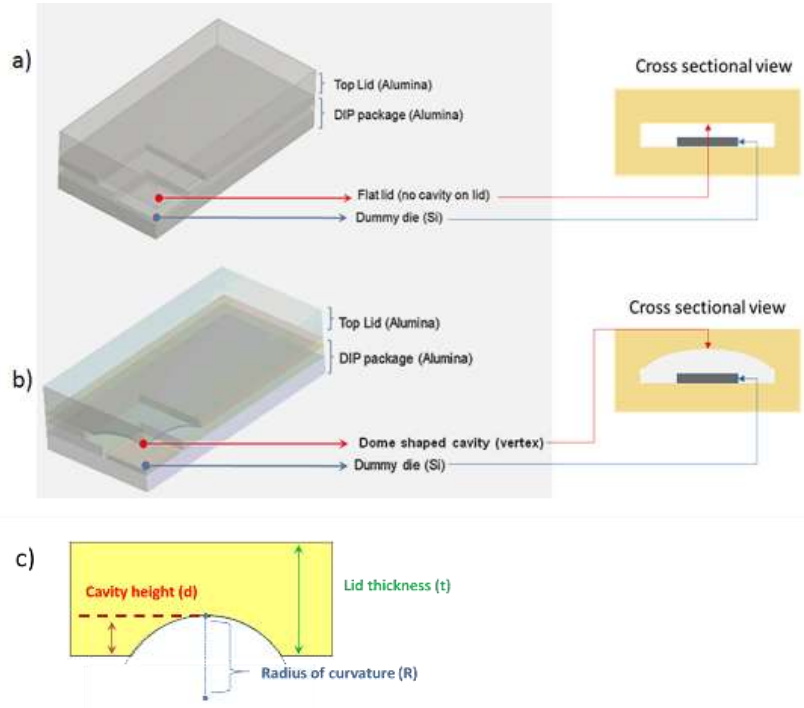

Figure B- 2 Representation of (a) ¼ of the ceramic flat box lid design. (b) ¼ of the ceramic dome cavity lid design. c) Mid-plane cut of dome cavity lid with naming conventions adopted in the simulations.

B3 Choice of materials

The material chosen for the lid is alumina (99.5%) as it has certain advantages over other ceramics for 300°C applications, including compatible coefficient of thermal expansion (CTE) with high temperature bonding materials such as glass frit, a high compressive strength of at least 1 GPa and a thermal conductivity of 33 W/m-K. Alumina is the common substrate used for high temperature DIP packaging in high temperate applications

Referring to Figure B-2 (c), the three main design parameters are: lid thickness (*t*), dome cavity height (*d*) and radius of curvature (*R*). The length and width of the lid are kept constant at 30.48 mm and 15.2 mm, respectively. Lid thickness represents the overall ceramic lid thickness and is kept between 1 mm to 5 mm, with industrial preference of smaller thickness. Cavity height represents the dome height which would house the die beneath. Ideally, this must be high enough to ensure possible die placement and wire-bonding. Radius of curvature depicts the degree of curvature which impacts the area of the cavity over the die. This parameter will also affect the distribution of stress directly over the die surface.

FEA was performed to evaluate the effectiveness of the dome cavity lid. In the simulations, a hydrostatic pressure environment was assumed with pressure directed normally onto the exposed package surface. As the objective is to evaluate the robustness of the package design for HPHT applications and these packages are not subjected to successive thermal or pressure fluctuations, the simulations were done under a constant environment of 300°C at 207 MPa.

In the simulations, both the lid and package material were assumed to be isotropic alumina, whereas the chip was isotropic silicon measuring 5 mm × 5 mm × 0.7 mm. Tetrahedral-type meshes were defined for the entire package with fine mesh densities. The package base was designated as the fixed support. The simulation was made more compact by “folding” the entire package into ¼ of the original size along its symmetrical axes.

All parameters such as lid thickness, radius of curvature and cavity height were optimized to achieve the following:

- Overall principle tensile and compressive stresses do not exceed the material fracture stress
- Smallest possible package geometry
- Minimal load transfer to the chip should there be any contact of lid vertex with chip due to low clearance height

In the design of experiments (DOE), simulations of flat lid without dome cavity were also generated for comparisons. Material properties used in the simulations are shown in Table B-1. Mode I fracture is the main failure mechanism assumed.

Table B- 1 Engineering properties used in ANSYS

Properties	Alumina (99.5%) at 20°C	Alumina (99.5%) at 500°C	PN (experimental)	Silicon
Young Modulus (GPa)	416	390	1.548	129.5
Compressive Modulus (GPa)	3	1.6	0.497	-
Tensile Strength (MPa)	380	267	50	64000
Poisson ratio	0.231	0.237	0.3	0.265
Specific Heat (J/Kg-K)	755	1165	1.08 (20°C) to 2.07 (300°C)	700
Thermal conductivity (W/m-K)	33	11.4	0.2	148

Both lid designs shown in Figure B-2 were used to reinforce a standard 24-pin DIP and simulations were carried out to predict the required minimum thickness for a hermetic package to survive HPHT testing. Figure B-3 shows the definitions adopted throughout the simulations, and the regions of stress in the lid which would be discussed further. The vertex zone (first stress zone) is usually the first failure region but simulations show that with variations in lid design, a second stress zone near to the line edge also has to be given due considerations. The line-edge region (second stress zone) is located at the die cavity edge which interfaces directly with the lid. It experiences a high compressive bending and is the region whereby lid would be in contact with structures such as wire bonds and bond pad metallization on high compressive pressure, thus causing damage.

The line edge region is mostly a region of compressive stress as opposed to the vertex zone where failure is mostly generated due to maximum tensile stress exceeding the interpolated limit of 377 MPa for alumina (Table B-1).

B4 Finite element simulation for flat lids under HPHT and HP conditions

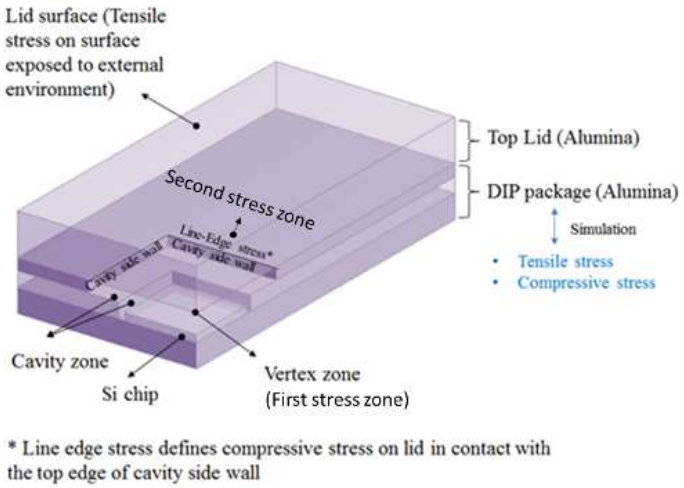

Figure B-3 Different stress zones on a flat lid at regions above the square cavity of the DIP package.

Figure B-4 shows ANSYS™ simulation results on the deformation and maximum principle stresses of the lid under HPHT environment (207 MPa and 300°C). As the lid thickness increases, less deformation is experienced. It can be observed that the high stress at the centre region of the vertex gradually decreases with increasing lid thicknesses (Figure B-4 (d) to (f)). Correspondingly, the deformation above the cavity also reduces with higher lid thicknesses (Figure B-4(a) to (c)). The stress intensity indicates that failure would occur with lid thickness below 3 mm, and that the deformation is mainly due to flexural stresses.

From Figure B-4(d) to (f), a second stress zone at the line edge is observed that is compressive in nature. However, alumina has a compressive strength of about 2183 MPa (at 300°C). This implies that the line edge stress, varying from 191 MPa to 311 MPa, will not be the cause of failures in alumina lids in HPHT environment. On the other hand, focus must be placed on the tensile modes of failure where the failure onset can occur at a much lower stress of 377 MPa.

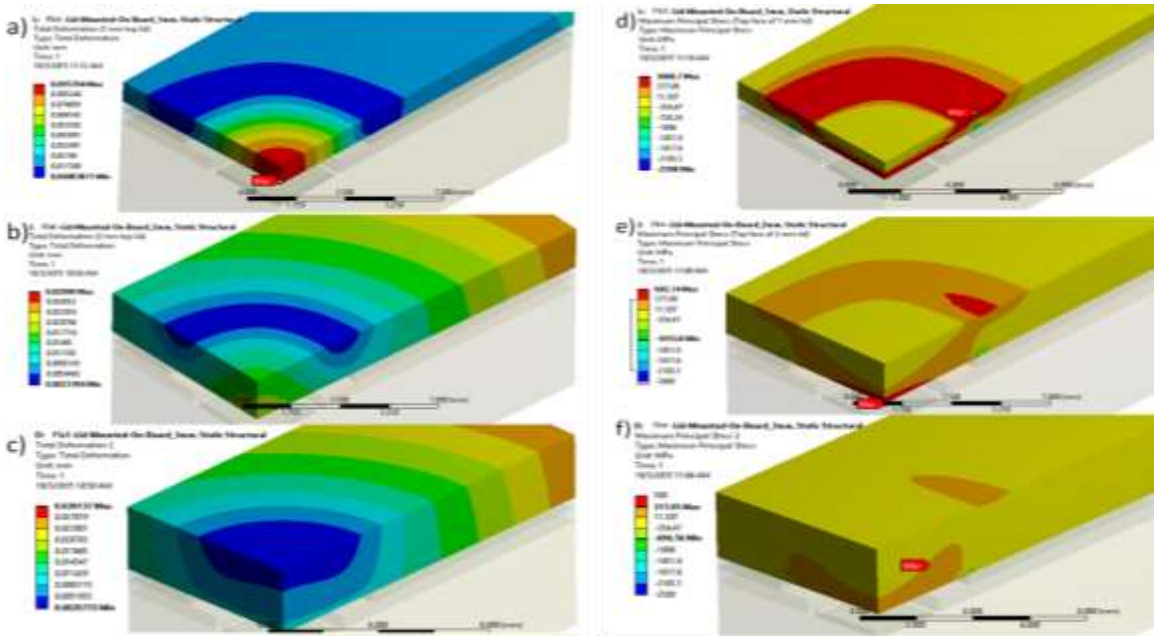

Figure B-4 Total deformation for (a) 1 mm, (b) 2 mm, and (c) 3 mm thick lid. Maximum principle stress for (d) 1 mm, (e) 2 mm, and (f) 3 mm thick lid. All conditions are HPHT.

Figure B-5 (a) and (b) show the corresponding deformation and maximum principle stress variation with increasing lid thickness, respectively under HPHT test condition (i.e. 207 MPa, 300°C). The two regions where stress concentrates are the centre of the lid on the inner side (vertex), and the package cavity edge that interfaces with the lid (line edge). As a reference, the maximum flexural strength of 377 MPa for alumina is shown in Figure B-5(b) to indicate expected failure of the lid when the maximum principle stress exceeds this value.

An exponential increase in deformation is predicted once the lid thickness decreases below 2 mm as observed in Figure B-5(a). With a lid thickness greater than 2 mm, the deformation is nearly constant. A similar trend is observed on the maximum principle stress shown in Figure B-5(b). The tensile stress starts to fall below 377 MPa with a thickness greater than 3 mm. With a thickness less than 3 mm, the stress will exceed the 377 MPa limit. The lid surface tensile stress follows the same trend closely but starts to deviate slightly from 3 mm onwards, indicating that the maximum tensile stress location is moving away from the surface and into the lid.

Alumina has excellent compressive strength of 2183 MPa (interpolated) at 300°C. The flexural strength however is much lower at about 377 MPa. Based on Fig. B-5(b), a minimum thickness of 3 mm is needed for flat lids to survive in a working pressure of 207 MPa alongside an operational temperature of 300°C.

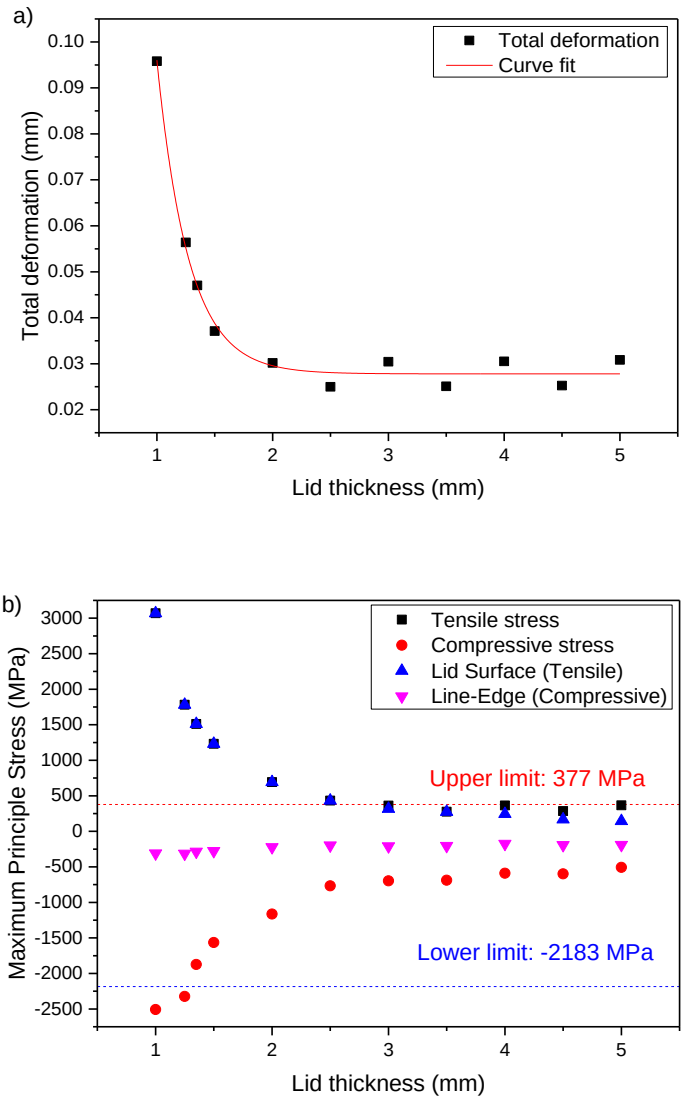

Figure B-5 (a) Lid deformation against thickness, (b) Flexural and compressive stresses on flat lid against thickness at HPHT condition (207 MPa, 300°C).

Figure B-6(a) shows the deformation results as a function of lid thickness under high pressure (HP) condition, (i.e. from a similar ANSYS™ simulation with the temperature at 20°C and pressure at 207 MPa). It can be observed that the total deformation under HPHT condition (Figure B-6(a)) is higher than that in HP condition (Figure B-5(a)) of

the same lid thickness. This can be attributed to the effect of dimensional changes at elevated temperature. As shown in Figure B-6(b), the failure stress increases slightly to 380 MPa under HP condition at 20°C. Correspondingly, the compressive limit increases to 3000 MPa for HP condition as compared to 2183 MPa in a HPHT environment at 300°C.

From the values shown, it can also be observed that the maximum stress gradually moves away from the top surface of the lid as it becomes thicker. It is further noted the maximum principle stress on the lid only drops below 380 MPa at a lid thickness of 3 mm.

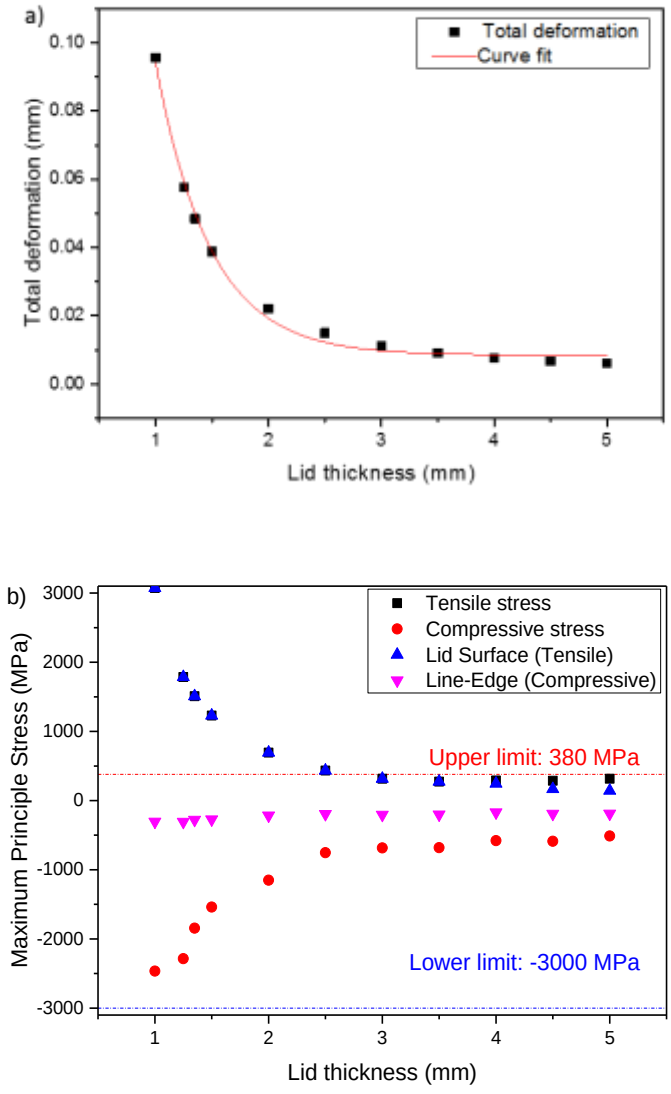

Figure B- 6 (a) Lid deformation against thickness, (b) Flexural and compressive stresses on flat lid against thickness at HP (207 MPa) condition.

High flexural stress is observed for lid thicknesses of less than 3 mm under HPHT. This is an important parameter to consider as it is an industrial demand to achieve lower package thickness. Based on the simulation results, it is not safe for such lids to be less than 3 mm when they are to be exposed to 207 MPa of external pressure, regardless whether it is at room temperature or 300°C, although lower lid surface tensile stress is observed in HPHT (Figure B-5(b)) condition as compared to HP condition (Figure B-6(b)).

It is also possible to compare and illustrate with FEA of the maximum stresses on dome cavity lids and flat lids by giving similar general dimensions. Figure B-7 shows the top view of dome cavity lids with different thickness. Referring to Figure B-7(a), the red region of high stress reaches a maximum of 359.64 MPa for a 2 mm thick dome cavity lid. Comparatively, a flat lid of 2 mm thickness as shown in Figure B-4(e) experiences a maximum stress of 692.74 MPa at the vertex zone (which is above alumina HPHT limit of 377 MPa).

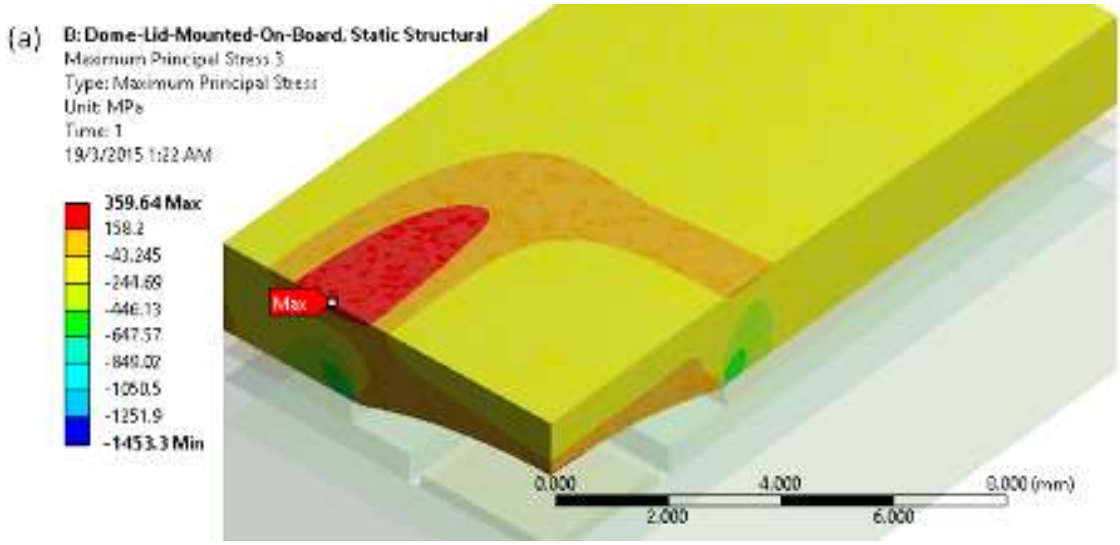

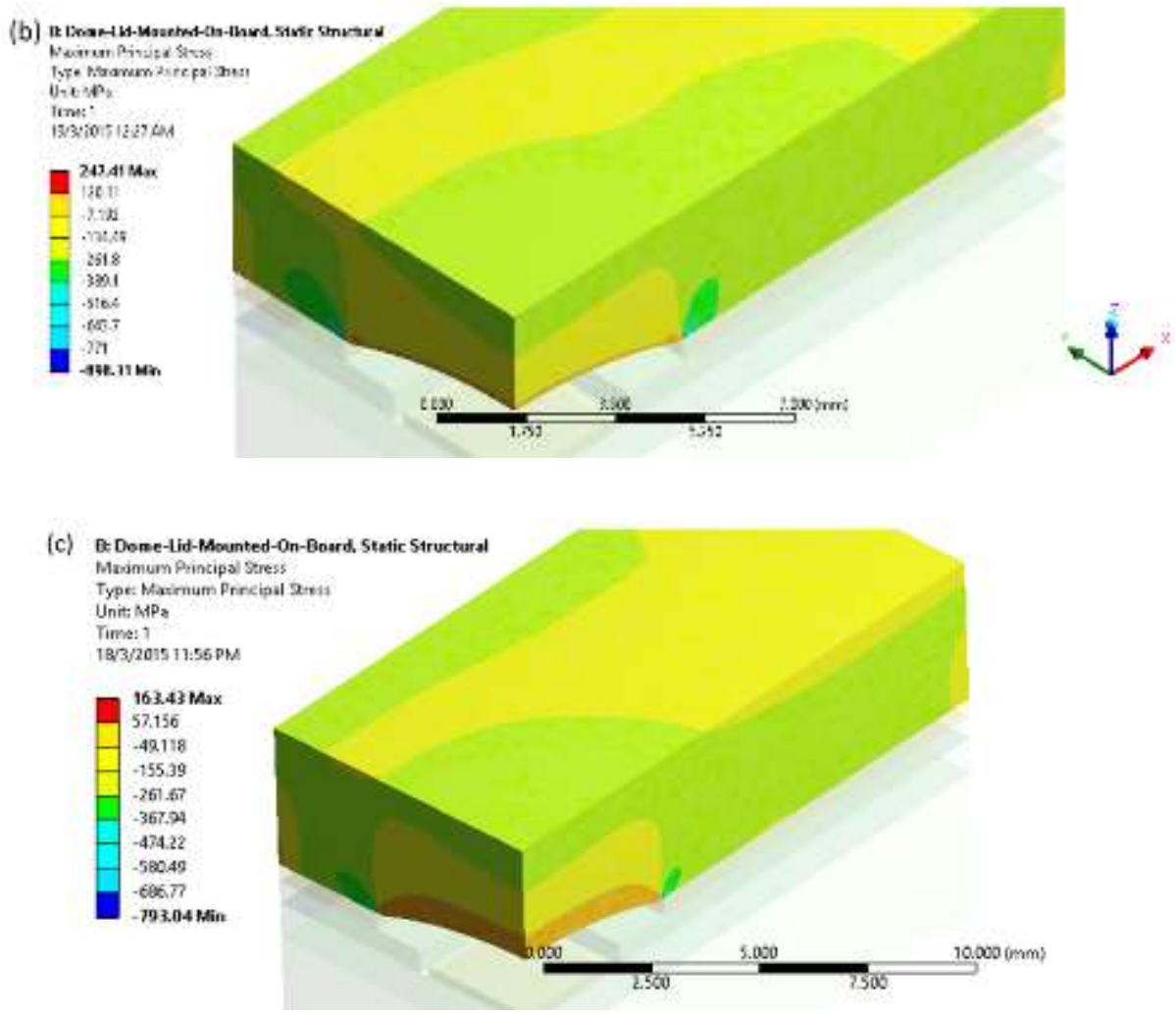

Figure B- 7 Top view of dome cavity design at thickness of (a) 2 mm (b) 3 mm (c) 4 mm. All conditions are HPHT.

B5 HP testing with fabricated flat box type and dome cavity type lids

A comparison of the high-pressure testing results with ANSYS™ simulations revealed a good match in observed crack patterns with the predicted crack patterns simulated on the lids surfaces. Crack marks observed from optical images of the ceramic flat lids after HP testing corresponded with the stress zones at which failures were predicted as shown in Figure B-8. The red zones shown in Figure B-8(a) indicate locations where the maximum principle stress exceeded the failure stress for 2 mm lid thickness. This stress decreased to below the failure limit when a 3 mm thick lid was used instead (Figure B-8(b)). A summary of the results is tabulated in Table B-2.

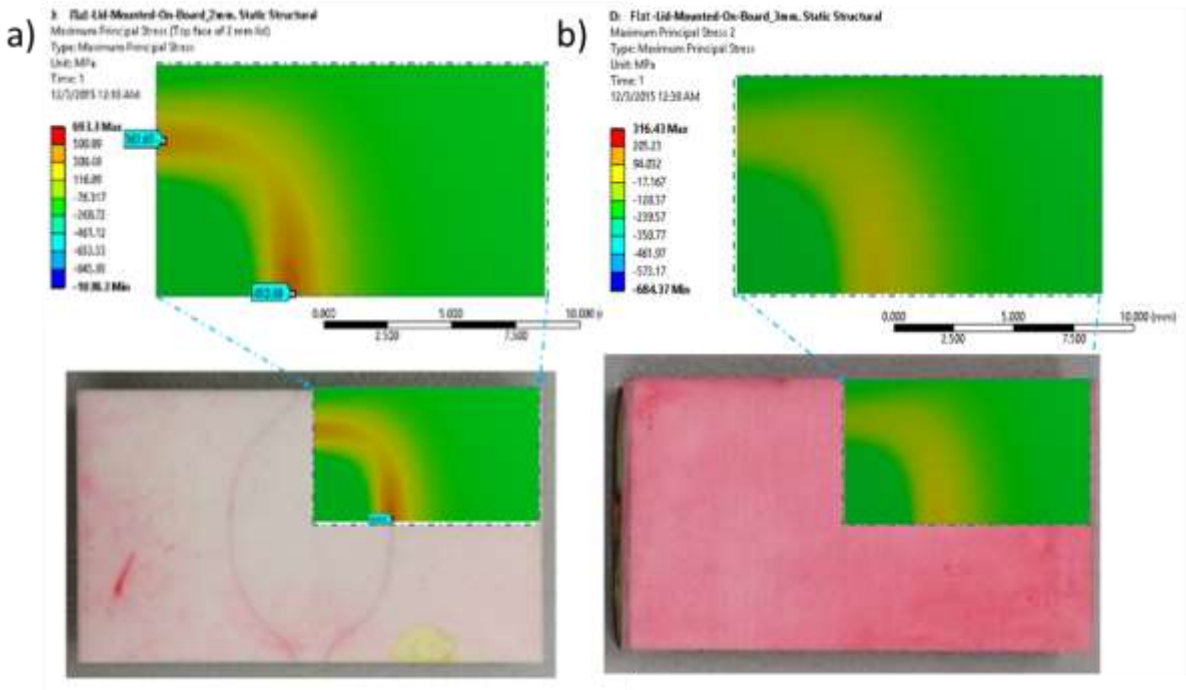

Figure B- 8 Simulations and physical experiments on (a) 2 mm and (b) 3 mm thick lids.

Table B- 2 Sample description for high pressure testing

Top Lid Thickness	Centre	Bottom Base Thickness	Result
4 mm	24 pin DIP	5 mm	No failure
3 mm	24 pin DIP	5 mm	No failure
2 mm	24 pin DIP	5 mm	Cracks on 2 mm top lid
2 mm	24 pin DIP	None	Cracks on top lid and DIP
3 mm	24 pin DIP	None	Cracks on top lid and DIP
4 mm	24 pin DIP	None	No failure

The physical test results correlate accurately with the predicted thicknesses at which the failure stress would occur, triggering the onset of crack formation and leading to brittle failure. Crack patterns observed on the samples also matched with the predicted zones of failure. By overlaying the maximum principle stress simulation results with the photographic images of cracks formed on the top lid, it can be deduced that failure stress had initiated from the high stress region (red zone) and propagated to form the crescent crack pattern observed on the surface, matching the patterns obtained on the total deformation results as observed in Figure B-4.

The match in simulated and actual failure patterns shows that maximum principle stress theory can be used to predict the combinational stresses accrued from high pressure and high temperature on a package level. With reference to a 2 mm thick flat lid, it can be observed that there is consistent failure under a 207 MPa pressurized environment. Figure B-9 is a 3D CT X-ray image which shows the extent of damage to the commercial DIP package when it was tested in a 207 MPa pressurized environment with only a 2mm thick lid. Clear cracks can be seen which cut through the centre metallization within the DIP package. In this case, a thicker dome shaped design lid would be more suitable for the same operation requirements. This substantiates the accuracy of the simulation results and provides ground for further lid fabrication using parameterized design of experiments.

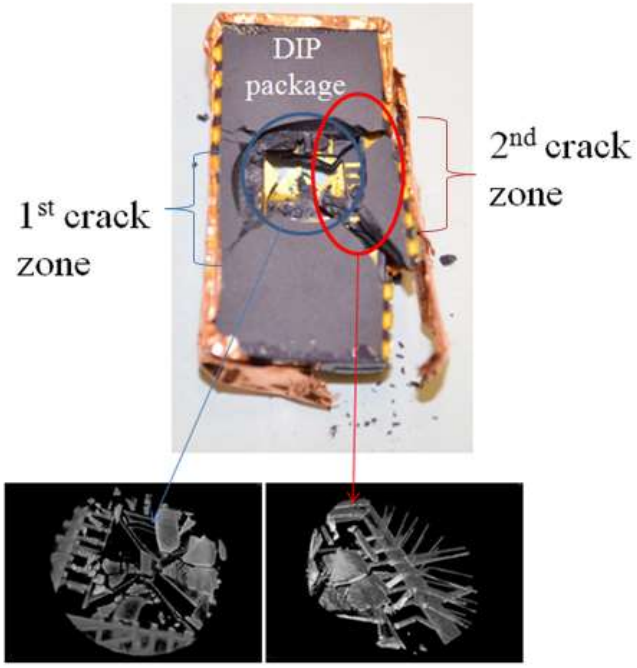

Figure B- 9 Optical and 3D CT X-ray images of DIP package after 207 MPa testing.

B6 Finite element simulation of stress distribution on a dome cavity lid

With the objective of exploring the limits of using a thinner lid with a dome cavity, an extensive simulation was performed using a lid thickness between 1.7 mm to 5 mm. The study was done with a dome radius of curvature between 6 mm to 13 mm and cavity height between 0.35 mm and 0.95 mm. Figures B-10 and B-11 show the stress distribution as a function of lid thickness, radius of curvature and cavity height at the vertex point and second stress zone, respectively, in a HPHT environment.

Referring to both Figure B-10 and Figure B-11, it can be observed that the lid thickness contributes significantly to the strength of the lid in a 300°C and 207 MPa environment. Correlating that with the observation for high stress regions in Figure 5 (most apparent in 2 mm thick lid), whereby the region of stress is not confined only to the lid vertex but also in the region immediately surrounding it (i.e. line edge, refer to Figure B-3), another correlation study was performed. Significantly higher stress values are observed (Figure B-11) whereby maximum principle stress in the second stress zone at the line edge can reach a maximum of over 600 MPa as lid thickness drops below 2 mm as compared to vertex stress which exceeds 400 MPa below 2 mm. From Figure B-11, it can also be observed that the strength of the lid is strongly dependent on the lid thickness as compared to cavity height and radius of curvature.

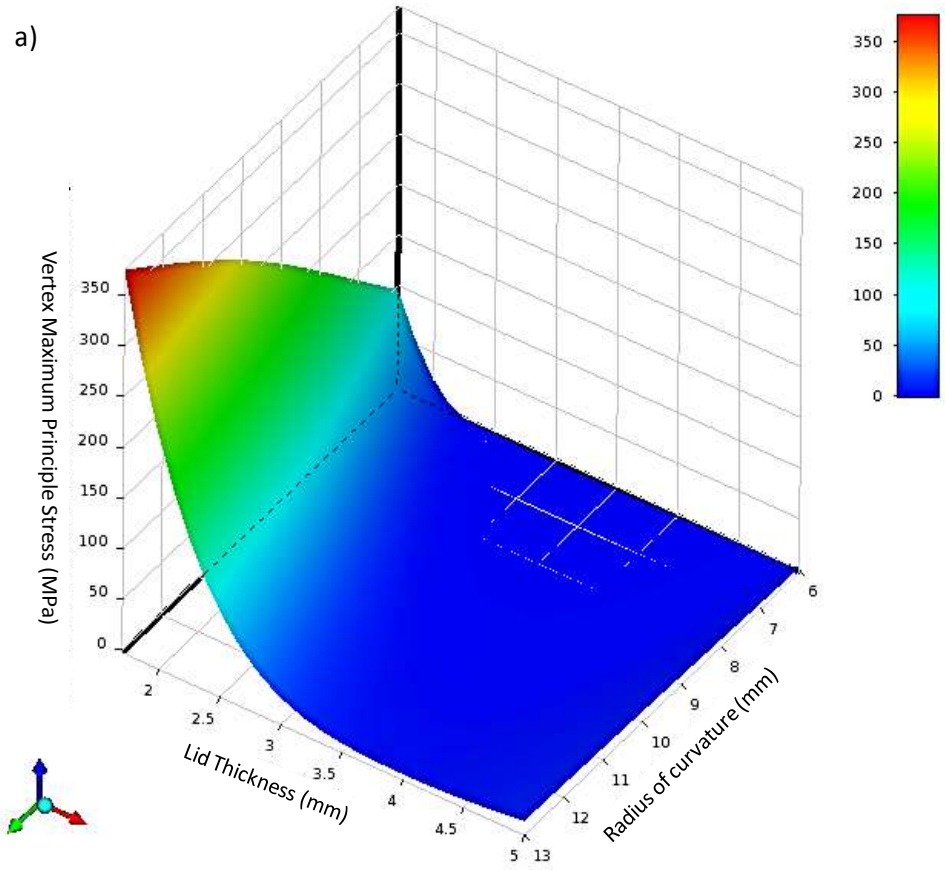

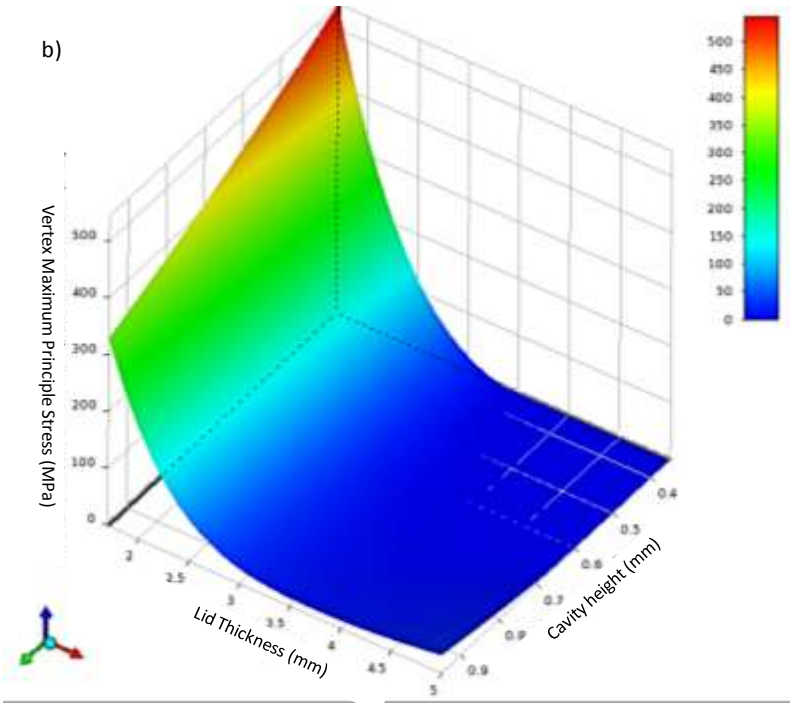

Figure B-10. Maximum vertex stress in correlation to lid thickness and (a) radius of curvature; (b) cavity height, under HPHT.

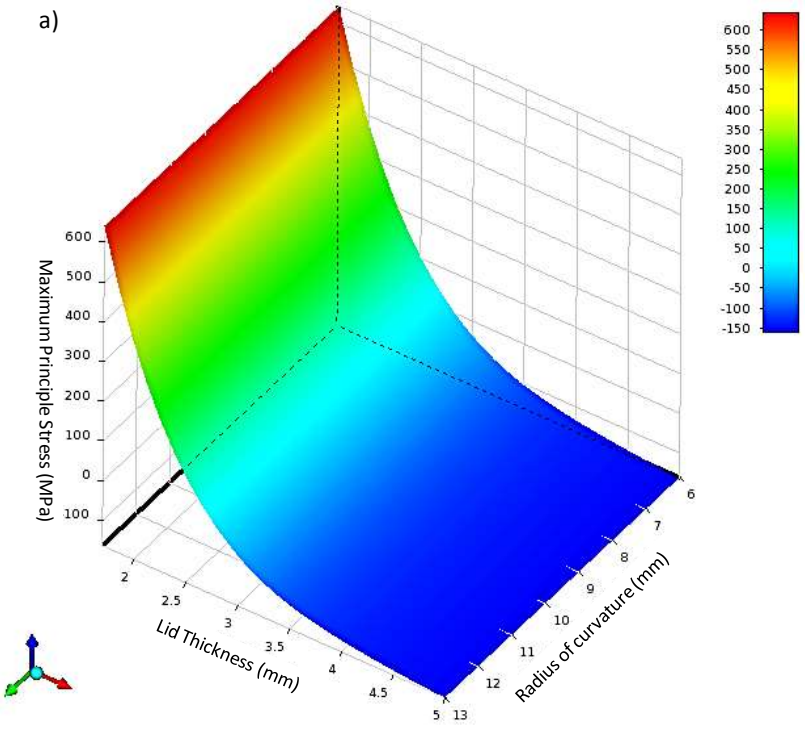

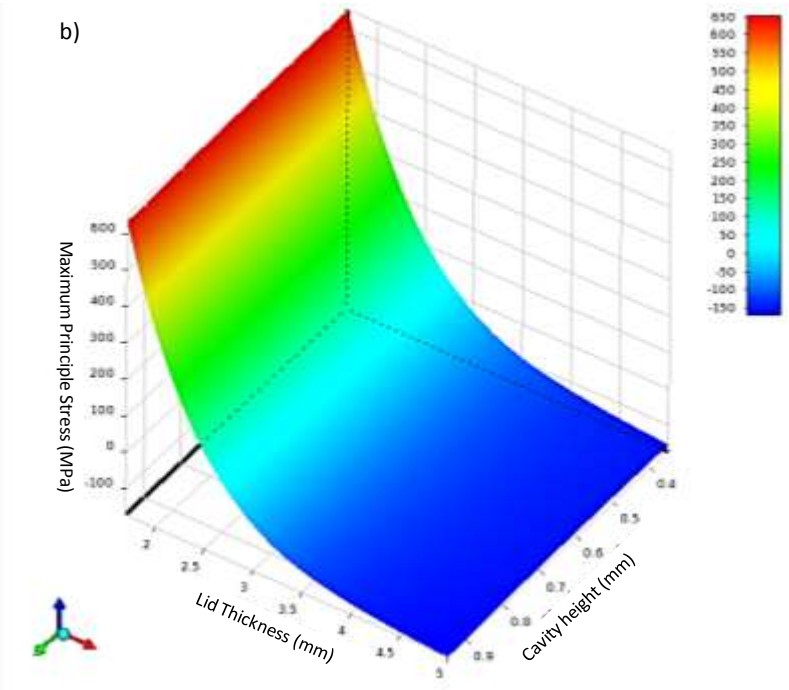

Figure B-11. Maximum stress at line edge region in correlation to lid thickness and (a) radius of curvature; (b) cavity height, under HPHT

With considerations from the optimized dimensions calculated and shown in Figure B-10 and Figure B-11, Table B-3 shows the dimensions of lid prototypes fabricated based on the optimized parameters. As shown in Figure B-12, Design 1 was fabricated to investigate failure patterns under high pressure testing. Conversely, Design 2 which is predicted to pass with the dimensions of t = 4 mm, d = 13 mm and cavity height of 0.8 mm, was also fabricated to verify the theoretical predictions. At the vertex, the thinnest part of the 4 mm thick dome cavity lid, the effective lid thickness is only 3.2 mm after deducting the cavity height.

Table B- 3 Fabricated package dimensions for proof of concept

Parameter (dimensions in mm)	**Design 1**	**Design 2**
Lid thickness	2	4
Radius of curvature	13	13
Cavity Height	0.8	0.8

With reference to Table B-3, it is observed that Design 1 as shown in Figure B-12 has cracks which extended from the centre vertex to the edges. This coincides with the vertex stress position which is predicted to be at a maximum on the lid vertex as shown in Figure B-12 (A Nikon D5100 was used with extra side lighting to enhance surface contrast as shown in the image for Design 1) The improved 4 mm thick lid with an effective thickness of 3.2 mm at the lid vertex showed no cracks and is in tandem with the simulation result where the maximum stress does not exceed the specification limit of 380 MPa (reference to 20°C).

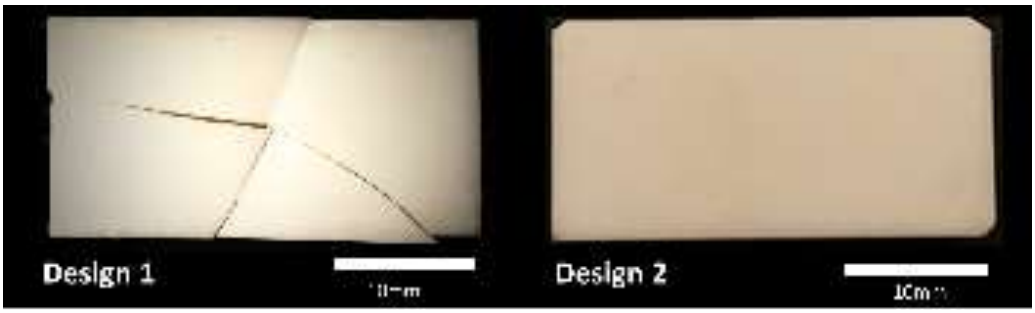

Figure B- 12 Optical images of Design 1 (2 mm) and Design 2 (4 mm) dome cavity lids after HP testing.

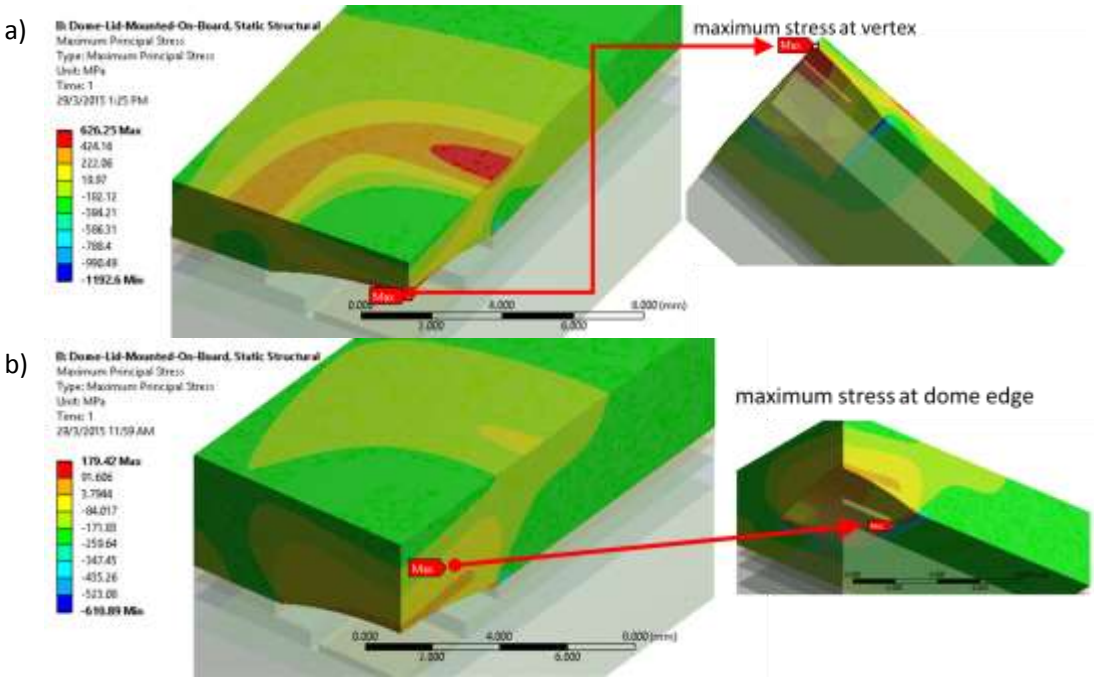

Figure B- 13 Simulation results for (a) 2 mm and (b) 4 mm thick dome cavity lids under HP tests conditions.

It can be observed from experimental results that crack initiations resemble closely to predictions from finite element analysis. This validates the hypothesis that dome cavity lid designs help to lower the maximum stress as compared to flat lid designs with similar thicknesses.

Appendix C: Scientific contributions

Intellectual Properties/Technical Disclosures

1. Multi-parameters accelerated test system for reliability characterization of test chips (as co-inventor)
2. Phthalonitrile (PN) based encapsulation for electronic packages used in high pressure high temperature (HPHT) applications (currently filed as NTU Propriety confidential information) – as inventor
3. Shaped Optimized Packaging for High Temperature and Pressure Application (Provisional patent) – as co-inventor

Journals/Conferences

1. R. I Made, E. J. R. Phua, S. S. Pramana, C. C. Wong, Z. Chen, A. I. Y. Tok, and C. L. Gan, "Improved mechanical and thermomechanical properties of alumina substrate via iron doping," Scr. Mater., vol. 68, no. 11, pp. 869–872, Jun. 2013.
2. L. F. Long, I. M. Riko, W. N. Putra, E. P. J. Rong, L. J. Zhang, L. J. Dy, W. C. Cheong, C. Zhong, V. C. Nachiappan, and G. C. Lip, "Study of electrical property of Au-Ge eutectic solder alloys for high temperature electronics," in Electronics Packaging Technology Conference (EPTC), 2012 IEEE 14th, 2012, pp. 30–33.
3. L. J. Dy, E. P. J. Rong, I. M. Riko, A. Sharif, L. J. Zhang, L. F. Long, G. C. Lip, C. Zhong, D. R. MinWoo, and W. C. Cheong, "Study of thin film metallization adhesion in ceramic multichip module," in Electronics Packaging Technology Conference (EPTC), 2012 IEEE 14th, 2012, pp. 67–71.
4. R. I. Made, E. J. R. Phua, A. Sharif, S. S. Pramana, C. C. Wong, Z. Chen, A. I. Y. Tok, V. C. Nachiappan, B. Y. Ho, and S. Gao, "Study of metal additives to alumina ceramics substrate for high temperature and pressure application," 2012.
5. I. M. Riko, S. S. Pramana, E. P. J. Rong, W. C. Cheong, C. Zhong, A. T. I. Yoong, and G. C. Lip, "Study of metal additives to alumina substrate for high temperature and pressure application," in Electronics Packaging Technology Conference (EPTC), 2012 IEEE 14th, 2012, pp. 48–51.
6. V. Chidambaram, E. P. J. Rong, G. C. Lip, and R. M. W. Daniel, "Cyanate Ester-Based Encapsulation Material for High-Temperature Applications," J. Electron. Mater., Jul. 2013.

7. Eric Jian Rong Phua, R. I. M. “Electronic Packages for High Pressure Applications: A Dome-Shaped Cavity Design,” in IEEE Electronic Components and Technology Conference, 2013.

8. M.-Y. Cheng, M. Je, K. L. Tan, E. L. Tan, R. Lim, L. Yao, P. Li, W.-T. Park, E. J. R. Phua, C. L. Gan, and A. Yu, “A low-profile three-dimensional neural probe array using a silicon lead transfer structure,” J. Micromechanics Microengineering, vol. 23, no. 9, p. 095013, Sep. 2013.

9. V. Chidambaram, E. P. J. Rong, G. C. Lip, and M. W. D. Rhee, “Performance enhancement of Au-Ge eutectic alloys for high-temperature electronics,” presented at the Electronics Packaging Technology Conference (EPTC 2013), 2013 IEEE 15th, 2013, pp. 202–207.

10. L. C. Wai, W. W. Seit, E. P. J. Rong, M. Z. Ding, V. S. Rao, and D. R. MinWoo, “Study on Silver Sintered Die Attach Material with Different Metal Surfaces for High Temperature and High Pressure (300°C/30kpsi) Applications,” Singapore. 2013 IEEE 15th Electron. Packaging. Technol. Conf., 2013.

11. H. H. Yuan, E. W. L. Ching, C. Y. Sing, V. Chidambaram, L. J. Bum, E. P. J. Rong, G. C. Lip, and D. R. M. Woo, “Extreme high pressure and high temperature package development,” in Electronics Packaging Technology Conference (EPTC 2013), 2013 IEEE 15th, 2013, pp. 379–383.

12. N. S. Nobeen, R. Imade, B. R. Lee, E. J. R. Phua, C. C. Wong, C. L. Gan, and Z. Chen, “Transient liquid phase (TLP) bonding using Sn/Ag multilayers for high temperature applications,” in 2013 IEEE 15th Electronics Packaging Technology Conference (EPTC 2013), .

13. H. H. Yuan, H. Kuruveettil, E. W. L. Ching, E. P. J. Rong, G. C. Lip, and D. R. M. Woo, “Development of ruggedized timer and temperature sensor packaging for 300° C/30kpsi downhole environment,” in Electronics Packaging Technology Conference (EPTC 2015)

14. E. J. R. Phua, M.Liu, B.Cho, Q.Liu, S.Amini, X.Hu, C.L.Gan, “Novel high temperature polymeric encapsulation material for extreme environment electronics packaging,” Mater. Des., vol. 141, pp. 202–209, Mar. 2018.